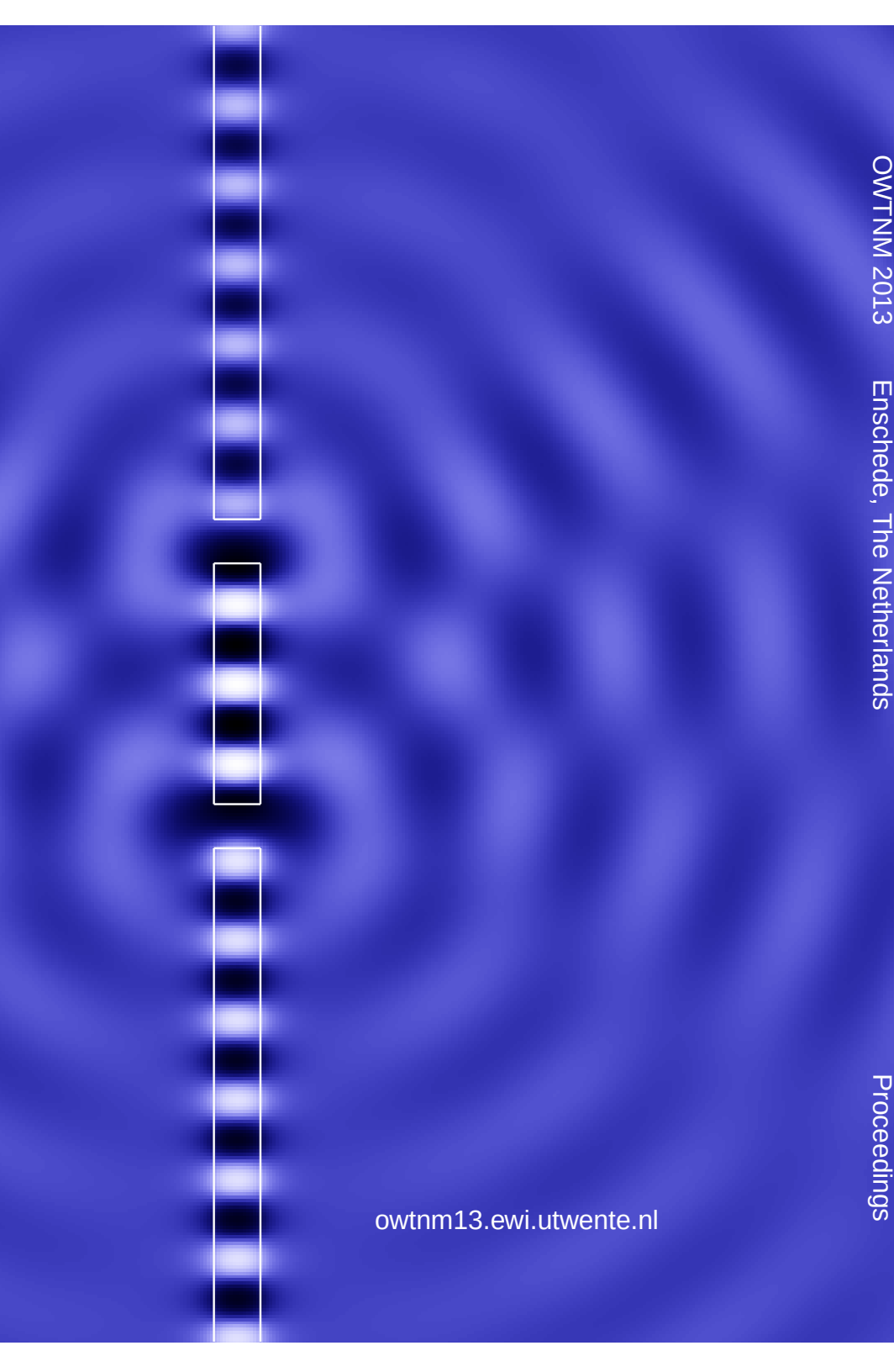

owtnm13.ewi.utwente.nl

OWTNM 2013 Enschede, The Netherlands Proceedings

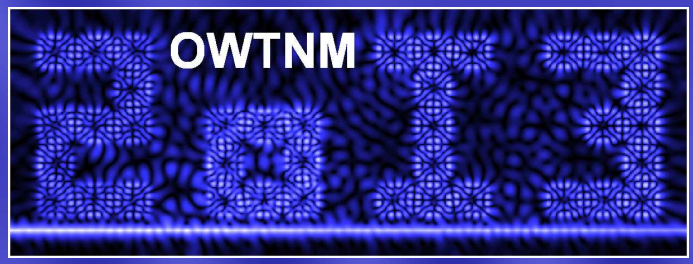

XXI International Workshop on Optical Wave & Waveguide Theory and Numerical Modelling

Enschede, The Netherlands
April 19 & 20, 2013

Proceedings

Contact information:
Dr. Manfred Hammer
University of Twente,
Faculty EEMCS,
P.O. Box 217,
7500 AE, Enschede,
The Netherlands;
Phone: +31 (0)53 489 3448, +31 (0)53 489 4768
Fax: +31 (0)53 489 3996
E-mail: owtnm13@ewi.utwente.nl
Web: http://owtnm13.ewi.utwente.nl/

Printed in Enschede, The Netherlands
ISBN: 978-90-365-3538-0

OWTNM 2013

XXI International Workshop on Optical
Wave & Waveguide Theory and Numerical Modelling

19-20 April 2013, Enschede, The Netherlands

Proceedings

UNIVERSITY OF TWENTE.

Acknowledgments

The organizers thank the following companies and institutes for their interest and support:

PhoeniX Software, Software for micro- and nano technologies,
P.O. Box 545, 7500 AM Enschede, The Netherlands

MESA+ Institute for Nanotechnology, University of Twente,
P.O. Box 217, 7500 AE Enschede, The Netherlands

JCMwave GmbH
Bolivarallee 22, D-14050 Berlin, Germany

Optiwave, Design software for Photonics
7 Capella Court, Ottawa, ON K2E 7X1, Canada

IEEE Photonics Society
http://www.photonics-benelux.org/

Lumerical Solutions, illuminating the way
Suite 300 – 535 Thurlow Street, Vancouver, BC V6E 3L2, Canada

Focal Machine Vision and Optical Systems
Zutphenstraat 10-28, 7575 EJ Oldenzaal, The Netherlands

LioniX
PO Box 456, 7500 AL Enschede, The Netherlands

Preface

The 21st edition of the *International Workshop on Optical Wave & Waveguide Theory and Numerical Modelling (OWTNM)* will be held in Enschede, the Netherlands, on April 19 & 20, 2013. Since 1992, the annual workshop has been a forum for enthusiastic scientists in the field of integrated optics to exchange ideas, and to discuss problems, related to optical theory, computational modelling, and novel device concepts. The organizers hope and expect that the 21st OWTNM will be just as successful as the previous meetings.

Integrated optics must nowadays be seen in an evolutionary context of related fields such as photonic nanostructures, metamaterials, and plasmonics, not to speak of the established areas of optical micro-resonators or photonic crystals. With the continuously increasing available computing power, the emphasis of simulation techniques shifts towards the modelling of larger or more complex systems, towards higher dimensionality, or towards more rigorous simulations. The field has thus seen quite some broadening, when compared to its origins. Respective suggestions from the 2012 meeting of the OWTNM technical committee led to a slight modification of the title of the workshop, where the traditional term *waveguide* gave way to the broader *wave*. Some emphasis on the traditional problems of integrated optics remains with the *waveguide*-subscript. This change might be continued or reversed for future editions of the OWTNM; the slight shift of emphasis, however, is well perceptible in the technical program on the following pages.

The OWTNM 2013 encompasses 55 scientific contributions, including 9 invited talks, distributed over 8 oral and one poster session. The organization could benefit from the financial support of 8 companies and institutions, which will have posters on display in a separate section of the poster area. Adhering to a tradition of the OWTNM series, a special journal issue of *Optical and Quantum Electronics* will be organized on the occasion of the workshop.

We are looking forward to an enjoyable, scientifically inspiring OWTNM 2013.

Enschede, March 2013
The local organizing committee

Organizers

Local Organizing Committee OWTNM 2013

- Manfred Hammer, University of Twente, Netherlands
- Hugo J.W.M. Hoekstra, University of Twente, Netherlands
- Remco Stoffer, PhoeniX Software, Enschede, Netherlands
- Sonia Garcia-Blanco, University of Twente, Netherlands
- Milan Maksimovic, Focal Optical Systems, Netherlands
- Liantian Chang, University of Twente, Netherlands
- Mustafa Akin Sefunc, University of Twente, Netherlands

OWTNM Technical Committee

- Trevor Benson, University of Nottingham, UK
- Jiří Čtyroký, Institute of Electronics and Photonics, Czech Republic
- Manfred Hammer, University of Twente, Netherlands
- Andrei V. Lavrinenko, COM-DTU, Lyngby Kgs., Denmark
- Xavier Letartre, LEOM, Ecole Centrale de Lyon, France
- John Love, Australian National University, Australia
- Andrea Melloni, DEI-Politecnico di Milano, Italy
- Olivier Parriaux, University of Saint Etienne, France
- Reinhold Pregla, FernUniversität Hagen, Germany
- Ivan Richter, Chech Technical University, Chech Republic
- Christoph Wächter, Fraunhofer IOF, Jena, Germany

Programme

Workshop schedule

Friday, April 19, 2013

08:55	Welcome address
09:00 – 10:15	O-1: Methods & algorithms I
	Coffee break
10:45 – 12:00	O-2: Active structures
	Lunch
13:00 – 14:15	O-3: Functional devices
	Coffee break
14:45 – 16:00	O-4: Nanophotonics
	Drinks
16:00 – 18:00	P: Poster session
19:00	*Workshop dinner*

Saturday, April 20, 2013

09:00 – 10:15	O-5: Methods & algorithms II
	Coffee break
10:45 – 12:00	O-6: Metamaterials & nanostructures
	Lunch
13:00 – 14:15	O-7: Physical phenomena
	Coffee break
14:45 – 16:00	O-8: Plasmonics
16:00	Closing remarks

Friday, 09:00 – 10:15: *Methods & algorithms I*

09:00 O-1.1 P.A. Postigo (invited),
Three-dimensional finite-difference time-domain (3D-FDTD) methods for photonic crystal lasers, solar cells and quantum nanophotonics

09:30 O-1.2 M. Maksimovic,
Resonances in high-contrast gratings with complex unit cell topology

09:45 O-1.3 D.D. El-Mosalmy, M. Farhat, O. Hameed, N.F.F. Areed, S.S.A. Obayya,
Radial basis function neural network based optimization approach for photonic devices

10:00 O-1.4 C. Kluge, L.T. Neustock, J. Adam, M. Gerken,
Calculation of leaky-wave radiation from compound binary grating waveguides

Friday, 10:45 – 12:00: *Active structures*

10:45 O-2.1 M. Pollnau, M. Eichhorn (invited),
Theory of lasing resonators: Quality factor and line width

11:15 O-2.2 A. Liu, J. Pond,
Nonlinear and gain simulation in waveguide systems: methods and applications

11:30 O-2.3 S. Malaguti, G. Bellanca, A. Bazin, F. Raineri, R. Raj, S. Trillo,
Hybrid III-V semiconductor/silicon three-port Filter on 1D-PhC wire

11:45 O-2.4 J. Ctyroky,
Full-vector analysis of photonic structures with a balance of loss and gain

Friday, 13:00 – 14:15: *Functional devices*

13:00 O-3.1 T. Mizumoto, Y. Shoji (invited),
Magneto-optical nonreciprocal devices on silicon

13:30 O-3.2 M. Farhat, O. Hameed, A.M. Heikal, S.S.A. Obayya,
Passive polarization rotator based on spiral photonic crystal fiber

13:45 O-3.3 B.B. Oner, M. Turduev, I.H. Giden, H. Kurt,
Enhancing light manipulation by graded index photonic crystal media

14:00 O-3.4 A.-L. Fehrembach, K. Chan Shin Yu, A. Monmayrant, O. Gauthier-Lafaye, P. Arguel, A. Sentenac,
1D crossed guided mode resonant gratings for tunable filtering

Friday, 14:45 – 16:00: *Nanophotonics*

14:45 O-4.1 J. Knoester (invited),
Collective optical excitations in self-assembled molecular nanotubes for light-harvesting

15:15 O-4.2 V. Grigoriev, A. Tahri, S. Varault, B. Rolly, B. Stout, J. Wenger, N. Bonod,
Decomposition of Mie scattering coefficients and polarizabilities of nanoshell structures into Lorentzian resonances

15:35 O-4.3 S. She, Y.Y. Lu,
Extraordinary optical transmission through circular metallic cylinder arrays

15:45 O-4.4 D. Ketzaki, O. Tsilipakos, T.V. Yioultsis, E.E. Kriezis,
Electromagnetically induced transparency with hybrid silicon-plasmonic traveling-wave resonators

Friday, 16:00 – 18:00: Poster session

P-01 D.K. Sharma, A. Sharma,
Low-loss splicing of microstructured optical fibers and single-mode fibers: an analytical study

P-02 K. Gehlot, A. Sharma,
Simple analytical approach to optimize structure parameters of photonic crystal waveguide coupler

P-03 A. Parini, G. Calo, G. Bellanca, V. Petruzzelli,
Vertical links for multilayer optical-networks-on-chip topologies

P-04 Q. Cao, S. Li, D. Teng, H. Gao,
A terahertz waveguide coupler with a tapered dual elliptical metal structure

P-05 P. Kwieicen, V. Kuzmiak, I. Richter, J. Ctyroky,
Nonreciprocal waveguiding EM surfaces and structures for THz region

P-06 A.M. Heikal, M. Farhat, O. Hameed, S.S.A. Obayya,
Coupling characteristic for novel hybrid long-range plasmonic waveguide including bends

P-07 S.I.H. Ibrahim, S.S.A. Obayya,
Novel mixed finite element method analysis of leaky photonic nanowires

P-08 S.I.H. Ibrahim, S.S.A. Obayya, R. Letizia,
Efficient bidirectional beam propagation method for multiple longitudinal optical waveguide discontinuities

P-09 R. Stoffer,
Mode Polishing for 3D Finite Element BPM

P-10 M.G. Can, B.B. Oner, H. Kurt,
Numerical modeling of human eye with electromagnetic approach

P-11 A.-L. Fehrembach, A. Sentenac,
A vectorial simplified model for Fano resonances of guided-mode resonant gratings

P-12 A.-L. Fehrembach, D. Shu, E. Popov,
Electro-optic effect in guided mode resonance gratings for tunable narrow-band filtering

Friday, 16:00 – 18:00: Poster session

P-13 A. Auditore, M. Conforti, C. De Angelis, A.B. Aceves,
Solitons in binary waveguide arrays

P-14 Vinita, A. Kumar, V. Rastogi,
Bandgap maps for photonic crystal with honeycomb lattice for different shapes of scatterers

P-15 Z. Hu, Y.Y. Lu,
Standing waves on periodic arrays of circular dielectric cylinders

P-16 Babita, V. Rastogi,
Design and analysis of a low cost highly sensitive refractive index sensor

P-17 H.J.W.M. Hoekstra,
Integrated optics refractometry: sensitivity in relation to spectral shifts

P-18 F. Civitci, M. Hammer, H.J.W.M. Hoekstra,
Reflection of semi-guided plane waves at angled thin-film transitions

P-19 S.F. Helfert,
Time domain method of lines

P-20 M.A. Botchev,
Matrix exponential and Krylov subspaces for fast time domain computations: recent advances

P-21 J.P. Epping, M. Kues, P.J.M. van der Slot, C.J. Lee, C. Fallnich, K.-J. Boller,
Numerical modeling of seeded FWM in silicon nitride waveguides for CARS

P-22 E.K. Sharma, J. Anand,
Propagation of a periodic sequence of Gaussian pulses in a coaxial optical fiber: occurrence of "Talbot Effect" in the time domain

P-23 S.G. Moiseev, V.A. Ostatochnikov, D.I. Sementsov,
The peculiarities of optical spectra of photonic crystal with plasmonic defect

P-24 G. Boudarham, B. Rolly, B. Stout, R. Abdeddaim, J.M. Geffrin, N. Bonod,
Manipulating light matter interaction with Mie resonators

Saturday, 09:00 – 10:15: *Methods & algorithms II*

09:00 O-5.1 K. Busch (invited),
Discontinuous Galerkin methods in nano-photonics
09:30 O-5.2 A.A. Shcherbakov, A.V. Tishchenko,
Generalized source method in curvilinear coordinates
09:45 O-5.3 K. Gehlot, A. Sharma,
Modified optimal variational method to study modal characteristics of Si photonic wire waveguides
10:00 O-5.4 M. Blome, K. McPeak, S. Burger, F. Schmidt,
Back-reflector optimization in thin-film silicon solar cells by rigorous FEM light propagation modeling

Saturday, 10:45 – 12:00: *Metamaterials & nanostructures*

10:45 O-6.1 F. Lederer, S. Muhlig, C. Rockstuhl, R. Alaee, C. Menzel (invited),
Tailoring meta-atoms for specific metamaterial applications
11:15 O-6.2 J. Benedicto, E. Centeno, A. Moreau,
Lens equation for flat lenses made with hyperbolic metamaterials
11:30 O-6.3 S. Bin Hasan, C. Etrich, R. Filter, C. Rockstuhl, F. Lederer,
Tailoring the quadratic response of nanoantennas: use of a waveguide model
11:45 O-6.4 P.J. Compaijen, V.A. Malyshev, J. Knoester,
Transmission of optical excitations through a linear chain of metal nanoparticles in the presence of a reflector

Saturday, 13:00 – 14:15: *Physical phenomena*

13:00 O-7.1 J.L. O'Brien & collaborators (invited),
Integrated quantum photonics
13:30 O-7.2 W.L. Vos (invited),
Looking in and through opaque material
14:00 O-7.3 A.V. Tishchenko, O. Parriaux,
Intriguing relations between "pseudo-Brewster incidence" and the plasmon mode at a metal surface

Saturday, 14:45 – 16:00: *Plasmonics*

14:45 O-8.1 Z. Han, S.I. Bozhevolnyi (invited),
Modelling of plasmonic waveguides
15:15 O-8.2 W. Walasik, Y. Kartashov, G. Renversez,
Plasmon-soliton waves: towards realistic modelling
15:30 O-8.3 P. Kwiecien, J. Ctyroky, I. Richter,
Hybrid dielectric plasmonic slot guiding nanostructures — analysis with Fourier modal methods
15:45 O-8.4 A. Alparslan, Ch. Hafner,
Analysis of layered media plasmonic waveguides by Multiple Multipole Program

Abstracts

Three-dimensional finite-difference time-domain (3D-FDTD) methods for photonic crystal lasers, solar cells and quantum nanophotonics

Pablo A. Postigo

[1]*IMM-Instituto de Microelectrónica de Madrid (CNM-CSIC), Isaac Newton 8, PTM, E-28760 Tres Cantos, Madrid, Spain.*

* pabloaitor.postigo@imm.cnm.csic.es

We have used the three-dimensional finite-difference time-domain (3D-FDTD) method to design new optoelectronic devices based in two-dimensional photonic crystals. Two–dimensional photonic crystals have the big advantage of being highly compatible with many optoelectronic devices, allowing for a high control of the light in the nanoscale. Here we will present the 3D-FDTD method for 1) the design of photonic crystal lasers with low threshold and high quality factor [1], 2) simulations of the strong coupling regime in a photonic crystal cavity for quantum photonics [2] and 3) the design of photonic crystals for efficient light trapping in solar cells [3].

References

[1] I. Prieto, L. E. Munioz-Camuniez, J. Canet-Ferrer, A. Gonzalez-Taboada, J.M. Ripalda, G. Muñoz-Matutano, J. Martinez-Pastor and P. A. Postigo, *Room temperature lasing at 1.3 microns in GaAs-based photonic crystal cavities with a single layer of InAsSb quantum dots*, 31st ICPS 2012, Zurich, Switzerland, 2012.

[2] J. M. Llorens, I. Prieto, L. E. Muñoz, and P. A. Postigo, *FDTD description of strong coupling regime in InP photonic crystal microcavity*, Optics of Excitons in Confined Systems (OECS12), Paris, 2011

[3] J. Buencuerpo, L. E. Munioz-Camuniez, M. L. Dotor, and Pablo A. Postigo, *Optical absorption enhancement in a hybrid system photonic crystal – thin substrate for photovoltaic applications*, Optics Express 20, A452-A464 (2012)

Resonances in high-contrast gratings with complex unit cell topology

Milan Maksimovic
Focal Vision and Optics, Oldenzaal, The Netherlands
milan.maksimovic@focal.nl

We analyze origin and properties of the spectral resonances in sub-wavelength high-contrast gratings with complex unit cell topology. We show examples of novel resonances absent from the spectrum of simple periodic structures. Our results can be used as an initialization step in the grating topology optimization.

Summary

High-contrast gratings (HCGs) are the ultra-thin elements with the period smaller than the wavelength and with the high-index grating material fully surrounded by low-index material. Recently a plethora of novel applications emerged utilizing HCGs e.g.: ultra-broadband high reflectivity mirrors, high-quality-factor resonators, wavefront phase control for planar focusing reflectors and lenses [1]. We specialize to analysis of the high-quality factor resonances in the transmission or reflection spectrum using standard rigorous coupled wave analysis (RCWA) for numerical simulations. First, we investigate spectral response of systematically perturbed periodic HCGs with otherwise simple periodic topology. We show that the spectral response of HCGs is robust to the symmetric perturbations (e.g. periodic defects in the topology), while asymmetric perturbations introduce significant changes to the spectral response. Second, we analyze origin and properties of the spectral resonances in HCGs with the complex unit cell topology fixed as a particular generation of a deterministic aperiodic sequence (e.g. Thue-Morse, see [2]). We choose the global period to be smaller than the wavelength to preserve sub-wavelength nature of HCGs. Spectral response reveals a highly fragmented resonance features displaying hierarchical structure with some of the spectral resonances not present in the case of HCGs with simple unit cell topology (see Figure below). These topics are scarcely explored in the literature on HCGs. Our analysis points to a systematic way to utilize new degrees of freedom in tailoring spectral response of HCGs similar to approaches used in the field of photonic quasi-crystals [2]. Moreover, our methodology and analysis can be used for selection of the efficient initial topology for the design and the topology optimization of the finite aperiodic HCGs.

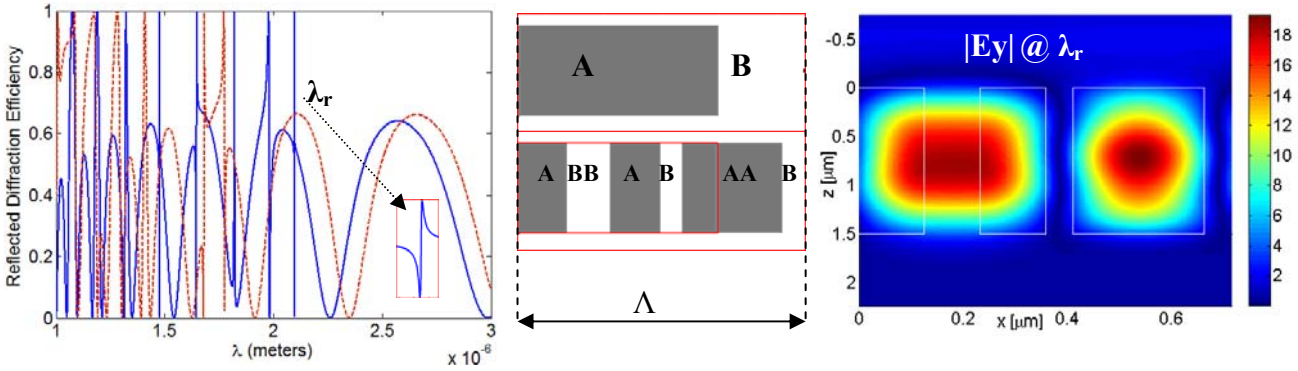

Spectral reflection response for TE –polarization (left) of HCG with the simple (dashed) and complex (solid)unit cell topology. Grating topology (center) for simple (center: top) and complex (center: bottom) unit cell with the high index bars of refractive index 3.48 (labeled A) embedded in air with refractive index 1 (labeled B). Parameter of gratings: height=1.494μm, period Λ=0.716 μm and duty cycle of 0.7 for simple unit cell (parameters chosen from [1] to enable comparison). Complex unit cell topology follows the 3rd generation Thue–Morse sequence (ABBABAAB) with the same global period and preserves volumetric content of the high and low index material as in the case of the simple unit cell Modulus of the electric field (right) in the complex unit cell at the resonance wavelength λ_r=2.0968 μm with nearly perfect reflection (boundaries show region with the high index material).

References

[1] C. J. Chang-Hasnain and W. Yang, *Advances in Optics and Photonics,* (4) 379, 2012
[2] E. Macia**,** *Reports on Progress in Physics*, (75) 036502, 2012

Radial Basis Function Neural Network Based Optimization Approach for Photonic Devices

Dalia D. El-Mosalmy[2], Mohamed Farhat O. Hameed[1], Nihal F. F. Areed[1], S. S. A. Obayya[1*]

[1]*Centre for Photonics and Smart Materials, Zewail City of Science and Technology, Sheikh Zayed District, 6th of October City, Giza, Egypt. * sobayya@zewailcity.edu.eg*

[2] *Faculty of Engineering, Mansoura University, Egypt*

A novel optimization technique based on radial basis function artificial neural network is proposed for designing photonic devices. The robustness of the suggested approach is demonstrated through the numerical precision and fast convergence of the design cycle performed on a slanted rib waveguide polarization rotator.

Analysis and Simulation Results

Our aim is to find an accurate method to optimize and design photonic devices with high accuracy and short computational time. The suggested approach relies on the use of radial bases function based artificial neural network (RBF-ANN) which shows excellent performance, and rapid convergence in comparison with conventional artificial neural network (ANN) technique. The RBF-ANN as shown in Fig. 1 consists of three layers, input, hidden and output layers. The RBF-ANN uses Gaussian transfer function as radial basis function in the hidden layer. The suggested approach is used for design and analysis of photonic devices such as passive polarization rotator (PR) based on slanted rib waveguide as shown in Fig.2 to obtain high conversion ratio with small device length. Therefore, it is required to maximize the ratio between the conversion ratio and the device length. In the RBF-ANN approach, the full vectorial finite difference method (FVFDM) and full vectorial finite difference beam propagation method (FVFD-BPM) to obtain the conversion lengths L_C and maximum conversion powers P_{max}, simultaneously of the studied PR with different rib refractive indices and with different slant angles θ within a certain range of wavelengths. The calculated values of the ratio $R= P_{max}/ L_C$ are used in the training process of the RBF-ANN. Therefore, the input layer of the RBF-ANN has three neurons in order to define the input parameters λ, rib refractive index n_g, and slant angle θ. The three input parameters and interconnection weights are processed by a summation function and passed first to the transfer function in the hidden layer and then to the output layer. The output layer contains only one neuron in order to define the required parameter, R. The trained RBF-ANN can then be used to evaluate the ratio R accurately for a given rib refractive index at a specific wavelength and slant angle θ within the trained data range. Consequently, PR structure can be obtained at the desired wavelength λ with maximum ratio R at which maximum power conversion and minimum conversion length occur. The radial basis function provides a rapid and an accurate learning process. This approach overcomes the meshing problems and time consuming of other numerical modelling methods. In addition, the numerical results of the proposed approach are in excellent agreement with that of the FVFDM and FVFD-BPM which proves the robustness of the suggested approach. More results will be presented in the conference.

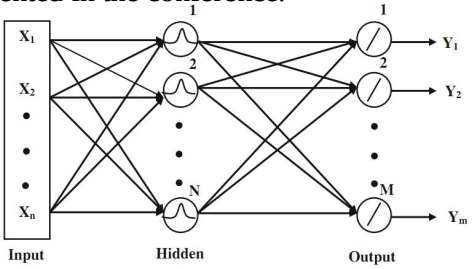

Fig.1 Schematic diagram of the RBF-ANN

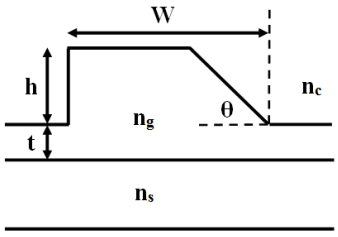

Fig.2 Schematic representation of a single-section PR

Calculation of leaky-wave radiation from compound binary grating waveguides

C. Kluge [1], L.T. Neustock [1], J. Adam [1,2], M. Gerken [1]

[1] *Institute of Electrical and Information Engineering, Christian-Albrechts-Universität zu Kiel, Kiel, Germany*
[2] *Electrical Engineering Department, University of California, Los Angeles, USA*
ckl@tf.uni-kiel.de

We present and validate rigorous coupled-wave calculations of waveguide binary gratings with multiple space-frequencies generated by superposition of different grating pitches. In the leaky-wave radiation pattern, the grating components produce pronounced directions.

Summary

In organic light-emitting diodes (OLEDs), high-index layer structuring is used to increase guided light outcoupling efficiency. Waveguide corrugation design is important to control the radiation pattern [1]. A single-pitch grating leads to sparse angle-dependent outcoupling peaks, which is potentially undesirable, e.g., in lighting applications. We investigate compound binary gratings combining two or more binary gratings with different pitches by logical disjunction [2]. We implemented a rigorous coupled-wave analysis (RCWA) [3] to find the leaky modes' complex propagation constants in a corrugated waveguide geometry (inset Fig. 1) and calculate the leaky-wave radiation without external excitation. The results are validated by finite-difference time-domain (FDTD) simulations (Fig. 1).

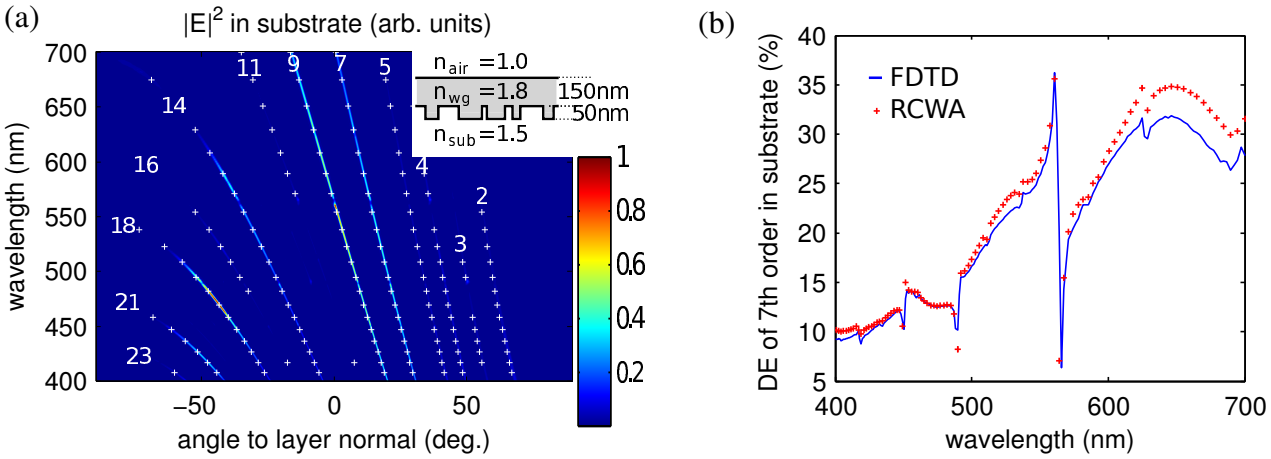

Fig. 1. The waveguide-to-substrate TE0 leaky-wave radiation, with a 350nm and 450nm pitch compound binary grating (total pitch 3150nm), shows good agreement between FDTD (background; solid line) and RCWA (crosses) calculations. (a) FDTD electric field intensity simulation, superimposed with RCWA diffraction angles. Numbers indicate the diffraction order. The 7th and 9th order correspond directly to the 450nm and 350nm grating component diffraction angles, respectively, and show the highest intensity over a wide wavelength range. (b) Exemplarily shown 7th order diffraction efficiency (DE).

References

[1] U. Geyer, J. Hauss, B. Riedel, S. Gleiss, U. Lemmer, and M. Gerken. *J. Appl. Phys.*, 104(9):093111, 2008.
[2] C. Kluge, M. Rädler, A. Pradana, M. Bremer, P.-J. Jakobs, N. Barié, M. Guttmann, and M. Gerken. *Opt. Lett.*, 37(13):2646, 2012.
[3] M. Moharam, E. Grann, D. Pommet, and T. Gaylord. *J. Opt. Soc. Am. A*, 12(5):1068, 1995.

Theory of Lasing Resonators: Quality Factor and Line Width

M. Pollnau[1,*], M. Eichhorn[2]
[1] *MESA+ Institute for Nanotechnology, University of Twente, Enschede, The Netherlands*
[2] *Institut Franco-Allemand de Recherches de Saint-Louis, Saint-Louis, France*
* m.pollnau@utwente.nl

This paper defines the quality factor of a continuous-wave laser and relates it to the laser line width.

The contradiction

The *Q*-factor of a passive resonator is defined as the energy stored in the resonator, E_{stored}, over the energy lost per oscillation cycle, E_{lost},

$$Q_c = 2\pi \frac{E_{stored}(t)}{E_{lost}(t)} = 2\pi \frac{\phi(t)}{-\frac{1}{\nu}\frac{d}{dt}\phi(t)} = 2\pi\nu\tau_c .$$

Here, the energy $E = h\nu V_{mode}\phi$ relates to the density ϕ of photons in the resonator via the single-photon energy $h\nu$ at frequency ν and the resonator mode volume V_{mode}. A Fourier transformation, resulting in

$$\tau_c = \frac{1}{2\pi\Delta\nu_c} ,$$

relates the photon decay time τ_c to the resonator line width $\Delta\nu_c$.

Current laser theories start from the assumption that in the resonator the gain equals the losses, i.e., the resonator losses quantified by the photon decay time τ_c are fully compensated by the generation of identical copies of photons in the resonator via stimulated emission. Consequently, there is no energy lost, $E_{lost} = 0$, and the *Q*-factor Q_L of a lasing resonator becomes infinitely high or is considered to be undefined. On the other hand, according to the derivation by Gordon, Zeiger, and Townes [1] for the microwave regime and its adaption to the optical regime by Schawlow and Townes [2] the laser line width is finite, thus resulting in a finite *Q*-factor,

$$Q_L = \frac{\nu}{\Delta\nu_L} .$$

The solution

By systematically including spontaneous emission into the calculation, we show that the *Q*-factor of a lasing resonator is finite, because the gain becomes smaller than the losses and, consequently, any coherent state inside the laser resonator decays with half the coherence time of the emitted laser light. The Schawlow-Townes line width of a laser is then straight-forwardly derived.

References

[1] J. P. Gordon, H. J. Zeiger, C. H. Townes, *The maser—New type of microwave amplifier, frequency standard, and spectrometer*, Phys. Rev. **99**, 1264–1274 (1955)

[2] A. L. Schawlow, C. H. Townes, *Infrared and optical masers*, Phys. Rev. **112**, 1940–1949 (1958)

Nonlinear and gain simulation in waveguide systems: methods and applications

A. Liu[1*], J. Pond[1]
[1] Lumerical Solutions, Inc, *Vancouver, BC, Canada*
* aliu@lumerical.com

We demonstrate how Lumerical's nonlinear material models, in combination with linear dispersion models, enable accurate modeling of nonlinear and gain phenomena in SOI waveguides and other systems. Examples include soliton propagation in waveguides, four-wave mixing, and lasing.

Simulation methodologies, the material plugin framework and anisotropy

As more complex nonlinear functionality is considered in waveguide systems [1], it is important to develop methods for omnidirectional propagation with arbitrary scattering. We show how a combination of eigenmode analysis and FDTD simulations can be used to model nonlinear effects in bidirectional and omnidirectional guided wave components by including an arbitrary polarization (or magnetization) update which can be added to any existing linear dispersive material. This polarization update is introduced using an open plugin framework. Nonlinear $\chi^{(2)}$, Raman and Kerr $\chi^{(3)}$, and four-level two-electron models with customizable source code have been created, and other models can be easily added and modified. Anisotropic nonlinear terms can be handled by performing a local unitary transformation to update the polarization in a reference frame where the nonlinearity is isotropic, such as one aligned with the crystalline axes [2].

Soliton propagation in SOI systems, four-wave mixing (FWM), gain models and lasing

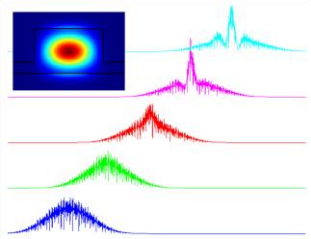

Soliton formation for the waveguide shown in the inset [3].

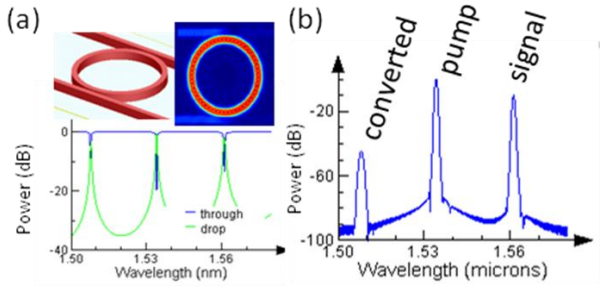

FWM in an SOI ring similar to a design in InP [4]. (a) Linear through and drop power. (b) Spectrum showing the pump, signal and converted light.

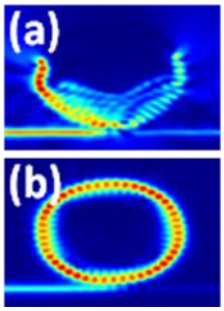

The field at 18ps (a) and 45ps (b) in a micro-disk laser as the mode is established

References

[1] Q. Lin, O.J. Painter, G. Agrawal, *Nonlinear optical phenomena in silicon waveguides: Modeling and Applications*, Opt. Express **15**, 16604-16644, 2007

[2] U.S. Patent Application No. 61/650,774, Unpublished (filing date May 23, 2012) (James Pond, applicant)

[3] V.M.N. Passaro, F. De Leonardis, *Solitons in SOI Optical Waveguides*, Adv. Studies Theor. Phys., **2**, 769-785, 2008

[4] C. Koos, M. Fujii, C.G. Poulton, R. Steingrueber, J. Leuthold, W. Freude, *FDTD-Modelling of Dispersive Nonlinear Ring Resonators: Accuracy Studies and Experiments*, IEEE J. of Quantum Electronics, **42**, 1215–1223, 2006

Hybrid III-V Semiconductor/Silicon Three-Port Filter on 1D-PhC Wire

S. Malaguti[1*], G. Bellanca[1], A. Bazin[2], F. Raineri[2], R. Raj[2], S. Trillo[1]
[1]*Department of Engineering, University of Ferrara, Via Saragat 1, 44122 Ferrara, Italy*
[2]*Laboratoire de Photonique et de Nanostructures, CNRS, Marcoussis, France*
*stefania.malaguti@unife.it

In this work we report on the design of a three port channel drop filter at 1550 nm on InP embedded on SOI substrate. The structure is built with two cavities realized on a 1D-PhC wire and properly coupled to exploit the resonant-tunneling reflection-feedback effect. A suitable mirror on the drop photonic wire waveguide has also been used to maximize the drop efficiency. The structure is fed through a silicon wire, vertically coupled with the 1D-PhC double-cavity structure. Simulation results will be compared with measurements.

Introduction

Heterogeneous integration of III-V semiconductors on Silicon is one the key technology for next-generation on-chip optical interconnects. This technology, in fact, enables the realization of sources [1], detectors [2] and control circuits [3] on the same chip by combining the superior silicon waveguiding capabilities with the efficient stimulated emission properties of direct band-gap of III-V materials.

Results

A sketch of the proposed Si/III-V semiconductor three-port filter is represented on the left side of Fig. 1. The bus is realized with a Si waveguide on a silica substrate embedded in BCB. InP photonic wires embedded in silica, on the contrary, are used for the double cavity and bus waveguide. Preliminary results illustrated on the right side of Fig. 1 report good drop efficiency (78%) and extinction ratio (-21dB). The 3dB linewidth of the proposed filter is of about 2.2 nm.

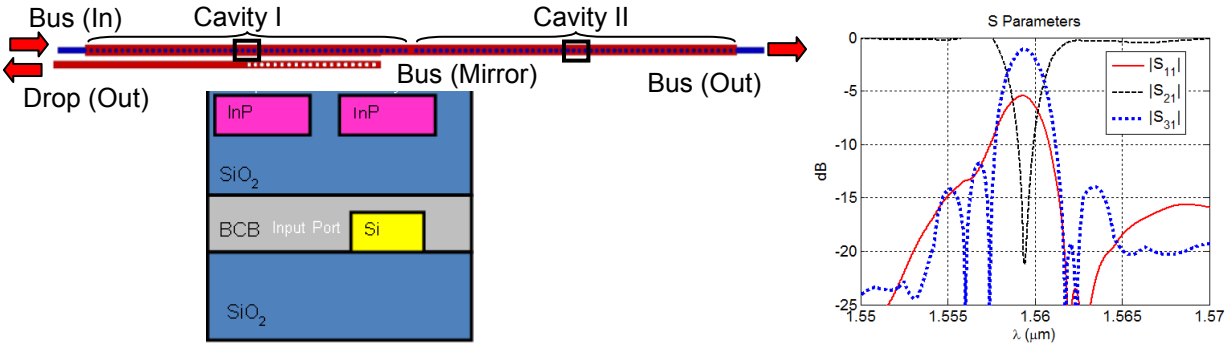

Fig. 1 On the left: sketch of the proposed device. Top view of the double cavity structure coupled with the bus waveguide and lateral view of the layered structure in vertical direction. On the right: S parameters computed by 3D-FDTD of the filter as a function of the wavelength. S_{11}: reflection coefficient at the input port; S_{21} transmission trough the bus; S_{31} transmission through the drop port.

References

[1] Y. Alioua et al., *Hybrid III-V semiconductor/silicon nanolaser*, Optics Express, Vol. 19, No. 10, 2011.

[2] L. Ottaviano et al., *High-speed photodetectors in a photonic crystal platform*, CLEO (CM1A), San Jose, California, May 6 (2012).

[3] S. Combrié et al., *Demonstration of Optically Controlled re-Routing in a Photonic Crystal Three-Port Switch*, IPRSN, Colorado Springs, CO, USA, 17th June 2012.

Full-vector analysis of photonic structures with a balance of loss and gain

J. Čtyroký
Institute of Photonics and Electronics AS CR, v.v.i., Prague, Czech Republic
ctyroky@ufe.cz

Waveguide structures with a balance of loss and gain are still more frequently discussed in the photonic community not only as photonic analogues of quantum-mechanical systems with parity-time symmetry (breaking), but also as components with potentially interesting technical applications. In this contribution we study the properties of gain/loss structures in full-vector approach, and consider also some more general cases of permittivity distribution exhibiting the behaviour analogous to *PT*-symmetry breaking.

Waveguide structures with a balance of loss and gain

Peculiar features of optical wavegide structures with a balance of loss and gain have been analyzed already more than 15 years ago [1]. Only comparatively recently these structures become rather popular as photonic analogues of quantum-mechanical systems with parity-time (*PT*) symmetry [2-4]. Since then, a number of other studies, mostly theoretical, have been published. In our first paper [1] we showed the existence of the critical (branching) point on the dispersion curves of the two-mode structure with permittivity distribution satisfying the relation $\varepsilon(-x) = \varepsilon^*(x)$ in the 2D, i.e., essentially scalar approximation. In this contribution we show that the basic character of gain/loss structures – the existence of a critical gain/loss value at which the behaviour of the structures is dramatically changed – is fully retained also in the 3D full-vector case, and to some extent also in a more general case of 2D permittivity distribution retaining the symmetry of the type $\varepsilon(-x,y) = \varepsilon(x,-y) = \varepsilon^*(x,y)$.

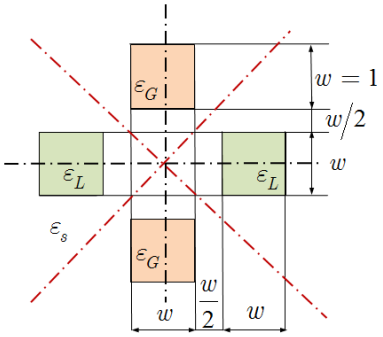

Figure 1. The cross section of the waveguide structure

Just as an example of the latter structure we briefly discuss results of the full-vector numerical analysis [5] of a 4-channel waveguide structure shown in Fig. 1. If each individual channel supports propagation of 2 (degenerate) modes of different polarizations, four from the total of 8 modes propagate without any singularity on the dispersion curves and exhibit either loss or gain, while the other four modes create two pairs of modes that exhibit the behaviour analogous to the "*PT* symmetry breaking". Weak perturbation of the gain/loss balance results in a rather smooth modification of the dispersion curves similar to the 2D case. Other cases will be discussed, too.

References

[1] H.-P. Nolting, G. Sztefka, M. Grawert, and J. Čtyroký, "Wave Propagation in a Waveguide with a Balance of Gain and Loss," in *Integrated Photonics Research '96*, Boston, USA, 1996, pp. 76-79.

[2] R. El-Ganainy, K. G. Makris, D. N. Chrisodoulides, and Z. H. Musslimani, "Theory of coupled optical PT-symmetric structures," *Optics Letters*, vol. 32, pp. 2632-2634, 2007.

[3] K. G. Makris, R. El-Ganainy, and D. N. Chrisodoulides, "Beam Dynamics in PT Symmetric Optical Lattices," *Physical Review Letters*, vol. 100, pp. 103904(1)-103904(4), 2008.

[4] C. E. Ruter, K. G. Makris, R. El-Ganainy, D. N. Christodoulides, M. Segev, and D. Kip, "Observation of parity-time symmetry in optics," *Nature Physics*, vol. 6, pp. 192-195, 2010.

[5] J. Čtyroký, "3-D Bidirectional Propagation Algorithm Based on Fourier Series," *J. Lightwave Technol.*, vol. 30, pp. 3699-3708, 2012.

Magneto-optical Nonreciprocal Devices on Silicon

T. Mizumoto* and Y. Shoji
Department of Electrical and Electronic Engineering, Tokyo Institute of Technology, Japan
** tmizumot@pe.titech.ac.jp*

Optical nonreciprocal devices such as isolators and circulators play unique roles in photonic circuits. The magneto-optic effect is important to realize the optical nonreciprocal function. In this article, magneto-optical nonreciprocal devices are discussed that are based on silicon waveguide platforms.

Introduction

The optical isolator provides one-way transmittance of light waves, which is used to prevent unwanted lightwave from launching into optically active devices. The optical circulator is important for constructing a highly functional photonic circuit. For example, it is used to build an optical add drop multiplexer together with a Bragg reflector. In an optical waveguide, it is hard to take TE-TM mode phase matching inevitable in a mode conversion isolator, which is similar to a bulk Faraday isolator. In order to overcome the difficulty, use of nonreciprocal phase shift given by a magneto-optical effect is effective especially in building nonreciprocal devices on a silicon waveguide platform.

Optical nonreciprocal devices based on magneto-optical phase shift

A magneto-optical phase shifter provides $-\pi/2$ phase difference between two interferometer arms in the rightward propagation direction and $\pi/2$ in the leftward direction, where the phase difference is measured in the upper arm with respect to the lower arm. A built-in phase bias provides a phase difference of $\pi/2$ independent of the light propagation direction. Constructive and destructive interferences occur in in the rightward and leftward directions, respectively, by combining the magneto-optical phase shift and the phase bias. An isolation of 28 dB was reported in a Mach-Zehnder interferometer (MZI) isolator, where a magneto-optical garnet Ce:YIG was directly bonded to a silicon waveguide [1].

A ring resonator equipped with a magneto-optical phase shift exhibits different resonant wavelengths depending on the propagation direction. Therefore, the transmittance in a bus line coupled with the resonator is dependent on the propagation direction at resonant wavelengths. An isolation of 20 dB was reported in a device fabricated by depositing a polycrystalline Ce:YIG on a silicon ring resonator [2].

By replacing the optical branching devices of MZI isolator with 3 dB directional couplers, a 4-port optical circulator was fabricated in a silicon nanowire waveguide with a maximum isolation of 15.3 dB at 1531 nm [3].

References

[1] Y. Shirato, Y. Shoji, T. Mizumoto, *High isolation in silicon waveguide optical isolator employing nonreciprocal phase shift*, OFC 2013, Anaheim, USA, OTu2C.5, 2013

[2] L. Bi, J. Hu, P. Jiang, D.-H. Kim, G. F. Dionne, L. C. Kimerling, and C. A. Ross, *On-chip optical isolation in monolithically integrated non-reciprocal optical resonators*, Nature Photon., 758-762, 2011

[3] K. Mitsuya, Y. Shoji, T. Mizumoto, *The first demonstration of silicon waveguide optical circulator*, OFC 2013, Anaheim, USA, JTh2A.25, 2013

Passive Polarization Rotator Based on Spiral Photonic Crystal Fiber

Mohamed Farhat O. Hameed, A. M. Heikal, S. S. A. Obayya*

*Centre for Photonics and Smart Materials, Zewail City of Science and Technology, Sheikh Zayed District, 6th of October City, Giza, Egypt. * sobayya@zewailcity.edu.eg*

A novel design of passive ultra-compact polarization rotator (PR) based on spiral tellurite photonic crystal fiber is proposed and analyzed using full vectorial finite difference approaches. The reported PR offers 97% polarization conversion ratio with ultra compact device length of 98 μm.

Simulation Results

Figure 1 shows cross section of the suggested polarization rotator (PR). The proposed design relies on using tellurite spiral PCF (TS-PCF) with eight arms and a central air hole. The central air hole of radius r_{h2} can be shifted equally in x and y directions to achieve complete polarization rotation. The first hole in each spiral arm is considered at a distance, $r_0 = r_c + r_h$ from the center where r_c and r_h are the radius of the core and cladding air holes, respectively. The distance of the second air hole of each arm from the center is taken as $r_1 = r_0 + 0.8(2r_h)$ with an angular displacement of $\theta_1 = 360^o/(2N)$, where N is the number of arms. Therefore, the n'th air hole in each arm is at a distance of $r_n = r_{n-1} + 0.8\times(2r_h)$ with an angular displacement of $\theta_n = (n\times 360^o)/(2\times N)$ from the first one. Therefore, the first, second, and third hole of each arm constitute the first, second, and third ring, respectively. In this study, r_c, r_h are taken as 0.7 μm, 0.3μm, respectively. In addition, the central hole of radius 0.25 μm is shifted equally in x and y directions by 0.36 μm. Moreover, the tellurite refractive index is fixed to 2.0278 at the operating wavelength 1.55 μm. The suggested TS-PCF PR offers polarization conversion ratio of almost 97% with a ultra compact device length of 98 μm as shown in Fig.2. The reported structure does not require a complex fabrication process like the semiconductor waveguide with slanted sidewalls. Therefore, the spiral TS-PCF PR is much shorter than single and multiple sectioned passive PRs with L-shaped core region [1] of device lengths of 1743 μm and 1265 μm, respectively. Moreover, the suggested PR is shorter than the triangular lattice silica PCF PR with device length of 206 μm [2]. More results will be presented in the conference.

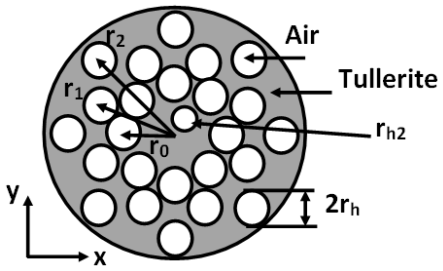

Cross section of the suggested spiral PCF PR

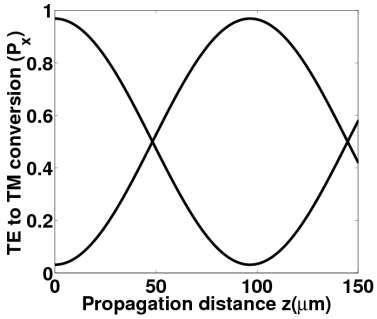

Evolution of the TM powers for the TE excitation along the propagation direction

References

[1] M. F. O. Hameed, S. S. A. Obayya, H. A. El-Mikati, and H. A. El-Mikati," Passive Polarization Converters Based on Photonic Crystal Fiber With L-Shaped Core Region " *J. of Lightwave Technol.*, vol. 30, pp. 283-289, 2012

[2] M.F.O. Hameed, Maher Abdelrazzak, S.S.A. Obayya, "Novel Design of Ultra-Compact Triangular Lattice Silica Photonic Crystal Polarization Converter", *IEEE J. Lightwave Technology*, vol. 31, no. 1, page 81-86, January 1, 2013

Enhancing Light Manipulation by Graded Index Photonic Crystal Media

B. B. Oner[1]*, M. Turduev[1], I. H. Giden[1], H. Kurt[1]
[1] *Nanophotonics Research Laboratory, Department of Electrical and Electronics Engineering TOBB University of Economics and Technology, 06560, Ankara, Turkey*

* bilgehan.oner@gmail.com

Various light manipulation scenarios including self-collimation, mode conversion, beam bending, and coupling properties of graded index (GRIN) media are explored. Specifically designed GRIN media yields impressive results with broad bandwidths that cover both lower and higher frequency regimes.

Photonic crystals (PCs) are periodic dielectric media that enable extraordinary manipulation of electromagnetic waves. Although the concept of GRIN media comprises different elemental parts from the basic PCs, combining GRIN and PC concepts enlarges the range of the photonic devices' area of usage. Refractive index profile of a GRIN medium gradually varies from point to point. Adjusting the gradient profile of the media enables one to design various integrated optical devices, such as couplers, spatial mode converters and waveguide bends [1-3]. In order to obtain the GRIN profiles, lattice spacing in the transverse direction of each cell is chosen as a variable while lattice spacing in the longitudinal directions is fixed at unit distance.

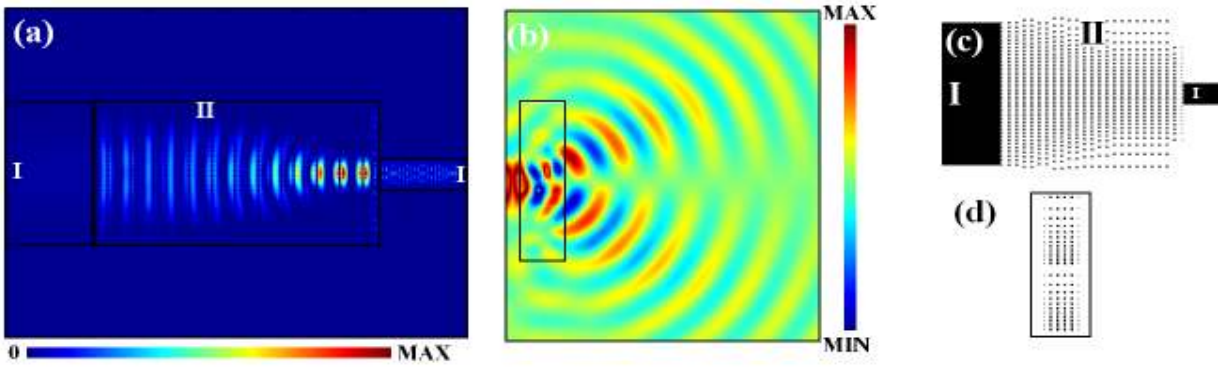

Figure 1 (a) *Intensity distribution of the GRIN PC coupler and (b) electric field distribution of GRIN PC spatial mode converter. Schematic representations of (c) GRIN PC coupler and (d) GRIN PC spatial mode converter.*

To date numerous studies about GRIN media and its' applications are reported. Nevertheless, many of them suffered from narrow bandwidth or being able to realize only for lower frequency regime. Our GRIN PC design method provides high transmission efficiency over broad bandwidth. Besides, we also realize superior property of being polarization insensitive. Fig. 1(a) demonstrates a compact optical waveguide coupler whose schematic forms is indicated in Fig. 1(c). Mode conversion process is shown in Fig. 1(b) and the corresponding schematic view is presented in Fig. 1(d). The details of the designs and optical characteristics of the inhomogeneous media will be presented in the conference.

References

[1] H. Kurt, B. Oner, M. Turduev, and I. Giden, *Modified Maxwell fish-eye approach for efficient coupler design by graded photonic crystals*, Opt. Express **20**, 22018-22033 (2012).

[2] B. Oner, M. Turduev, I. H. Giden, and H. Kurt, *Efficient mode converter design using asymmetric graded index photonic structures*, Opt. Lett. **38**, 220-222 (2013).

[3] H. Kurt and D. S. Citrin, *Graded index photonic crystals*, Opt. Express **15**, 1240-1253 (2007).

1D crossed guided mode resonant gratings for tunable filtering

A.-L. Fehrembach [1], K. Chan Shin Yu [2,3], A. Monmayrant [2,3], O. Gauthier-Lafaye [2,3], P. Arguel [2,3] and A. Sentenac [1]

[1] *Aix Marseille Université, CNRS, Ecole Centrale Marseille, Institut Fresnel, 13013 Marseille, France*
[2] *CNRS; LAAS; 7 avenue du Colonel Roche, F-31077 Toulouse, France*
[3] *Université de Toulouse, UPS, INSA, INP, ISAE; LAAS; F-31077 Toulouse, France*
anne-laure.fehrembach@fresnel.fr

We propose a narrow band, polarization independent filter tunable with respect to the angle of incidence over a 100 nm range. We explain its physical principles and show that its performances are reachable experimentally.

Guided mode resonance filters (GMRF) are composed with a planar waveguide structured with a subwavelength periodic pattern. The excitation of an eigenmode via a diffraction order leads to a resonance peak in the reflectivity spectrum of the structure. The peak can be very narrow (Q factor greater than 15000 in practice) and its centering wavelength is linearly tunable with respect to the angle of incidence. These properties are very interesting for example for imaging spectroscopy. But the peak depends strongly on the polarization of the incident wave in basic configurations.

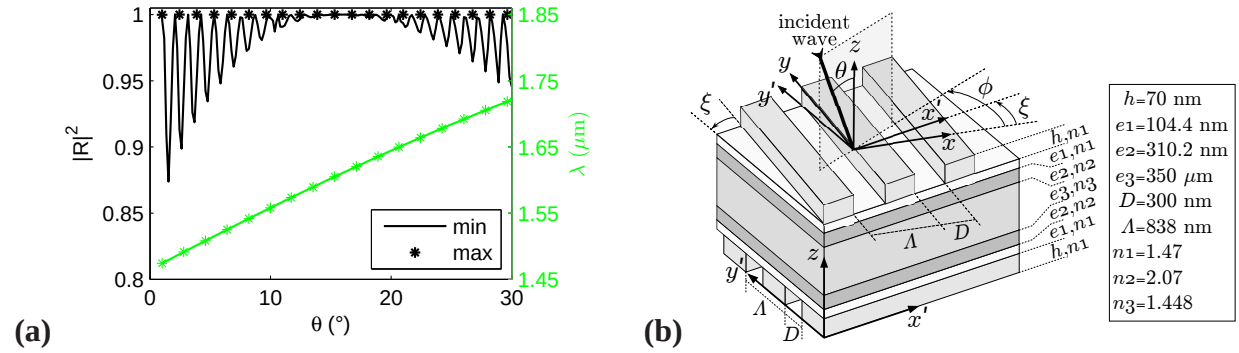

Fig. 1. (a) configuration, (b) minimum and maximum of reflectivity when the incident polarization varies, and resonance wavelength versus the polar angle of incidence.

We present a simple, yet promising configuration [1] able to generate a 0.1nm width (at 1550nm) polarization independent peak, angularly tunable over a wide range (100 nm) (see Figure (a)). The structure is composed with two identical multilayer stacks deposited on each side of a substrate, on top of which two identical 1D gratings are engraved, but with different directions of periodicity (see Figure (b)). This configuration differs from the reported configurations [2] in its basic principle, and being composed with 1D gratings, it is easier to fabricate. A prototype is into characterization process.

ACKNOWLEDGEMENT: The financial support of the CNES in this work is gratefully acknowledged.

References

[1] A. Monmayrant, O. Gauthier-Lafaye, A.-L. Fehrembach, K. Chan Shin Yu, A. Sentenac, P. Arguel, and J. Loesel. Filtre optique a reseaux resonnants insensible a la polarisation accordable en fonction de langle dincidence, 2011.

[2] A.-L. Fehrembach and A. Sentenac. Study of waveguide grating eigenmodes for unpolarized filtering applications. *J. Opt. Soc. A.*, 20:481–488, 2003.

COLLECTIVE OPTICAL EXCITATIONS IN SELF-ASSEMBLED MOLECULAR NANOTUBES FOR LIGHT-HARVESTING

Jasper Knoester[1]

[1] *Zernike Institute for Advanced Materials, University of Groningen, Nijenborgh 4, 9747 AG Groningen The Netherlands*
E-mail: j.knoester@rug.nl

Self-assembly is a promising route towards designing new nanoscale functional materials. In this talk, I will address self-assembled systems consisting of thousands of dye molecules with optical functionality. The collective optical excitations in such systems are Frenkel excitons. Their static and dynamic properties are responsible for the optical response of the aggregate. The excitons are governed by a complex interplay between intermolecular resonance interactions that delocalize the excitations and interactions with slow and fast degrees of freedom in the environment that lead to static and dynamic disorder, which counteract exciton delocalization and cause decoherence. Optical properties of special interest are motional narrowing, exciton superradiance, strong optical nonlinearities, and ultrafast energy transport. While these properties are interesting in their own right, they also may be used for applications, for instance in artificial light-harvesting systems and all-optical switches.
In this talk, I will focus in particular on tubular aggregates [1], which currently attract much attention. These systems, consisting, for instance, of cyanine molecules [2] or porphyrin derivatives [3], have recently attracted strong attention. They closely resemble in size (diameter approx 10 nm, length up to microns) and properties antenna systems that occur in bacterial light-harvesting systems. I will report on joint experimental-theoretical studies of the exciton dynamics and the resulting optical response of such aggregates [1-4]. Near-field optical experiments as well as various ensemble measurements can be well explained using phenomenological modeling and yield a model for the microscopic structure of the aggregate. Current research aiming at a first-principles modeling of the structure and optics of molecular aggregates will be introduced.

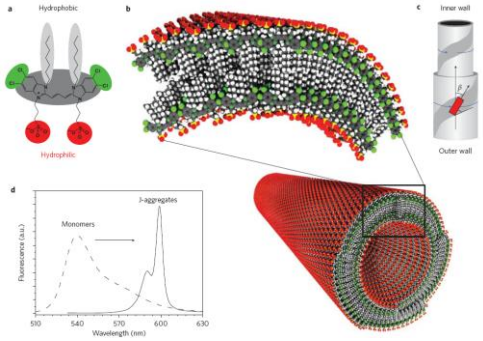

Figure: Double-walled aggregate of the amphiphilic cyanine dye C8S3, with fluorescence spectrum [2].

[1] C. Didraga, J.A. Klugkist, and J. Knoester, J. Phys. Chem. B **106**, 11474 (2002).
[2] D.M. Eisele, J. Knoester, S. Kirstein, J.P. Rabe, and D. Vanden Bout, Nature Nano **4**, 658 (2009).
[3] S.M. Vlaming, R. Augulis, M.C.A. Stuart, J. Knoester, and P.H.M. van Loosdrecht, J. Phys. Chem. B **113**, 2273 (2009); A. Stradomska and J. Knoester, J. Chem. Phys. **133**, 094701 (2010).
[4] D.M. Eisele, …, J. Knoester, J.P. Rabe, and D.A. Vandenbout, Nature Chemistry **4**, 655 (2012).

Decomposition of Mie scattering coefficients and polarizabilities of nanoshell structures into Lorentzian resonances

V. Grigoriev*, A. Tahri, S. Varault, B. Rolly, B. Stout, J. Wenger, N. Bonod
Institut Fresnel, CNRS, Aix Marseille Université, Ecole Centrale Marseille, Marseille, France
* victor.grigoriev@fresnel.fr

The analytical properties of the scattering matrix are applied to explain the frequency response of nanoshell structures. Their polarizabilities are decomposed exactly into resonances of Lorentzian shape regardless of material dispersion and nonlocal effects, if the size of particles becomes comparable to wavelength of light.

Coupled oscillator models for nanostructures

The ability to engineer the resonant properties of nanoparticles helps to strengthen their interaction with light, which is of utter importance for a number of practical applications. Such engineering is usually achieved by hybridization of plasmonic modes in nanoshell structures [1]. Nevertheless, the models based on coupled oscillators do not establish a firm link between the resonant properties of the structures and their actual frequency response. In particular, they do not treat consistently the excitation of multiple resonances and ignore nonlocal effects caused by the retardation of the signals.

Perfectly emitting and absorbing modes as a uniform basis for decomposition

We show that the frequency response of nanoshell structures can be completely restored from the analytical properties of the scattering matrix $S(\omega) = a_{\text{out}} / a_{\text{in}}$, which relates the amplitudes of outgoing a_{out} and incoming a_{in} spherical waves. The resonances reveal themselves as poles ω_r^- and zeros ω_r^+ of the *S*-matrix, so that the application of the Weierstrass factorization theorem gives

$$S(\omega) = A\exp(iB\omega)\prod_{r=-\infty}^{+\infty}\frac{\omega-\omega_r^+}{\omega-\omega_r^-} = A\exp(iB\omega)\left[1+\sum_{r=-\infty}^{+\infty}\frac{\sigma_r}{\omega-\omega_r^-}\right],$$

where the constants A and B are responsible for the external retardation effects, and the residues σ_r describe the strength of the Lorentzian resonances. All other spectra can be expressed in terms of the *S*-matrix, including the Mie coefficients $M = (S-1)/2$ and polarizabilities $\alpha \sim M$. An example of such decomposition is shown in the figure below. This approach offers new opportunities for the design of metamaterials, coherent absorbers, superscatterers and nanoantennas.

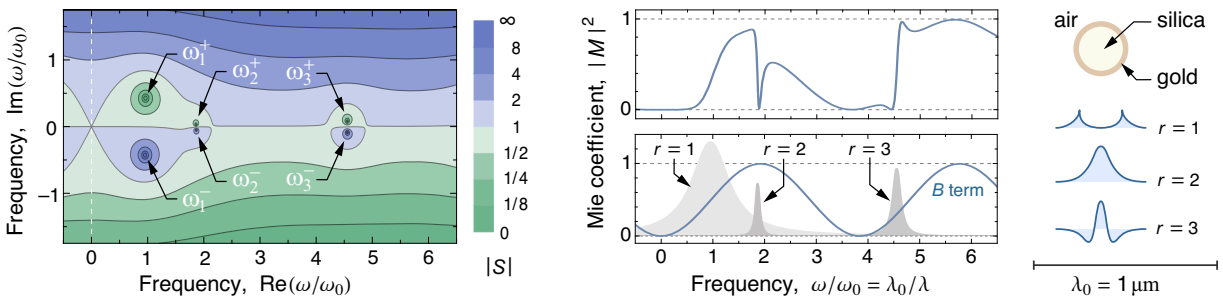

A contour plot of S-matrix (electric dipole) in the complex frequency plane. Spectrum of the Mie coefficient and its decomposition. A schematic picture of the nanoshell structure and its modes.

References

[1] E. Prodan, C. Radloff, N. J. Halas, and P. Nordlander, Science **302**, 419 (2003).

Extraordinary Optical Transmission Through Circular Metallic Cylinder Arrays

Shichang She, Ya Yan Lu

Department of Mathematics, City University of Hong Kong, Kowloon, Hong Kong
shichashe2@student.cityu.edu.hk

Light transmission through arrays of circular metallic cylinders with subwavelength gaps is analyzed theoretically. Features of the the transmission spectra are explained using band structures, a single Bloch mode model and complex-frequency resonant modes.

Introduction

The phenomenon of extraordinary optical transmission (EOT) through subwavelength apertures in metal films has been intensively investigated by many authors. We consider periodic arrays of circular metallic cylinders, and theoretically analyze light transmission through the metallic cylinder arrays. Numerical results indicate that high transmission is possible even when the gaps between nearby cylinders are much smaller than the wavelength. In particular, the transmitted light may carry much more power than the fraction of incident light illuminated directly on the gaps. Moreover, high transmission is concentrated on two wavelength intervals.

Results

We consider N one-dimensional arrays of circular silver cylinders (radius $r = 225$nm) arranged on a square lattice (lattice constant $a = 500$nm) and surrounded by air, where each array is infinite and periodic in the x direction. The gap between two nearby cylinders is $d = 50$nm. The case for $N = 3$ is shown in the figure below (left panel). For a normal incident plane wave in the H polarization, the

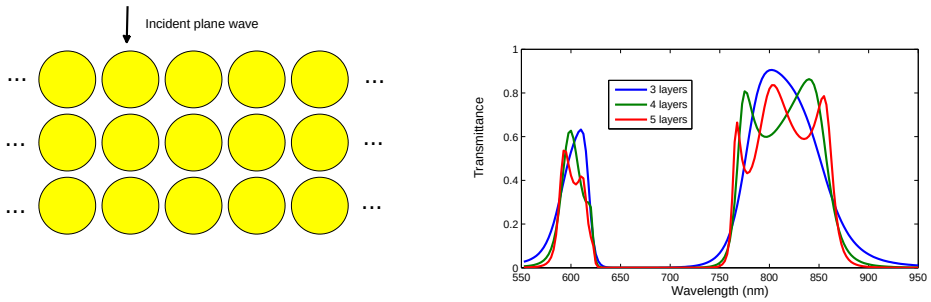

transmission spectra for a few values of N are given in the right panel of the figure. Notice that high transmission is only possible in two wavelength intervals. For some wavelengths the transmittance is more than 80% while the gap-period ratio d/a is only 0.1.

To understand the unusual light transmission behavior through the metallic cylinder arrays, we perform additional computations concerning band structures, Bloch modes, and complex frequency resonant modes. These results allow us to explain the location of two high transmission intervals, to develop a single mode theory based on the leading Bloch mode, and to explain a transmission peak as a resonant-tunneling effect.

Electromagnetically Induced Transparency with Hybrid Silicon-Plasmonic Traveling-Wave Resonators

Dimitra A. Ketzaki*, Odysseas Tsilipakos, Traianos V. Yioultsis, Emmanouil E. Kriezis
Department of Electrical and Computer Engineering, Aristotle University of Thessaloniki, Greece
* dketzaki@auth.gr

Spectral filtering and electromagnetically induced transparency (EIT) with hybrid silicon-plasmonic traveling-wave resonators are theoretically investigated. The rigorous three-dimensional vector finite element method (3D-VFEM) simulations are complemented with temporal coupled mode theory (CMT).

Introduction

Hybrid plasmonic waveguides have recently drawn considerable attention due to the favorable compromise between mode confinement and propagation loss they offer [1]. The recently-proposed conductor-gap-silicon (CGS) waveguide [Fig. 1(a)] can be bent with sub-micron radii and is moreover compatible with standard silicon-on-insulator waveguides [2]. As a result, it is a prime candidate for building integrated nanoscale structures comprising traveling wave resonators.

Results

The filtering capabilities of CGS-based microring resonator filters are investigated by means of 3D-VFEM modeling [3]. We show that resonators with sub-micron radii can efficiently filter the lightwave with minimal insertion loss (IL < 0.2 dB) and high quality factors (Q > 120), Fig. 1(b). By cascading two slightly-detuned resonators and providing an additional route for resonator interaction, a response reminiscent of EIT is observed [Fig. 1(c)]. The transmission peak can be shaped by means of resonator detuning ($\Delta\lambda_{res}$) and resonator separation (s). For example, a resonator detuning of 15 nm, corresponding to a radius variation of approx. ±5 nm, introduces an EIT peak with a quality factor of ~250 and an IL of -3 dB (resonator separation is $s = 3\lambda_g \sim 2.5R_0$).

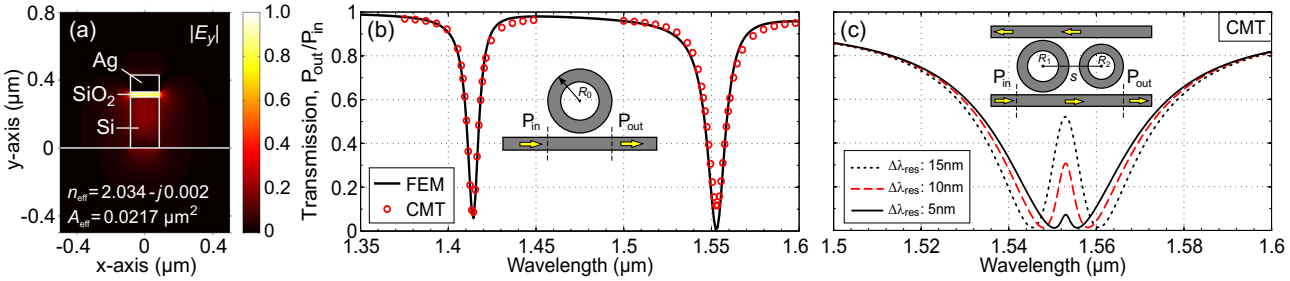

Fig. 1. (a) CGS waveguide (w = 170 nm, h = 300(Si) + 30(SiO_2) + 100(Ag) nm) and corresponding mode profile ($|E_y|$). (b) Transmission vs. wavelength for a 930-nm-radius microring resonator filter. CMT is fed with intrinsic and loaded quality factors determined from 3D-VFEM eigenvalue simulations of the coupled and uncoupled resonator, respectively. (c) EIT with two slightly detuned resonators for three detuning scenarios. Note the fundamental trade-off between peak transmission maximum and quality factor.

This work has been supported in part by the THALES Project ANEMOS, co-financed by the European Union (European Social Fund) and Greek National Funds through the Operational Program "Education and Lifelong Learning" of the National Strategic Reference Framework.

References

[1] R. F. Oulton, V. J. Sorger, D. A. Genov, D. F. P. Pile, X. Zhang, *Nat. Photon.*, **2**, 496, 2008

[2] M. Wu, Z. Han, V. Van, *Opt. Express*, **18**, 11728, 2010

[3] O. Tsilipakos, *et al.*, *Opt. Quant. Electron.*, **42**, 541, 2011

Low-Loss Splicing of Microstructured Optical Fibers and Single-Mode Fibers: An Analytical Study

Dinesh Kumar Sharma, Anurag Sharma
Physics Department, Indian Institute of Technology, New Delhi-110016, India
dk81.dineshkumar@gmail.com, *asharma@physics.iitd.ac.in*

Low-loss splicing of microstructured optical fibers (MOFs) and standard single-mode fibers (SMFs) can be achieved by enlarging the mode field diameter (MFD) of MOFs using, e.g., the controlled all air-hole collapse method. This leads to an optimum mode field match at the interface. We study analytically the splicing between such an MOF and an SMF using our analytical field model.

Introduction

The study of low-loss fusion splicing of MOFs with other types of optical fibers is essential for the practical realization of MOF based devices and sensors [1,2]. Conventional fusion splicing technologies are not usable for MOFs, as the characteristic air-holes pattern often collapses during the splicing process, which significantly increases the loss by distorting the light guiding structure of MOF near the joint interface. To overcome this problem, controlled air-hole collapse method has been used [2]. Here, we have analytically simulated interfacing of MOFs to SMFs using our earlier developed analytical field model [3].

Results and Discussion

On heating the MOF, air-holes are collapsed due to surface tension of the material and it is assumed that the total area of the MOF material remains constant, which yields the following relation [1,2];

$$\Lambda = \Lambda_0 \sqrt{\left(\sqrt{3}/2 - \pi/4\left(d_0/\Lambda_0\right)^2\right) \Big/ \left(\sqrt{3}/2 - \pi/4\left(d/\Lambda\right)^2\right)}$$

where d and Λ are the hole size and pitch of collapsed MOF, d_0 and Λ_0 are the parameters of initial MOF. Our field model based on variational method provides the optimized value of the propagation constant and the field parameters [3], which can be analytically expressed by fitting the polynomial of the 8th degree. We evaluated the splicing loss between an MOF having $d_0/\Lambda_0 = 0.612$ and $\Lambda_0 = 3.35\mu m$ and an SMF with core diameter 6.0μm, NA = 0.08 and $\Delta = 0.0154$, for $\lambda = 0.80\mu m$, using mode overlap integral. The splicing loss is 2.6dB without any air-hole collapse of MOF and with the increases of collapse ratio, we obtained the lowest loss of 0.08dB (see Fig.1). For high degree of collapse ratio the results deteriorate and the model based on three rings structure and one ring field is not adequate; one must add more number of rings in the field. Further work is in progress.

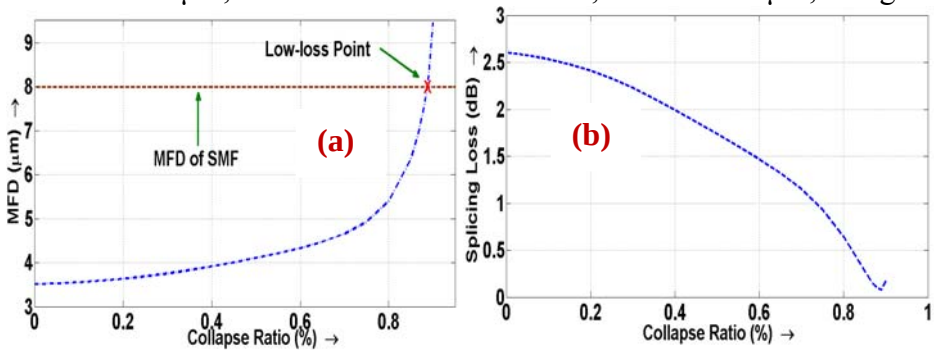

Fig.1 (a) MFD Vs collapse ratio. (b) Splicing loss Vs collapse ratio.

This work was supported by grant from the Council of Scientific and Industrial Research (CSIR), Govt. of India.

References

[1] J. Laegsgaard and A. Bjarklev, *Opt. Commun.*, **237**, 431 (2004).
[2] X. Xi, Z. Chen, G. Sun, and J. Hou, *Appl. Opt.*, **50**, E50 (2011).
[3] D.K. Sharma and A. Sharma, *OQE*, **44**, 415, (2012); also *OWTNM 2009* and *OWTNM 2012*.

Simple Analytical Approach to Optimize Structure Parameters of Photonic Crystal Waveguide Coupler

Kanchan Gehlot, Anurag Sharma

Department of Physics, Indian Institute of Technology Delhi, New Delhi 110 016, India
gehlot.kanchan@gmail.com, asharma@physics.iitd.ac.in

Simple analytical approach of optimal variational method (VOPT) is used to optimize structure parameters of a photonic crystal waveguide coupler to obtain desired power coupling ratio. In analysis of photonic crystal waveguides by VOPT, separate set of parameters are identified that control the guiding mechanism and Bragg reflections. This helps in optimizing the structure for desired application.

Summary

Optimal variational method (VOPT) [1] is based on variational principle and assumes field to be separable in two orthogonal directions. In [2], it is shown that VOPT approximates a two dimensional photonic crystal waveguide to a 1-D Bragg reflector and a multilayer slab waveguide. Reflection/transmission spectra of the structure are obtained from the Bragg reflector and modal field profile is obtained from the modes of multilayer waveguide. Analytical results obtained by VOPT are further used to optimize a photonic crystal waveguide coupler of configuration shown in Fig.1. The structure is excited asymmetrically from the input end and we find power distribution between two cores of coupler at the output. Optical field profile and the power coupling ratio predicted by VOPT method and FDTD analysis are very close.

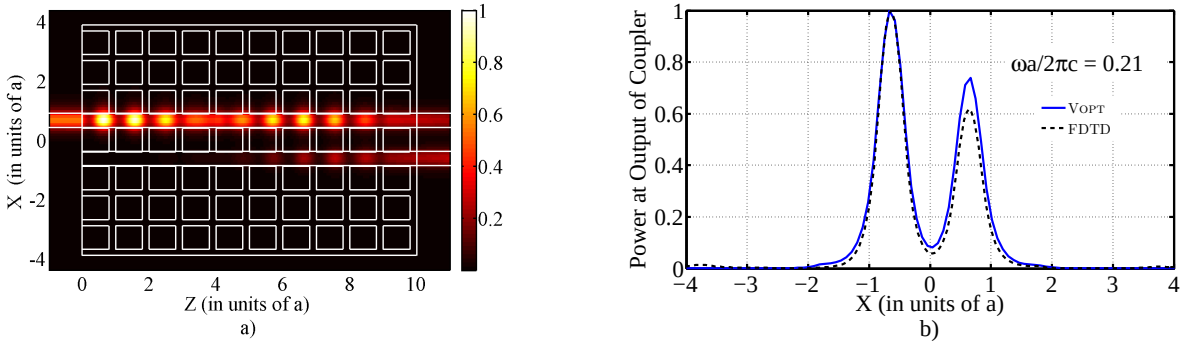

Fig. 1. a) Optical intensity profile of 2D photonic crystal waveguide coupler at normalized frequency, $\omega a/2\pi c = 0.21$, where a is the period of photonic crystal. The schematic of coupler is shown with white lines. Width of two cores of GaAs ($\epsilon = 12.96$) is $d = 0.375a$ and area of square air hole is $\pi(0.45a)^2$ b) Comparison of output intensity profile with FDTD results.

This analysis provides a simple model to understand properties of photonic crystal waveguides and devices. The analytical process reduces the computational time considerably and simplifies optimization of the structure.

This work was supported by grant from Council of Scientific and Industrial Research (CSIR), Govt. of India.

References

[1] A. Sharma, *Opt. Quant. Electron.*, **21**, 517–520 (1989)
[2] K. Gehlot, A. Sharma, *OWTNM-2012*, Barcelona, Spain, (2012)

Vertical Links for Multilayer Optical-Networks-on-Chip Topologies

A. Parini[1,3*], G. Calò[2], G. Bellanca[3], V. Petruzzelli[2]
[1]*Laboratory for Micro and Submicro Enabling Technologies of the Emilia-Romagna Region (MIST E-R), Via P. Gobetti 101, 40129 Bologna, Italy*
[2]*Dipartimento di Ingegneria Elettrica e dell'Informazione, Politecnico di Bari, Via Re David 200, 70125 Bari, Italy*
[3]*Department of Engineering, University of Ferrara, Via Saragat 1, 44122 Ferrara, Italy*
* alberto.parini@unife.it

In this work we propose two possible technological solutions that may allow the connection in the vertical direction between different layers of an Optical-Network-on-Chip (ONoC). The first solution relies on Multi-Mode Interference devices (MMI), while the second exploits a cascading between vertically stacked parallel waveguides. Comparisons in terms of efficiency, bandwidth and footprint will be reported.

Introduction

Networks-on-Chip (NoCs) can take advantage of the fully compatible CMOS silicon photonic integration to realize optical based interconnection links. In fact, optical (instead of electrical) interconnections among the different computational cores can provide a huge communication bandwidth with a favorable power budget [1]. At present, planar topologies are mainly proposed in the literature [2]. However, the inherent complexity of the optical circuitry and the constraints on the footprint lead toward the realization of vertically stacked layers, in order to avoid crossings, allow an efficient placing and routing of the different optical devices, and increase the integration density of the functional elements. In this work we design and compare two different techniques that can be used to implement vertical connections between two superposed optical layers.

Results

An MMI based solution to connect two waveguides, vertically separated by a gap of 820nm, is reported on the left panel of Fig. 1. The 3D-FDTD simulation shows an average efficiency of 90% on a 60nm band. The right panel of the figure presents an alternative strategy for the same connection, which exploits a cascaded coupling among three vertically stacked waveguides. In this second case, the Coupled Modes Theory provides an average efficiency of 97%. The existing trade-off between footprint, vertical distance and transmission efficiency must be carefully assessed.

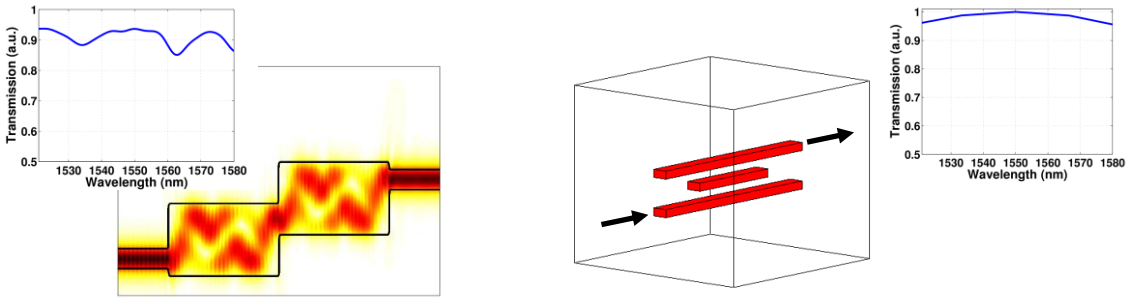

Figure 1: (Left panel) Vertical cross-section of the electrical field in the MMI based structure; the inset shows the transmission in the band 1520nm-1580nm. (Right panel) Coupled waveguides based solution: 3D sketch of the coupler and relative transmission curve.

References

[1] C. Batten et al., *Designing Chip-Level Nanophotonic Interconnection Networks*, IEEE Journal on Emerging and Selected Topics in Circuits and Systems, Vol. 2, No. 2, 2012.

[2] L. Chen et al., *Integrated GHz silicon photonic interconnect with micrometer-scale modulators and detectors*, Optics Express, Vol. 17, No. 17, 2009.

A Terahertz Waveguide Coupler with a Tapered Dual Elliptical Metal Structure

Qing Cao*, Shuang Li, Da Teng, and Hua Gao
Department of Physics, Shanghai University, 99 Shangda Road, Baoshan District, Shanghai 200444, China
**qcao@shu.edu.cn*

Abstract: A high efficient plasmon coupler is suggested for the coupling of terahertz wave from an approximate plate waveguide to a two-wire waveguide. We numerically show that the coupling efficiency of this kind of coupler can be as high as about 94%.

It was reported that the two-wire THz waveguide has the advantages of low bending loss and low attenuation [1-2]. Here, we present a new coupling structure for the highly efficient coupling from an approximate plate waveguide to a two-wire waveguide. This new coupler is composed of two tapered elliptical metal structures. As shown in Fig.1, through putting the long axis b decreases slowly, the two-ellipse structure gradually degenerates into two metal wires. As a result, the reflection can be eliminated and thus a high coupling efficiency can be obtained.

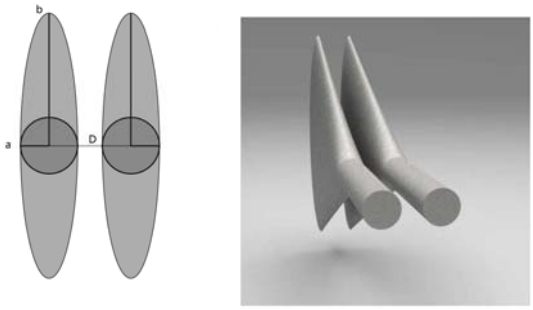

Fig.1. A tapered dual elliptical plasmon waveguide

We numerically test the coupling efficiency of the tapered dual elliptical plasmon waveguide coupler by use of the commercial software of COMSOL Multiphysics. At the output plane, each of the wires has a radius of 0.5 mm and the two wires are separated by a 2 mm distance. At the input plane, the long axes b and the short axes a are 5 mm and 0.5 mm, respectively. The coupling length l is 0.1 m. We first calculate the effective index n_{eff} of each 2-D cross-section of the tapered dual elliptical plasmon waveguide by use of the COMSOL software. We find that the mode coupling process meets the WKB approximation [3] very well. According to the WKB approximation, the coupling efficiency η can be calculated by the following formula. Through numerical calculations, we find that the coupling efficiency can be as high as about 94%.

$$\eta = \exp\left[-2k_0 \int_0^l \mathrm{Im}(n_{eff})dz\right]$$

References

[1] M. Mbonye, R. Mendis, and D. M. Mittleman, *A terahertz two-wire waveguide with low bending loss*, Appl. Phys. Lett. **95**, 233506, 2009

[2] H. Pahlevaninezhad, T. E. Darcie, and B. Heshmat, *Two-wire waveguide for terahertz*, Opt. Express **18**, 7415–7420, 2010

[3] A. Rusina, M. Durach, K. A. Nelson, and M. I. Stockman, *Nanoconcentration of terahertz radiation in plasmonic waveguides*, Opt. Express **16**, 18576–18589, 2008

Nonreciprocal waveguiding EM surfaces and structures for THz region

P. Kwieicen[1], V. Kuzmiak[2], I. Richter[1*], J. Čtyroký[2]

[1] *Czech Technical University in Prague, Faculty of Nuclear Sciences and Physical Engineering, Department of Physical Electronics, Břehová 7, 11519 Prague 1, Czech Republic*

[2] *Institute of Photonics and Electronics AS CR, v.v.i., Chaberská 57, 182 51 Praha 8, Czech Republic*

* ivan.richter@fjfi.cvut.cz

Based on combination of magnetooptic Fourier modal method (MOaRCWA) simulations and (quasi)analytical dispersion relation predictions, we have studied the magnetoplasmons in plasmonic nanostructures composed of highly-dispersive polaritonic InSb material, within the THz spectral region.

Introduction

Recently, among possible stable EM waves propagating within photonic nanostructures, surface waves constrained to the media interfaces have found an increasing scientific interest (and even application potential) in such areas as sensing, metamaterials, and nonreciprocal systems. Among these, surface plasmons polaritons (SPP) have become established in many practical areas, especially in surface plasmon resonance biosensing, waveguiding, and others [1]. One of only few possibilities how to impose nonreciprocity in these structures is to apply an external magnetic field [2] (mainly in the transverse, or Voigt configuration). In such a case, one-way (nonreciprocal) propagation of SP is not only possible but may bring many interesting phenomena in connection with magnetoplasmons (MSP) [3]. However, in order to properly simulate such MSP propagation, an appropriate numerical tools is necessary.

Results

Based on our previous studies [4], we have developed an efficient 2D numerical technique based on MO aperiodic rigorous coupled wave analysis (MOaRCWA). In our in-house tool, the artificial periodicity is imposed within a periodic 1D RCWA method, in the form of the complex transformation and / or uniaxial perfectly matched layers. Our approach, in which several key improvements have been implemented, is able to properly cope not only with SPP propagation in nanostructures, but also with a general form of permittivity / permeability anisotropy, and hence also with the Voigt MO effect. Next, we have combined the MOaRCWA simulations with (quasi)analytical predictions in order to study MSP performance of plasmonic nanostructures with highly-dispersive polaritonic InSb material, in the presence of external magnetic field. Here, Voigt MO effect can be used to impose nonreciprocity (one-way propagation) bringing new interesting phenomena in connection with MSP. As an example, Fig. 1 shows one of these structures studied [5], together with the InSb permittivity tensor dispersions, and corresponding nonreciprical dispersion diagram. In particular, we have explored nonreciprocal behavior of the MSP which reflects variety of interesting features associated with both surface and bulk polaritonic modes within the THz frequency range. The results of our studies will be shown and discussed in a detail.

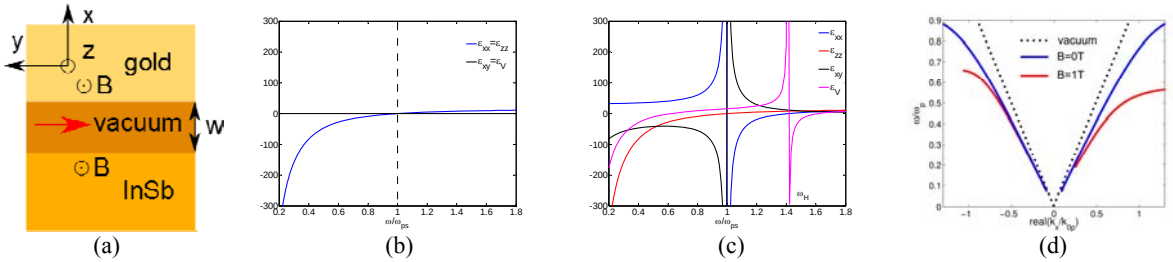

(a) (b) (c) (d)

Fig. 1: (a) Schematic picture of the one-way plasmonic waveguide operating at the THz range; the frequency dependence of the permittivity tensor (ε_{XX}, ε_{YY}, ε_{ZZ}, ε_{XY}) and the corresponding Voigt dielectric constant ε_V of InSb material: (b) case with no magnetic field, $\omega_b/\omega_p = 0$, (c) case with magnetic field, $\omega_b/\omega_p = 1$, ω_b is the cyclotron frequency, (d) THz magnetoplasmon dispersion relations for the structure w/o external magnetic field.

Acknowledgements: This work was financially supported by the Czech Science Foundation (projects P205/10/0046 and P205/12/G118).

References

[1] S.A. Maier, *Plasmonics: Fundamentals and Applications*, Springer, 1. ed. (2007).
[2] A. Figotin, I. Vitebsky, Phys. Rev. E **63**, 066609 (2001).
[3] A. Boardman, N. King, Y. Rapoport, L. Velasco, New J. Phys. **7**, 191 (2006).
[4] S. Eyderman, V. Kuzmiak, M. Vanwolleghem, in Proc. SPIE **7713**, 77130P-1 (2010).
[5] B. Hu, Q.J. Wang,Y. Zhang, Optics Letters **37**, 1895 (2012).

Coupling Characteristic for Novel Hybrid Long-Range Plasmonic Waveguide Including Bends

A. M. Heikal, Mohamed Farhat O. Hameed S. S. A. Obayya*

*Centre for Photonics and Smart Materials, Zewail City of Science and Technology, Sheikh Zayed District, 6th of October City, Giza, Egypt. * sobayya@zewailcity.edu.eg*

A novel design of hybrid long-range plasmonic waveguide is introduced and analyzed using full-vectorial finite difference method. The suggested design has high index material as a cap to reduce the propagation loss and optimum bending radius as well. The bending and coupling analysis of the reported design has been introduced.

Simulation Results

Figure 1 shows the suggested novel hybrid long-range plasmonic waveguide structure. The reported waveguide consists of a gold strip of thickness t_m = 20 nm, width W_m and has a permittivity ε_m= -131.95+j12.65. The metal strip is embedded in a rib waveguide with high index dielectric thin cap. In this study, Benzocyclobutene (BCB) of permittivity, ε_2 = 2.356225 is used as a rib core with total width W_r = 6.5 µm and total height h_r = 1.6 µm. In addition, SiO_2 is used as a substrate with permittivity ε_1 = 2.0736. The very thin dielectric cap has a thickness t_{Si} = 0.3 µm and a permittivity of ε_3 = 144.98327281. Figure 2 and 3 illustrate the variation of the effective index n_{eff} and propagation loss of the suggested structure with the bending radius, respectively with Si cap, with BCB cap and without cap at two different widths W_m, 0.5 µm and 3.0 µm. It is evident from Fig. 3 that the high index cap decreases the propagation loss. In addition, the propagation loss is decreased by increasing the refractive index of the cap. Therefore, the propagation loss without cap is higher than that with BCB cap and Si cap. It is also revealed from these figures that the effective index of the suggested structure with Si cap is greater than that with BCB cap. However, the propagation loss L_{pro} and optimum bending radius r_{opt} with Si cap with minimum propagation length, is smaller than that with BCB cap. At W_m = 3 µm, L_{pro} = 0.91 dB/mm and r_{opt} = 90 µm are obtained with BCB cap while L_{pro} = 0.77 dB/mm and, r_{opt} = 80 µm are achieved with Si cap. The numerical results also reveal that the effective index and propagation loss at W_m=3.0 µm are greater than those of W_m=0.5 µm as shown in Fig 2 and Fig.3. It is also shown from Fig. 2 that the effective index n_{eff} decreases by increasing the bending radius from r =70 µm to 1000 µm. If the bending radius is further increased, n_{eff} starts to be constant. The simulation results are obtained using full vectorial finite difference method [1]. More results will be presented in the conference.

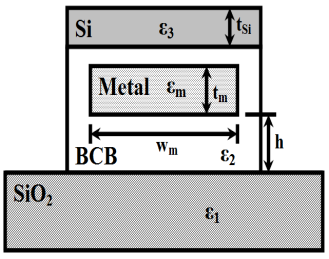

Figure 1 Schematic diagram of hybrid long-range plasmonic waveguide

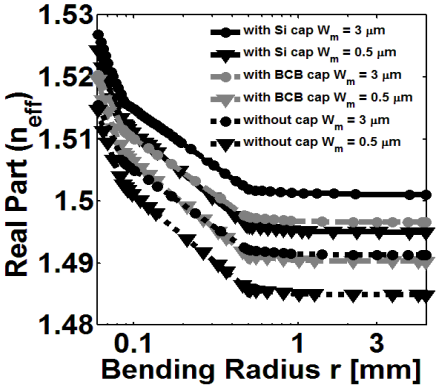

Figure 2 Variation of real part (n_{eff}) with the bending radius r

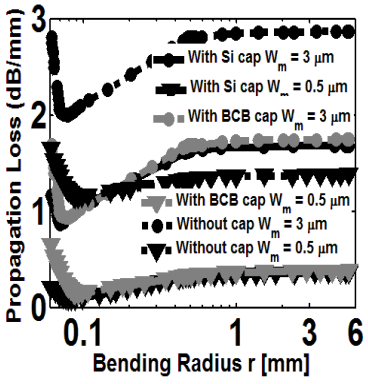

Figure 3 Variation of propagation loss (L_{prop}) with the bending radius r

References

[1] A. B. Fallahkhair, K. S. Li, and T. E. Murphy, "Vector Finite Difference Modesolver for Anisotropic Dielectric Waveguides," J.Lightwave Technol., vol.26 (11), pp. 1423-1431, 2008

Novel Mixed Finite Element Method Analysis of Leaky Photonic Nanowires

Shaymaa I.H.Ibrahim, S.S.A.Obayya*
Centre for Photonics and Smart Materials, Zewail City of Science and Technology, Sheikh Zayed District, 6th of October City, Giza, Egypt. *sobayya@zewailcity.edu.eg

A modified symmetric mixed finite element method is introduced and validated. Besides the benefits of conventional curl conforming mixed elements, the symmetric element has the advantage of being independent on the selection of facet related basis functions.

Summary and Results

Mixed finite elements are widely used for their ability to accurately apply boundary conditions to prohibit spurious modes and to eliminate unnecessary degrees of freedom. Figure 1 shows a second order vector element. The element has six tangential unknowns along with two facet unknowns. The facet related basis is hence asymmetric. This asymmetry may cause some problems: the choice of any two of possible three facet functions may influence the numerical accuracy of results. Special attention must be paid to numerical implementation of the asymmetric elements. Peterson introduced an efficient second order element that satisfies the Nedelec's constraints, however, it suffer from the asymmetry [1]. Modifying the facet related functions in [1] to get a set of dependent functions, we obtain a symmetric element. The developed finite elements technique is used analyze leaky photonic nanowire shown in Fig. 2 [2]. Photonic silicon nanowires are now a very important component in integrated photonics research as well as sensing applications.. Silicon nanowires enjoy a very good field confinement due to its high index contrast. However, this index contrast causes the field to be highly discontinuous at the interfaces which needs to be modeled correctly. A precise modal characterization of a silicon nanowire is extremely important as it forms the building block for almost all other circuitry components. Figure 2(b) shows the field discontinuities at the silicon-air interface and at oxide-silicon interfaces of the nanowire. The mode effective index calculated using the developed method shows an excellent agreement with other well-established mode solvers in [2]. In addition different choices of facet basis functions in our modified element almost give the same result unlike those calculated using facet function in [1] which gives different results for different selections, especially, on the imaginary part of the mode effective index which is the most sensitive parameter in sensing applications.

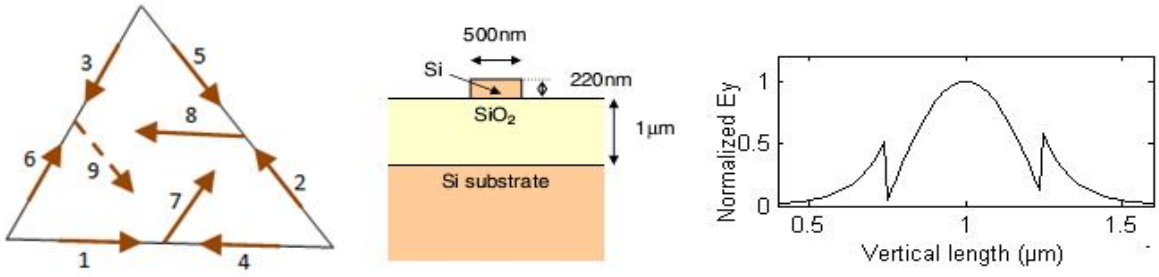

Figure 1 Second order mixed finite element. Figure 2(a) Leaky silicon nanowire, (b) Field discontinuities at the interfaces.

References

[1] Peterson, A.F.; , "Vector finite element formulation for scattering from two-dimensional heterogeneous bodies," *Antennas and Propagation, IEEE Transactions on* , no.3, pp.357-365, 1994.

[2] Bienstman, P. and Selleri, S. and Rosa, L. and Uranus, H.P. and Hopman, W.C.L. and Costa, R. and Melloni, A. and Andreani, L.C. and Hugonin, J.P. and Lalanne, P. and Pinto, D. and Obayya, S.S.A. and Dems, M. and Panajotov, K. (2006). Optical and Quantum Electronics, 38 (9-11). pp. 731-759. ISSN 0306-8919

Efficient Bidirectional Beam Propagation Method for Multiple Longitudinal Optical Waveguide Discontinuities

Shaymaa I.H.Ibrahim[1], S.S.A.Obayya[1]*, R. Letizia[2]

[1]*Centre for Photonics and Smart Materials, Zewail City of Science and Technology, Sheikh Zayed District, 6th of October City, Giza, Egypt.* *sobayya@zewailcity.edu.eg

[2]*Department of Engineering, Lancaster University, Lancaster, UK*

A new finite-element bidirectional beam-propagation method (FE-Bi-BPM) for the analysis of multiple longitudinal optical waveguide discontinuities is introduced. The method is very accurate with a very limited computational cost. Results show its agreement with well-established methods in the literature.

Summary and Results

Multiple longitudinal discontinuities are often encountered in optical devices. The analysis of such structures requires a bidirectional wave propagation technique to account for transmission and multiple reflections at the discontinuities. In the developed method, the square root of the characteristic matrix of both discontinuity sides is efficiently approximated using the Taylor's series expansion. By the enforcement of the boundary conditions at the discontinuity interface, both the reflected and the transmitted fields can be calculated while totally avoiding any matrix inversion and modal solutions. For multiple discontinuities, reflected and transmitted fields are solved at each interface and stored for each propagation trip until convergence is achieved.

To validate the proposed FE-Bi-BPM, a waveguide-loaded semiconductor laser [1], shown in Fig. 1, is simulated. Consider two symmetrical and single-mode waveguides connected by an air gap with 1μm height, where the TE_0 mode is injected as source at the operating wavelength, λ, is 1.55 μm. In Fig. 2, the variation of reflected, transmitted, and radiated power with the total number of propagation trips are shown. It may be noted that convergence of the numerical solution is achieved after only 4 propagation trips. Next, in Fig. 3, the reflected, transmitted, and radiated power are reported against the real-valued fundamental mode phase shift constant β_0. It is clear that the suggested technique has a low sensitivity to the variation of β_0. The results excellently agree with those obtained through FSRM technique [1].

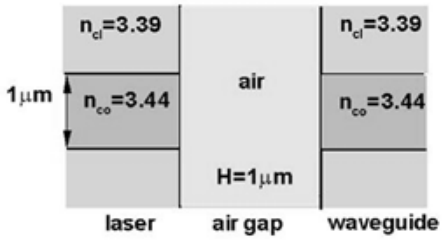

Figure 1 Schematic diagram of a waveguide-loaded semiconductor laser

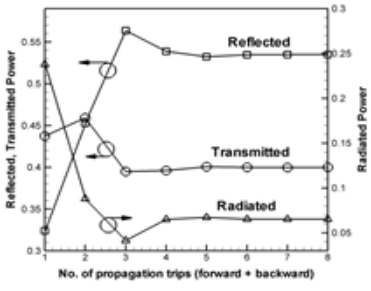

Figure 2 Convergence with the number of propagation trips

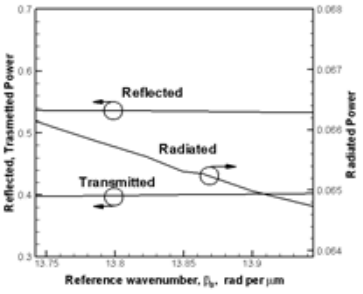

Figure 3 Variation with the reference wavenumber β0

References

[1] Smartt C. J., Benson T. M., Kendall P. C.: 'Free space radiation mode method for the anaysis of p ropagation in optical waveguide devices', IEE Proc.-Optoelectron., 1993, 140, (1), pp. 56-61

Mode Polishing for 3D Finite Element BPM

Remco Stoffer

PhoeniX Software, Enschede, The Netherlands
remco.stoffer@phoenixbv.com

A method to polish the modes to launch and analyze in a 3D Finite Element BPM is presented. It ensures that the modes that are used are eigenmodes of the numerical scheme.

Introduction

In the fixed-grid finite element vectorial 3D Beam Propagation Method (BPM), as presented in [1] and implemented in PhoeniX Software's Optodesigner, a relatively coarse grid can be used, since interfaces between materials are taken into account inside each element.

A numerical waveguide mode of the BPM will never be exactly equal to the analytical mode of a guide. If the analytical mode is simply used directly in the BPM for both launching and overlapping modal fields, unexpected bahaviour may occur, such as perceived gain in simple straight waveguides. Therefore, we developed a routine that polishes the analytical mode into the numerical BPM mode.

Implementation

We use a shift–and–invert method to obtain the modal field. The BPM algorithm (approximately) solves the equation $(\mathbf{A}\partial_{zz} + \mathbf{M})\mathbf{u} = 0$, where $\mathbf{A}$ and $\mathbf{M}$ are matrices describing the refractive index profile and the spatial derivatives, and $\mathbf{u}$ is a vector of discretized field components. Thus for a mode with propagation constant β_i, $(-\mathbf{A}\beta_i^2 + \mathbf{M})\mathbf{u_i} = 0$. If we then take trial β_t and (normalized) $\mathbf{u_t}$, which are close to β_i resp. $\mathbf{u_i}$, and calculate the expression $(-\mathbf{A}\beta_t^2 + \mathbf{M})^{-1}\mathbf{A}\mathbf{u_t}$, the component $\mathbf{u_i}$ in $\mathbf{u_t}$ will blow up: $(-\mathbf{A}\beta_t^2 + \mathbf{M})^{-1}\mathbf{A}\mathbf{u_t} \approx (\beta_i^2 - \beta_t^2)^{-1}\mathbf{u_i}$. This final expression can be used to obtain a better estimate for the numerical β_i. We find that two iterations of this procedure suffice to obtain a modal profile that propagates without noticeable distortion through the waveguide. An overlap of the field after some distance of propagation with another polished mode yields, as expected, a value of 1.

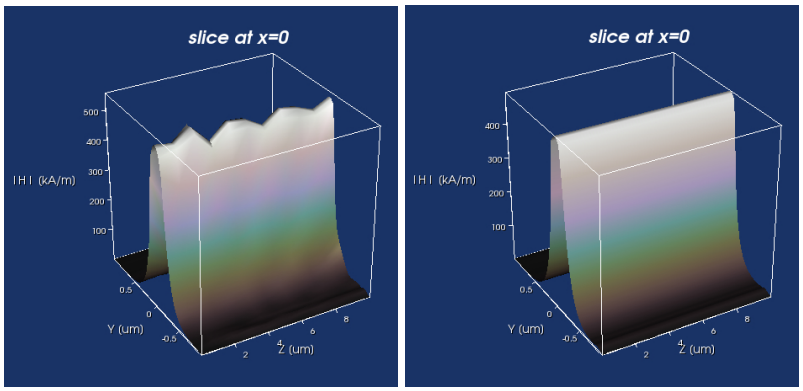

Slice of the field through a coarse grid BPM of a Silicon on Insulator waveguide. Left: Analytical mode launched into the structure. Right: Polished mode launched into the structure.

References

[1] R. Stoffer and J. Bos *Fixed-grid Finite Element Beam Propagation Method,* Proceedings of the OWTNM 2008, Eindhoven, The Netherlands, 2008, page 2

Numerical Modeling of Human Eye with Electromagnetic Approach

M. G. Can[1]*, B. B. Oner[1], H. Kurt[1]
[1] Nanophotonics Research Laboratory, Department of Electrical and Electronics Engineering
TOBB University of Economics and Technology, 06560, Ankara, Turkey
* m.can@etu.edu.tr

In this work we aimed to perform wave analysis of light propagation through the human eye implementing finite-difference time-domain (FDTD) method. Due to many orders of magnitude difference between the size of the human eye and operating wavelength in visible spectrum, we utilize additional asymptotic approach.

To the best of our knowledge, the electromagnetic wave approach is carried out for the first time to analyze the optical properties of the human eye. Wave theory of light has ability to explain interference, diffraction and aberrations contrary to ray optics approach that fails to take into consideration. Additionally, ray theory gives infinitesimal spot size at the focal point while wave theory analysis provides an exact full-width at half-maximum value of the focused light at the proximity of the retina.

The numerical computations are performed by means of the FDTD. The ratio between human eye size (~12 mm in diameter) and the visible light wavelength (400-750 nm) gives rise to numerical stability problem [1]. In order to overcome this issue, a proper description of the geometrical and dispersive properties of the eye is modelled by implementing asymptotic and numerical methods.

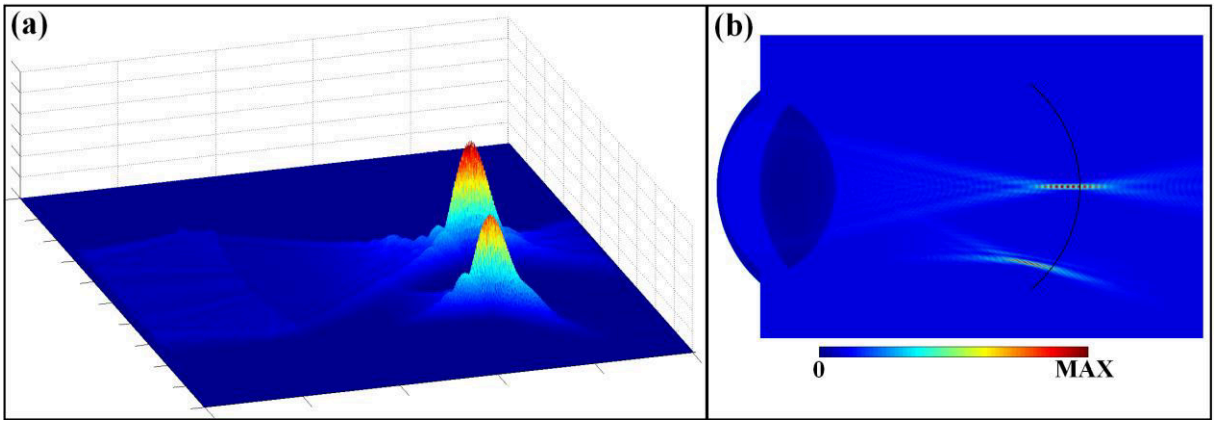

Figure 1 (a) Intensity distribution of the two focused beams with different incident angles. (b) A snapshot of the beams focused at the proximety of the retina (dark plotted arc represent retina).

Fig. 1(a) shows a snapshot of two different focused beams. The color bar represents the intensity variation for both Figs. 1(a) and 1(b). Beams have different incident angles (perpendicular and 20^0). While the perpendicular case gets focused on the retina, the tilted case focuses in front of the retina. The figure also indicates that the maximum intensity of the focused beam is getting low as we increase the incidence angle. Coma aberration and its properties are observed from the figure, not only coma but also other optical properties of our eye model are compatible with the literature. The details of the electromagnetic wave analysis of human eye will be presented in the conference.

References

[1] A. Taflove and S. C. Hagness, Computational Electrodynamics: The Finite-Difference Time-Domain Method, Artech House Publisher, 2005.

A vectorial simplified model for Fano resonances of guided-mode resonant gratings

A.-L. Fehrembach and A. Sentenac

Aix Marseille Université, CNRS, Ecole Centrale Marseille, Institut Fresnel, 13013 Marseille, France
anne-laure.fehrembach@fresnel.fr

We present a vectorial, semi-analytical model developed to understand the physics of guided mode resonant gratings and to express their properties with respect to the parameters of the structure.

Guided mode resonant gratings are simple structures, composed with a planar waveguide structured with a subwavelength periodic pattern. Their basic principle is simple: a leaky guided-mode can be excited by an incident wave via a diffraction order, which generates a resonance peak in the diffraction spectrum of the structure. Despite this outward simplicity, they are however very interesting for applications such as narrow band filtering, sensoring .... Yet, to obtain advanced properties (polarization independence, angular tolerance...) it is necessary to work with complex configurations (conical incidence, excitation of several modes...). Knowing the link between the parameters of the structure and its properties, or at least having some physical understanding in theses configurations is a crucial help in the design. Here, we present a semi-analytical model in the vectorial case, e.g. whatever the plane of incidence and the incident polarization. This is a further development of the scalar model which led us to propose configurations with enhanced angular tolerance [1, 2].

We start from Maxwell equations, and consider the grating as a perturbation over a reference, planar structure. We show that for an incident wave with wavelength λ and in-plane wavector $\vec{\kappa}$, the electric field diffracted at an abscissa z above or below the grating is solution of the equation

$$[\vec{F}(\lambda,\vec{\kappa},z)] = [\vec{E}_{ref}(\lambda,\vec{\kappa},z)] + h\mathbf{M}(\lambda,\vec{\kappa},z,0)[\vec{F}(\lambda,\vec{\kappa},0)] + o(h^2), \tag{1}$$

where $[\vec{F}(\lambda,\vec{\kappa},z)]$ is a vector containing the components of the electric field in the grating orders, $[\vec{E}_{ref}(\lambda,\vec{\kappa},z)]$ contains the incident field and the field reflected and transmitted by the reference structure, h is the grating depth, and $\mathbf{M}$ a matrix which depends on the reflection and transmission matrix $\mathbf{R}_{ref}$ and $\mathbf{T}_{ref}$ of the reference structure and of the gratings parameters.

Solving successively the homogeneous and the diffraction problems, we are able to express the reflection and transmission matrix of the structure with respect to the incident wavelength λ as

$$\mathbf{R} = \mathbf{R}_{ref} + h^2\frac{\mathbf{R}_{pert}}{\lambda-\lambda_{pole}} + o(h^2) \quad \text{et} \quad \mathbf{T} = \mathbf{T}_{ref} + h^2\frac{\mathbf{T}_{pert}}{\lambda-\lambda_{pole}} + o(h^2), \tag{2}$$

where $\mathbf{R}_{pert}$ and $\mathbf{T}_{pert}$ are matrix that express the coupling-in and out of the mode via the grating, and λ_{pole} is the eigen wavelength of the excited mode. We draw some physical interpretations out of these expressions and provide a numerical validation of the model.

ACKNOWLEDGEMENT: The financial support of the CNES in this work is gratefully acknowledged.

References

[1] A.-L. Fehrembach, F. Lemarchand, A. Talneau, and A. Sentenac. High q polarization independent guided-mode resonance filter with doubly periodic etched ta2o5 bidimensional grating. *I.E.E.E. J. Light. Tech.*, 28:2037–2044, 2010.

[2] A. Sentenac and A.-L. Fehrembach. Angular tolerant resonant grating filters under oblique incidence. *J. Opt. Soc. Am. A.*, 22:475–480, 2005.

Electro-optic effect in guided mode resonance gratings for tunable narrow-band filtering

A.-L. Fehrembach, D. Shu and E. Popov

Aix Marseille Université, CNRS, Ecole Centrale Marseille, Institut Fresnel, 13013 Marseille, France
anne-laure.fehrembach@fresnel.fr

We present a numerical study of guided mode resonant gratings including a layer of electro-optic material. The effect of the anisotropy of the electro-optic layer on the tunability and polarization dependence of the peak is taken into account.

A guided mode resonance filter is a simple structure composed of a stack of a few dielectric layers on which a sub-wavelength grating is engraved. Their main interest is the narrow spectral FWHM they can achieve: in practice, quality factors greater than 7000 have already been obtained. The potential application fields are: optical telecommunications, spectroscopy, lasers, sensoring, etc. We aim to develop the potential of resonant grating filters by studying the tunability of their center wavelength by electro-optic effect. Here, we present a numerical study of the properties of guided mode resonance filters including an electro-optic material [1]. We have used a numerical tool based on the Fourier Modal Method including anisotropic materials [2]. This is indispensable to analysis the effects related to the incident polarization.

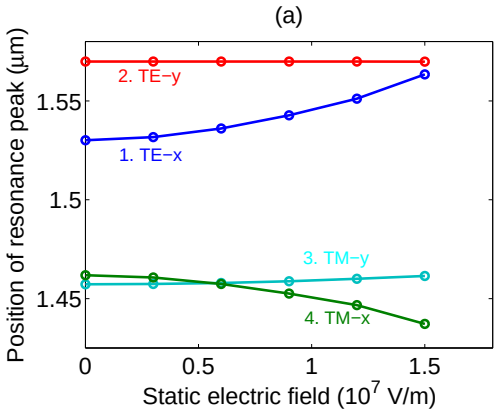

Fig. 1. Tunability of a guided mode resonance filter including a Barium Titanate layer

We work with two materials, Lithium Niobate and Barium Titanate, because of their large electrooptic coefficients. We compare several configurations, allowing either a strong (up to 90nm) or a weak tunability, toward greater or smaller wavelengths (see Fig. 1). For each case, a physical interpretation is given for the facts that are observed. We also study the behavior of the peak in the different configurations with respect to the incident polarization.

References

[1] D. Shu, E. Popov, and A.-L. Fehrembach. Electro-optic effect in batio3 for spectral tuning of narrow-band resonances. *J. Opt. Soc. Am. B*, 30, 2013.

[2] L. Li. Fourier modal method for crossed anisotropic gratings with arbitrary permittivity and permeability tensors. *J. Opt. A: Pure Appl. Opt.*, 5:345–355, 2003.

Solitons in binary waveguide arrays

Aldo Auditore[1], Matteo Conforti[1], Costantino De Angelis[1], Alejandro B. Aceves[2]

[1] *Dipartimento di Ingegneria dell'Informazione, Università degli Studi di Brescia, Brescia 25123, Italy.*
[2] *Department of Mathematics, Southern Methodist University, Dallas, Texas 75275, USA*
aldo.auditore@ing.unibs.it

We suggest a model describing light propagation in binary (linearly and nonlinearly) waveguide arrays. Performing a suitable continuum expansion, we find solitons for focusing, defocusing, and even for alternating focusing-defocusing nonlinearity. We also analyze modulational stability in the continuum limit and in the discrete system.

Model and results

We consider here a model that can be applied in different physical settings such as plasmonic, Bragg and photonic crystal waveguides [1, 2, 3, 4, 5]. The simplest form consists of a binary array designed in such a way that the coupling between successive waveguides switches periodically from C to $-C(1+\epsilon)$. For this case a gap centered at zero Bloch momentum in the linear dispersion relation opens, allowing the existence of bright solitons. Whereas, if the coupling coefficient have equal modulus, the gap closes, and a Dirac point emerges in the band structure at zero transverse momentum. Despite the absence of a gap in the linear spectrum, preventing the existence of bright gap solitons, a binary Kerr nonlinearity can open a gap, allowing for the existence of gap solitons sitting on a non-vanishing constant background. Our study has started considering coupled mode theory and taking into account third-order nonlinearities in the form of a pure Kerr effect, in order to obtain a system of equations describing the physical system. Performing a suitable Taylor expansion, we get two sets of coupled equations with constant coefficients describing beam propagation along the array. It is straightforward to write these equations in an Hamiltonian form; from the analysis of the associated dynamical system we obtain solitary-wave solutions corresponding to homoclinic or heteroclinic orbits in the phase plane. In this way, we describe in a simple and accurate fashion the entire spectrum of the soliton states of this system: bright-bright [3], bright-dark [4] and dark-antidark [5]. We also discuss the stability of plane wave solutions in both the discrete case and in the continuous long wavelength limit, finding that the discrete system can support stable plane wave propagation when the corresponding continuum approximation has no stable solutions.

References

[1] S. H. Nam, A. J. Taylor, and A. Efimov, *Diabolical point and conical-like diffraction in periodic plasmonic nanostructures*, Opt. Exp 18, 10120 (2010).
[2] N. K. Efremidis, P. Zhang, Z. Chen, D. N. Christodoulides, C. E. Rüter, and Detlef Kip, *Wave propagation in waveguide arrays with alternating positive and negative couplings*, Phys. Rev. A 81, 053817 (2010).
[3] M. Conforti, C. De Angelis and T. R. Akylas, *Energy localization and transport in binary waveguide arrays*, Physical Review A **83**, 043822 (2011).
[4] M. Conforti, C. De Angelis, T. R. Akylas and A. B. Aceves, *Modulational stability and gap solitons of gapless systems: continuous vs. discrete*, Physical Review A **85**, 063836 (2012).
[5] A. Auditore, M. Conforti, C. De Angelis, and A. B. Aceves, *Dark-antidark solitons in waveguide arrays with alternating positive-negative couplings*, Optics Communications, in press.

Bandgap maps for Photonic Crystal with Honeycomb lattice for different shapes of scatterers

Vinita[1], A. Kumar[1*], V. Rastogi[2]
[1] *Department of Applied Physics, Delhi Technological University, Delhi, India*
[2] *Department of Physics,Indian Institute of Technology Roorkee, Roorkee , India*
* ajeetdph@gmail.com

In this paper, two dimensional (2D) photonic crystal (PhC) with honeycomb lattice for non circular (square and hexagonal) shapes of rods has been investigated using plane wave expansion method. Photonic bandgap maps for different shapes of scatterers have been presented and their characteristics have been discussed.

Brief Summary

Photonic crystals (PhCs) are most valuable when they possess complete photonic bandgap (CPBG) where, propagating modes are forbidden regardless of polarization [1]. PhCs with triangular lattice have larger CPBG than square lattice but are difficult to fabricate. Previous work on honeycomb lattice for circular rods show CPBG at smaller filling fraction [2]. In this paper, CPBG and PBG maps for honeycomb lattice with non-circular shapes of dielectric rods in air column have been investigated. Results have been calculated for dielectric rods with GaAs material having relative dielectric constant, ε =11.4, since this is an important material for variety of PhC devices [1]. The gap maps for two shapes of rods (square and hexagonal) are presented in Fig. 1. For square rods, maximum CPBG has been found for l/a =0.38, where l is the length of the side of the square and a is lattice constant with maximum gap midgap ratio, ω_R = 5.8%. In case of hexagonal rods, two CPBG have been obtained. For first CPBG region, maximum CPBG has been found for d/a = 0.26, where d the length of side of the hexagon with maximum gap midgap ratio, ω_R = 10.5% while for second region, maximum CPBG has been found at d/a = 0.42 with maximum gap midgap ratio, ω_R = 5.4%. Hexagonal rods have the largest CPBG than square and circular rods at relatively smaller filling fraction. So, it is easy to fabricate devices for honeycomb structure with hexagonal rods than triangular lattice. As maximum gap midgap ratio is greater than 10% so it can be used as PhC mirrors with 100% reflection [2].

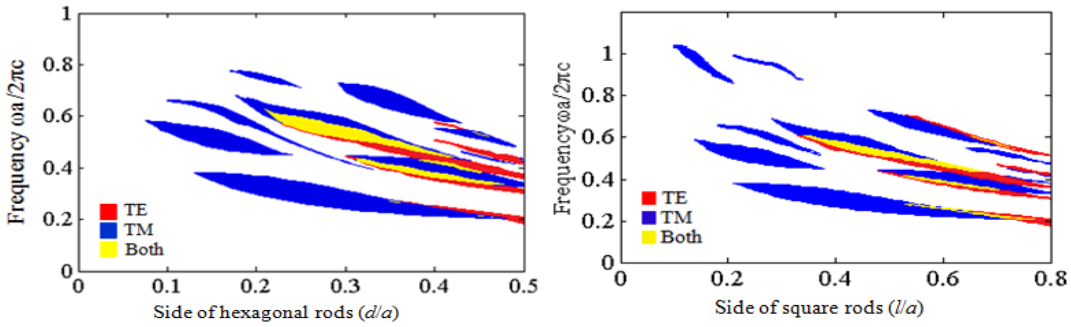

Fig.1 Gapmaps for (a) hexagonal rods, (b) square rods in honeycomb lattice

References

[1] A. V. Dyogtyev, I. A. Sukhoivanov, and R. M. De La Rue, *Photonic band-gap maps for different two dimensionally periodic crystal structures*, Journal of Applied Physics, 107, 013108, 2010

[2] J. D. Joannopoulos, R.D. Meade, and J. N. Winn, *Photonic Crystals*: *Molding the Flow of Light*, Princeton University Press, Chichester, West Sussex, 1995

Standing Waves on Periodic Arrays of Circular Dielectric Cylinders

Zhen Hu[1], Ya Yan Lu[2]

[1]*Department of Mathematics, Hohai University, Nanjing, Jiangsu, China*
[2]*Department of Mathematics, City University of Hong Kong, Kowloon, Hong Kong*
huzhen1230@gmail.com

Standing waves are known to exist on infinite arrays of dielectric circular cylinders. The frequencies of standing waves are calculated for different values of the dielectric constant and radius. The standing waves have real frequencies, and they correspond to resonances with infinite quality factor.

Introduction

Consider a periodic array (period a) of infinitely long and parallel (parallel to z axis) circular dielectric cylinders (radius r, dielectric constant ε) placed on the y-axis and surrounded by air. A standing wave on the array is periodic in y, and decays exponentially as $|x| \to \infty$.

Results

In Fig. 1, we show the lowest frequencies of the standing waves in the E polarization for different

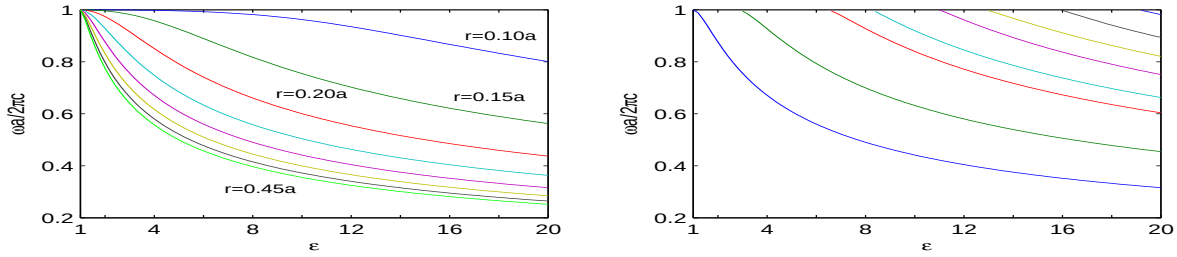

Fig. 1. Left: lowest frequencies for different r. Right: all frequencies for $r = 0.3a$.

values of r and ε, and the frequencies of all standing waves for $r = 0.3a$. For $\varepsilon = 11.56$, there are five standing waves whose frequencies are $\omega a/2\pi c = 0.4112$, 0.5897, 0.7841, 0.8590, and 0.9766, respectively. The electric field patterns of these standing waves are shown in Fig. 2.

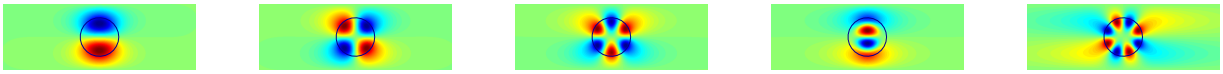

Fig. 2. Electric field patterns of the five standing waves for $r = 0.30a$ and $\varepsilon = 11.56$.

Acknowledgments

The work is partially supported by the National Science Foundation of China (project 11101122).

References

[1] S. Shipman and D. Volkov, SIAM J. Appl. Math. **67**, 687–713 (2007).

Design and Analysis of a Low Cost Highly Sensitive Refractive Index Sensor

Babita[1*], V. Rastogi[1]
[1] *Department of Physics, Indian Institute of Technology Roorkee, Roorkee-247667, India*
* babitaphy@gmail.com

A simple, compact, low cost and highly sensitive sensor for sensing refractive index of various biological and chemical samples has been presented. The maximum resolution of the sensor is of the order of 10^{-5} corresponding to 1% change in transmitted power.

Introduction

In biomedical applications, such as photodynamic therapy [1], functional imaging and optical biopsy light or laser beams are transported and distributed in biological tissues. When light enters in the biological tissue or in any chemical liquid, the optical properties of tissues like absorption coefficients, reflection, irradiance levels, and the scattering phase functions determine the light transmission and distribution. These phenomena are dependent on the refractive indices of tissues or liquids and reflect their structural organization, which can be used as an intrinsic marker for disease. Therefore, to understand the light behavior in biological tissues and chemical liquids, it has become imperative to have accurate data regarding refractive indices of the tissues or liquids. Here we present the design of a leaky planar optical waveguide based refractive index sensor. In the proposed design the test sample forms the leaky layer of the structure. Any change the refractive index of the leaky layer changes the leakage loss and hence transmittance of the structure and this forms the working principle of the sensor.

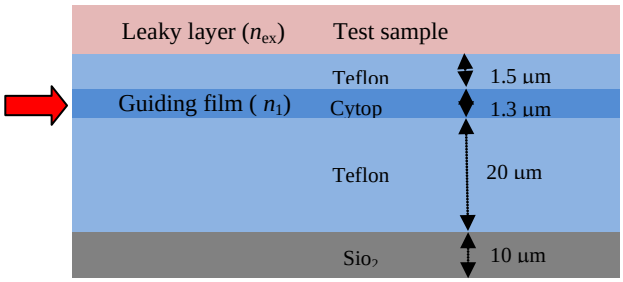

Fig. 1 (a) Schematic representation of sensor

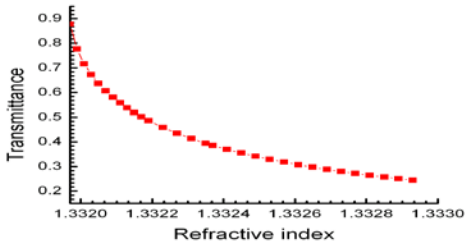

Fig. 1(b) Variation in transmittance with n_{ex}

Results and discussion

Schematic of the sensor design is shown in Fig. 1(a). Transmittance through guiding film has been modeled by using the transfer matrix method TMM [2]. Fig.1 (b) clearly shows that within the range 1.33197 to 1.33293 resolution of sensor is 1.5×10^{-5} for 1% change in output power at 633 nm wavelength. This range can be used to sense refractive index of proteins, glucose solution, sucrose solution, salt solution and for testing water adulteration.

References

[1] T. J. Dougherty, C. J. Gomer, B. W. Henderson, G. Jori, D. Kessel, M. Korbelik, J. Moan, and Q. Peng, *Photodynamic therapy*, J. Nat. Cancer Inst., 90 (12), 889-905, 1998.

[2] A. K. Ghatak, K. Thyagarajan, and M. R. Shenoy, *Numerical analysis of planar optical waveguides using matrix approach*, J. Lightwave Technol., 5 (5), 660-667 (1987).

Integrated Optics refractometry: Sensitivity in relation to spectral shifts

H.J.W.M. Hoekstra*, *MESA*$^{+}$ *Institute for Nanotechnology, University of Twente, Enschede, NL*
**h.j.w.m.hoekstra@ewi.utwente.nl*

A new variant of the Vernier-effect based sensor reported in ref. 1 is introduced. Both sensor types may show a huge index induced spectral shift. It will be shown in a poster presentation that with such sensors, as well as with surface plasmon based sensors, the constraints on the spectral resolution of the read out are strongly relaxed, but the sensitivity is not increased (unlike what is often reported in the literature).

Considered sensing devices

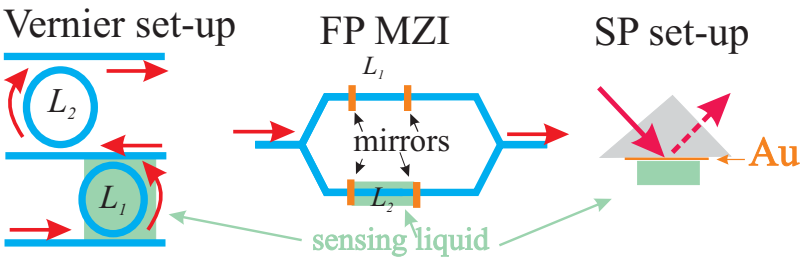

Figure 1. Schematics of the considered devices with potentially huge index-induced spectral shift enhancement.

The considered three sensing devices are depicted in fig. 1. Here we will discuss in some detail only the one based on the Vernier effect [1]. The lengths of the two cascaded ring resonators differ only slightly ($L_1 / L_2 = \eta/(\eta+1)$; η integer) so that the transmission combs of the resonators have a slightly different free spectral range (FSR, $\Delta\lambda$) and their transmission peaks coincide periodically according to a FSR of $\Delta\lambda_V = \eta\Delta\lambda$ (see fig 2a), corresponding to the spectral spacing of the transmittance maxima of the cascaded cavities (see fig. 2b). For a relatively small spectral shift of the transmission comb of one of the cavities, $\delta\lambda$, the broadened total transmittance shows an enhanced shift of $\delta\lambda_V \approx \eta\delta\lambda$.

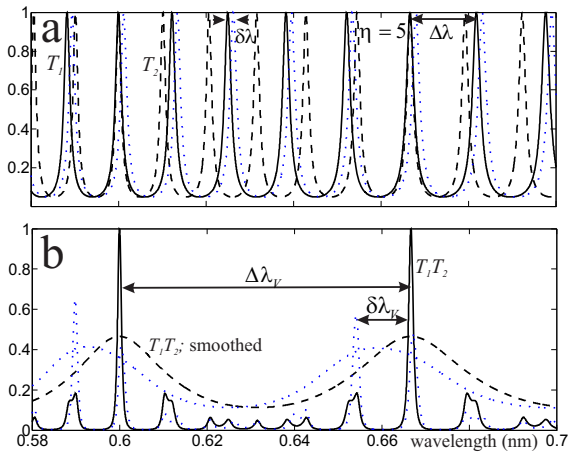

Figure 2. Graphs illustrating the Vernier effect based sensor, with (a) transmittances of the two separate cavities, T_1 (solid) and T_2 (dashed) and T_1 after a spectral shift $\delta\lambda$ (dotted, blue), and with (b) corresponding total transmittance T of the set-up (solid), T spectrally broadened (dashed) and both after the spectral shift (dotted, blue)

About sensitivity and spectral shift

The sensitivity of a device, *S*, can be defined by the maximum value of $|\partial \ln T / \partial n|$ and can be rewritten according to

$$S = |\partial \ln T / \partial n|_\lambda = |\partial \ln T / \partial \lambda|_n \, |\partial\lambda / \partial n|_T .$$

It is seen from the equation that the sensitivity of the Vernier set-up, with say only T_1 sensitive to index changes, is equal to that of the separate cavity with transmittance T_1. The huge spectral shift of the former is exactly neutralized by the smaller slope, i.e., generally $|\partial T / \partial\lambda| \ll |\partial T_1 / \partial\lambda|$. The key point for the sensitivity seems to be only the magnitude of the interaction between light and sensed matter; a point further elaborated during the poster presentation.

References

[1] T. Claes et al., *Experimental characterization of a Si photonic biosensor consisting of two cascaded ring resonators based on the Vernier effect etc.*, Opt. Expr. 18, 2010.

Reflection of semi-guided plane waves at angled thin-film transitions

Fehmi Çivitci, Manfred Hammer*, Hugo J.W.M. Hoekstra

MESA+ Institute for Nanotechnology, University of Twente, Enschede, The Netherlands
*m.hammer@utwente.nl

The propagation of thin-film guided, in-plane unguided plane optical waves, and their partial or total reflection at transitions between regions with different film thickness, is considered. The properties of reflected and refracted waves can be predicted reasonably by readily available Helmholtz- and/or eigenmode-solvers.

2-D optics

Classical concepts [1] for integrated optical components like mirrors, lenses, prisms, polarizers, but also for entire spectrometers [2], rely on the effects that a — tapered or step-like — transition between regions with different layering, specifically different core thickness, has on thin-film guided, in-plane unguided light. Results for the reflection and refraction of 1-D guided plane waves at such a discontinuity may form the basis for a description of the in-plane propagation by geometrical optics [1, 2]. Part (a) of the figure below shows a typical configuration. As a step beyond the classical effective index picture, we will discuss and compare two approaches on how this problem can be tackled — at least partly — by standard tools for integrated optics design.

(I) Accepting the scalar approximation, using an ansatz of a uniform harmonic field dependence on the interface coordinate y, the 3-D problem reduces to a 2-D Helmholtz problem, for guided wave input and transparent boundaries, where the permittivity depends on the incidence angle.

(II) By complementing the x-z-view with a mirrored interface at some faraway negative z-position, one obtains the 2-D cross section of a wide multimode rib channel. Constraints for transverse resonance permit to translate the propagation constants of its polarized modes into discrete samples of the phase factors experienced by an in-plane guided wave upon total internal reflection at the sidewalls.

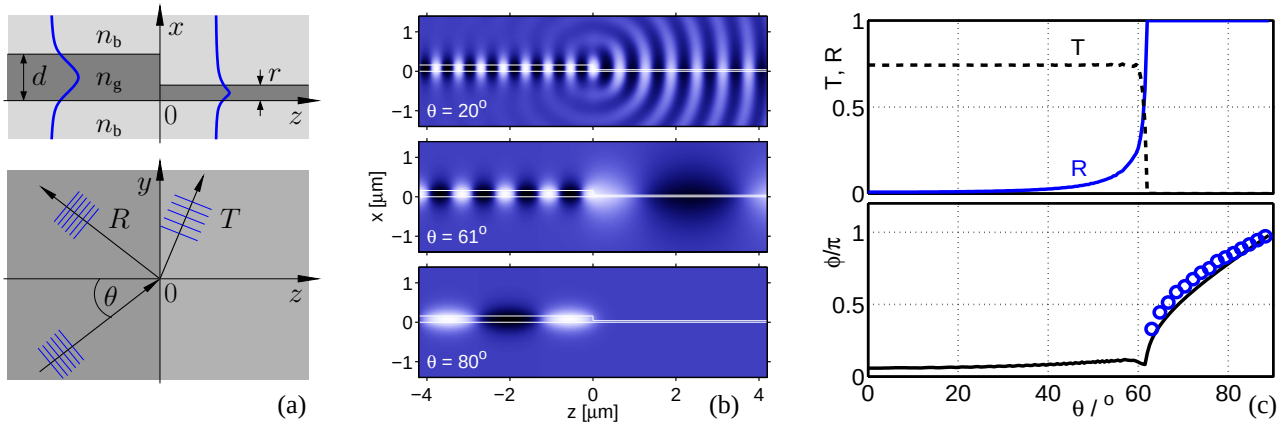

(a): Reflection of semi-guided plane waves at a thin film step discontinuity. (b): Snapshots for wave incidence at different angles θ. (c): Transmittance T, reflectance R, and phase shift ϕ upon reflection vs. incidence angle θ, predicted by a 2-D Helmholtz solver (I), and by mode analysis (II, markers) of an $8\,\mu$m wide rib. Parameters, cf. (a): $n_b = 1.4524$, $n_g = 2.0081$, $d = 160$ nm, $r = 40$ nm, TE-fields, vacuum wavelength $\lambda = 850$ nm.

References

[1] P. K. Tien. *Rev. Mod. Phys.*, 49(2):361, 1977; R. Ulrich, R. J. Martin, *Appl. Opt.*, 10(9):2077, 1971.
[2] F. Çivitci, H. J. W. M. Hoekstra. Europ. Conf. Integr. Optics (ECIO), Barcelona, Spain, paper 151, 2012.

Acknowledgement: This research is supported by the Dutch Technology Foundation STW (project 10051).

Time domain Method of Lines

S. F. Helfert

FernUniversität in Hagen, Chair of Optical Information Technology, Universitätsstr. 27
58084 Hagen, Germany
stefan.helfert@fernuni-hagen.de

In this presentation will be shown how the Method of Lines can be used to solve initial value problems in time domain. 1D numerical results are presented for standard dispersion free materials but also for dispersive media.

Introduction

The Method of Lines is a numerical algorithm that permits the solution of waveguide problems. Usually it is used in the frequency domain; the algorithm is described in detail e.g. in [1]. However, also time domain computations were performed in the past. In [2] the time dependency was treated with finite differences. A time dependency according to $\sin \omega_0 t$, $\cos \omega_0 t$ was applied in [3] and frequency solutions were combined with the discrete Fourier transform in [4]). In contrast to those papers, initial value problems with analytic time dependency will be treated here.

Numerical algorithm

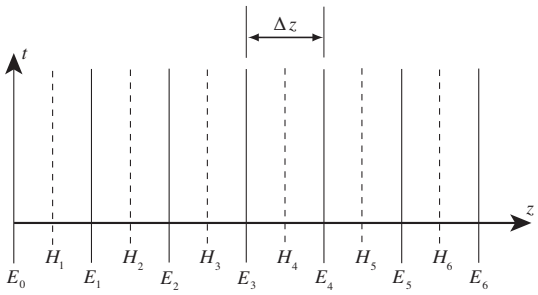

Fig. 1: Discretization in z-direction

To develop the algorithm we start with Maxwell's equations that are discretized in spatial directions. The 1D-case is shown in Fig. 1. Analytic expressions are used for the time-dependency, resulting in "time-lines". Different from frequency domain computations $E_0(t)$ will be given as initial value, here. Then, the discretized Maxwell' equations may be written as:

$$\frac{\partial \mathbf{F}}{\partial t} + \mathbf{Q}_1 \mathbf{F} = -\mathbf{Q}_0 E_0(t)$$

where $\mathbf{F}$ contains the discretized fields and the $\mathbf{Q}$-matrices contain finite difference approximations of the derivatives. Particularly, an inhomogeneous differential equation system is obtained. In the presentation will be shown how its solution is constructed from the inhomogeneous and the homogeneous differential equation. Numerical results will be shown for standard dispersion free materials, and for structures where a left handed material (LHM, see e.g. [5]) is sandwiched between two standard right handed materials. Since LHMs are dispersive it is also shown how such dispersive material may be incorporated into the algorithm.

References

[1] R. Pregla, *Analysis of Electromagnetic Fields and Waves - The Method of Lines*, Wiley & Sons, UK, 2008.
[2] W. E. Schiesser, *The Numerical Method of Lines Integration of Partial Differential Equations*, Academic Press, San Diego , USA, 1991.
[3] S. Nam, S. El–Ghazaly, H. Ling, and T. Itoh, *Electron. Lett.*, vol. 24, no. 2, pp. 128–129, 1988.
[4] J. Gerdes, in *ICTON Conf.*, Rome, Italy, 2007, vol. 4, pp. 324–327.
[5] G. V. Eleftheriades and Keith G. Balmain, (Eds.), *Negative-Refraction Metamaterials*, Wiley-Interscience, Hoboken, NJ, USA, 2005.

Matrix exponential and Krylov subspaces for fast time domain computations: recent advances

M.A. Botchev [1]

[1] *MESA$^+$ Institute for Nanotechnology, MaCS/EEMCS, University of Twente, Enschede, The Netherlands*
www.math.utwente.nl/ botchevma/, m.a.botchev@utwente.nl

We show how finite difference (or finite element) time domain computations can be accelerated by employing recent advances in the matrix exponential time integration and Krylov subspace techniques.

Matrix exponential time integration: no time stepping!

The finite difference time domain (FDTD) method is an efficient tool to model photonic nanostructures numerically. The standard FDTD method can be seen an application of the staggered leap frog time integration to the system of ordinary differential equations

$$y'(t) = -Ay(t), \quad y(0) = v, \qquad A \approx \begin{bmatrix} 0 & \mu^{-1}\nabla\times \\ \varepsilon^{-1}\nabla\times & \sigma\cdot \end{bmatrix} \in \mathbb{R}^{n\times n}.$$

Here A is the discrete Maxwell operator discretized in space by the standard staggered Yee method. μ, ε and σ are (relative) permeability, permittivity and conductivity, respectively. The vector function $y(t)$ contains unknown components of the magnetic and electric fields.

By using the matrix exponential operator, solution of the system can be written as $y(t) = \exp(-tA)v$. Numerical algorithms, which are based on this approach, are called exponential time integration methods. The essential point is that not the matrix exponential itself but rather *its action* on the vector v is computed. An attractive feature of the formula $y(t) = \exp(-tA)v$ is that it provides solution for virtually any time moment, without time stepping. Often, this leads to a significantly faster time solution than with the standard time integration, such as the classical FDTD method.

Rational shift-and-invert Krylov subspace techniques

An efficient way to compute the actions of $\exp(-tA)$ is by employing the so-called Krylov subspace methods. In this approach a projection of A onto the Krylov subspace $\mathrm{span}\{v, Av, A^2v, \ldots, A^{k-1}v\}$ is used and the approach is efficient as soon as $k \ll n$. Recently, an improvement has been proposed to the Krylov subspace methods for computing the actions of the matrix exponential, namely, the shift-and-invert Krylov subspace method. This method belongs to the class of the rational Krylov subspace methods. It provides a very fast and often grid independent convergence for the price of solving linear systems. We discuss its implementation issues.

Block Krylov subspaces to accommodate source terms

Source terms are often dealt with incorporating an inhomogeneous term $g(t)$ into the discretized Maxwell equations, e.g.,

$$y'(t) = -Ay(t) + g(t), \quad y(0) = v.$$

The presence of the source term renders the formula $y(t) = \exp(-tA)v$ invalid and usually one applies a time stepping where the matrix exponential approach can used at each time step. We propose another, often more efficient, approach. It is based on a low rank approximation of the source term $g(t)$ and a special block Krylov subspace method.

Numerical Modeling of Seeded FWM in Silicon Nitride Waveguides for CARS

J.P. Epping[1*], M. Kues[2], P.J.M. van der Slot[1], C.J. Lee[1,3], C. Fallnich[2], K.-J. Boller[1]
[1] *MESA+ Institute for Nanotechnology, University of Twente, Enschede, The Netherlands*
[2] *Institute of Applied Physics, Westfälische Wilhelms-Universität Münster, Germany*
[3] *FOM Institute DIFFER, Nieuwegein, The Netherlands*
* j.p.epping@utwente.nl

We propose and theoretically investigate a light source for CARS based on seeded four-wave mixing in silicon nitride waveguides. A tuning range (1290-2750 cm^{-1}) is expected via pumping at a wavelength of 1058 nm and the pump power is calculated to be one order of magnitude lower than what was previously reported.

Coherent anti-Stokes Raman scattering (CARS) offers label-free detection with chemical selectivity. In order to achieve spectral and therefore chemical resolution two synchronized narrowband pulses have to be provided by an appropriate light source. Here, we present theoretical investigations of a CARS light source based on seeded four-wave mixing (FWM) [1] in silicon nitride waveguides, which is of great interest for analyzing CARS spectra in a lab-on-a-chip setup.

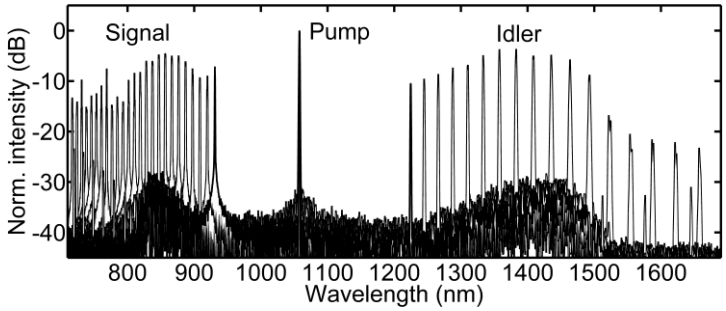

Fig. 1: *Superimposed spectra of cw seeded FWM for different seed wavelengths. The pump pulse has a center wavelength of 1058 nm and a pulse duration of 10 ps. The cw seed has a power of 100 mW and is tuned from 715 nm to 935 nm in 10 nm steps.*

We consider a silicon nitride waveguide and pump pulses with a pulse width of 10 ps and a peak power of 100 W. The center wavelength of 1058 nm is selected to lie in the normal dispersion regime. The waveguide dispersion is calculated using COMSOL Multiphysics. We calculate the seeded FWM by numerically integrating the generalized nonlinear Schrodinger equation [2]. For obtaining a spectral narrow idler wave a cw narrowband seed at the signal wavelength is also injected and tuned from 715 nm to 935 nm in order to generate synchronized idler pulses suitable for CARS. As can be seen in Figure 1 the idler pulses can be tuned from 1225 nm to 1492 nm (at -10 dB) corresponding to CARS signals from 1290 cm^{-1} to 2750 cm^{-1}. The pulse length of the idler wave is 6.4 ps and a maximum conversion efficiency of 46 % was calculated, while the pump power is one order of magnitude lower than in [1].

References

[1] M. Baumgartl, M. Chemnitz, C. Jauregui, T. Meyer, B. Dietzek, J. Popp, J. Limpert and A. Tünnermann, Widely tunable fiber optical parametric amplifier for coherent anti-Stokes Raman scattering microscopy, Opt. Exp. 20, 26583 (2012).

[2] M. Kues, N. Brauckmann, T. Walbaum, P. Groß, C. Fallnich, Nonlinear dynamics of femtosecond supercontinuum generation with feedback, Opt. Express 17, 15827 (2009)

Propagation of a Periodic Sequence of Gaussian Pulses in a Coaxial Optical Fiber: occurrence of "Talbot Effect" in the time domain

Enakshi K Sharma[1*] and Jyoti Anand[2]
[1] *Department of Electronic Science, University of Delhi South Campus, Delhi-110021, India*
[2] *Keshav Mahavidyalaya, University of Delhi, Delhi 110034, India*
* enakshi54@yahoo.co.in

We show that when a periodic sequence of Gaussian temporal light pulses propagates through a coaxial fiber each Gaussian pulse in the sequence splits into a series of narrow pulses within the broadened Gaussian envelope. However for a chosen repetition rate, the original Gaussian pulse sequence reappears.

Summary

Coaxial optical fibers [1] (Fig.1) support two symmetric modes (LP_{01} and LP_{02}) which at a certain wavelength (λ_o) have the same group velocity (v_o) and almost equal and opposite group velocity dispersion ($\pm\alpha_o$).When the coaxial fiber is excited by a periodic sequence of Gaussian temporal pulses (period T) of the form $f(t) = e^{j\omega_0 t}\left[E_0 e^{\frac{-t^2}{\tau_0^2}} * \frac{1}{T} Comb\left(\frac{t}{T}\right)\right]$ with $\omega_o = \frac{2\pi c}{\lambda_o}$ and $\tau_o = 1ps$,

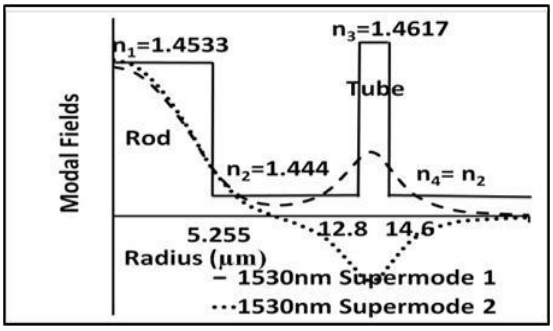

Fig. 1 Coaxial optical fiber and its modes

from a single mode fiber identical to the rod waveguide, both modes are excited [2] and due to same group delay, arrive at a distance, z, at the same time. If an output single mode fiber (identical to the input fiber) is spliced at any z, power from both the modes is coupled out and due to temporal interference between the spectral components, each Gaussian pulse splits into a series of narrow pulses within the broadened Gaussian envelope (Fig. 2). However if $T = \sqrt{2\alpha_o \pi z}$, defined as a " Talbot Revival Period" (TRP), the input sequence of pulses is reproduced, in general with a reduced amplitude. Further, in addition, if $z = \frac{2m\pi}{(\beta_1 - \beta_2)}$, (where $\beta_{1,2}$ are the propagation constants of the two modes, m is an integer) the amplitude of the pulses is also recovered. Fig. 3 shows the result at z=398m for which TRP is 25ps. The sequence of pulses with T=25ps is reproduced while at T=25$\pm$ 5ps, the pulses are distorted due to splitting and broadening (Fig. 3).

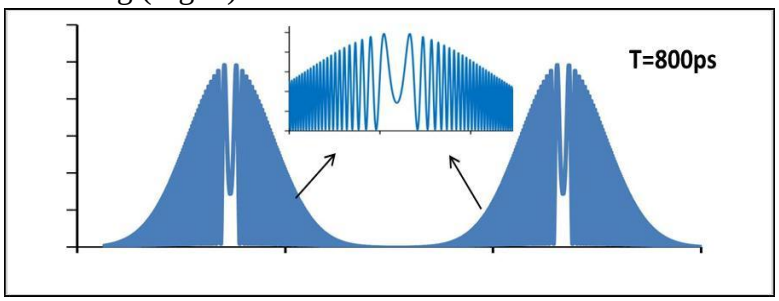

Fig. 2 Intensity of output pulse

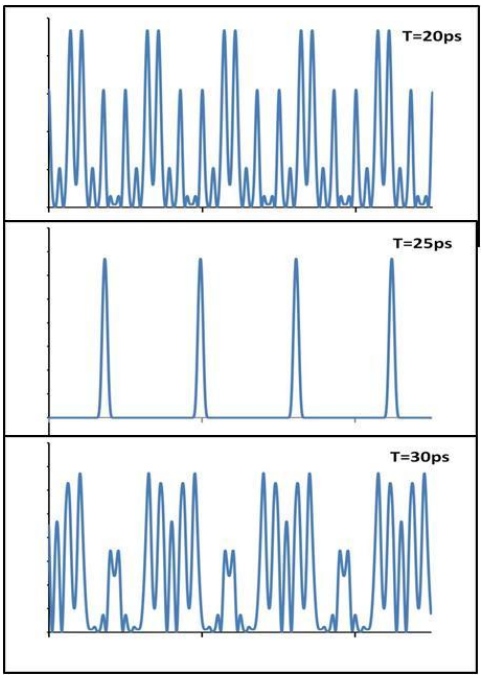

Fig. 3 Sequence of pulses at z=398m

References

[1] A C Boucouvalas, *J. Lightwave Technol.*, LT3, 1151-1158, 1985.
[2] Jyoti Anand, et al., *Optics & Laser Tech.*, 45, 688-695, 2012.

The Peculiarities of Optical Spectra of Photonic Crystal with Plasmonic Defect

S. G. Moiseev[1,2,3*], V. A. Ostatochnikov[1], D. I. Sementsov[1]
[1] *Ulyanovsk State University, Russia*
[2] *Ulyanovsk State Technical University, Russia*
[3] *Kotel'nikov Institute of Radio Engineering and Electronics of RAS, Ulyanovsk Branch, Russia*
* serg-moiseev@yandex.ru

Optical spectra of an artificial layered periodic structure with a finite number of periods and a plasmonic defect is analyzed. The case is considered when two orthogonal polarizations of an incident wave correspond to different plasmon resonance frequencies of the nanocomposite. If one of the plasmon frequencies coincides with the defect mode frequency in one of the photonic bandgaps, complete suppression of the defect mode in the transmission spectrum is possible, which makes the spectra of such structures polarization-sensitive.

In this work the possibility of using plasmonic nanocomposite with nonspherical inclusions as a tuning defect in a photonic crystal (PC) is considered and the features of the behavior of electromagnetic eigenmodes in an artificial layered periodic structure with a finite number of periods and a plasmonic defect are analyzed.

We consider a symmetric microcavity photonic crystal structure in which a nanocomposite layer is sandwiched between two dielectric photonic crystal mirrors inverted relative to one another. The structure has a double defect: inversion and inserted layer. The inversion is due to the change in the stacking sequence of the layers in going from one part of the structure to the other. The transfer matrix of the PC under consideration, with an inserted defect layer and two PC mirrors, has the form $\hat{G} = \hat{N}^a \hat{D} \hat{\bar{N}}^a$, where $\hat{N}^a = \left(\hat{N}_1 \hat{N}_2\right)^a$ and $\hat{\bar{N}}^a = \left(\hat{N}_2 \hat{N}_1\right)^a$ are the transfer matrices of defect-free PC mirrors having a periods. The PC mirrors have a finite number of structural periods, each consisting of two layers of isotropic dielectrics having permittivity ε_j and thickness L_j (j=1,2). We neglect absorption in the frequency range of interest, so ε_j is real-valued.

The defect layer in the PC structure under consideration consists of a nanocomposite, which has the form of a dielectric material containing evenly distributed metallic nanoparticles in the shape of ellipsoids of revolution. The nanoparticles are aligned with their polar axis parallel to the x axis. The nanocomposite has properties of a uniaxial crystal, and its effective permittivity is represented in the major axes by a diagonal tensor. The dependence of optical properties of the plasmonic defect on the geometric (shape and concentration of inclusions) and material (permittivities of the matrix and metal nanoparticles) parameters of composite are calculated within the Maxwell−Garnett effective-medium approximation.

It is shown, that reflection and transmission spectra of such defective periodic structure exhibit high polarization contrast. For radiation of the region near the spectral line of the defect mode, this PC absorbs the light polarized parallel to the long axis of spheroids, and for the light polarized parallel to the short axis of spheroids the structure is almost transparent. The performed analysis and the revealed features of wave characteristics of the PC with plasmonic defect can be used in the development of devices for the control of optical radiation on the basis of such structures.

This work was supported by the Russian Foundation for Basic Research and the Ministry of Education of the Russian Federation through project contracts within the framework of the Federal Target Program 'Science, Academic and Teaching Staff of Innovative Russia for 2009-2013'.

Manipulating light matter interaction with Mie resonators

G. Boudarham[1*], B. Rolly[1], B. Stout[1], R. Abdeddaim[1], J.M. Geffrin[1], N. Bonod[1]
[1]*Institut Fresnel, CNRS UMR 7249, Campus Universitaire de Saint-Jérôme, 13397 Marseille cedex 20, France*

* guillaume.boudarham@fresnel.fr

We explore the possibility to enhance and confine the magnetic near-field by using a dimer of dielectric resonators illuminated by a plane wave.

Electric and magnetic dipolar and quadrupolar Mie resonances in high-index dielectric particles exhibit high quality factor that compensates their low field confinement compared to the plasmon resonances of metallic particles [1]. In a host matrix of refractive index n=1.45, and when a dipolar electric or magnetic emitter is placed at the center of a dimer of Si spheres, we obtain enhancement factors of the magnetic versus electric decay rates of 4 around λ=1.54 µm [2], that could be interesting for manipulating decay rates of trivalent erbium ions (see Fig. 1 left). We derived the analytical expressions of the decay rates of an electric/magnetic dipole transition when coupled to an electric or magnetic dipolar or quadrupolar mode. We show that in parallel coupling, an electric mode (resp. magnetic) can increase the decay rates of both magnetic and electric dipoles. Motived by the results obtained by B. Rolly *et al* [2-3], we investigate in this contribution the reciprocal problem by studying the magnetic field enhancement within the nanogap of a dimer of dielectric resonators with moderate permittivity when illuminated by a plane wave [4].

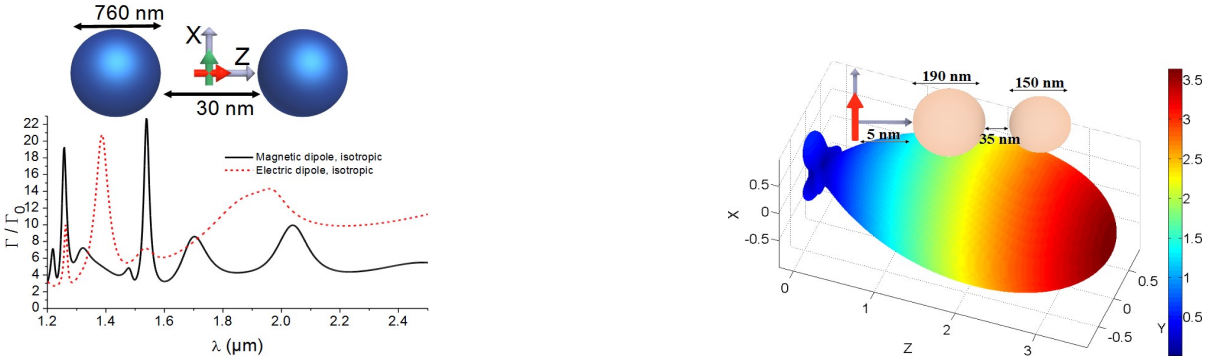

Fig 1: *left: isotropic averaged decay rates when an electric dipole (dashed red line) or magnetic dipole (solid black line) is placed in the centre of a Si dimer. right: radiation diagram at 570 nm of an electric dipole transversely coupled to two GaP spheres. Emission directivity is over 9 dBi.*

References

[1] A. García-Etxarri *et al*., "*Strong magnetic response of submicron Silicon particles in the infrared*," Optics Express 19, 4815-4826, 2011.
[2] B. Rolly *et al*., "*Promoting magnetic dipolar transition in trivalent lanthanide ions with lossless Mie resonances*", Physical Review B **85**, 245432, 2012.
[3] B. Rolly *et al*., "*Metallic dimers: When bonding transverse modes shine light*", Physical Review B **84**, 125420, 2011.
[4] G. Boudarham *et al*., submitted.

Discontinuous Galerkin Methods in Nano-Photonics

Kurt Busch
Humboldt-Universität zu Berlin, Institut für Physik, AG Theoretische Optik & Photonik, Newtonstr. 15, 12489 Berlin, and Max-Born-Institut, Max-Born-Str. 2A, 12489 Berlin, Germany
kurt.busch@physik.hu-berlin.de

The Discontinuous Galerkin Time-Domain Finite-Element approach and its applications to nano-photonic systems is reviewed. This includes technical aspects (curvilinear elements, graphic processors) as well as conceptual developments (electron energy loss spectroscopy, advanced material models).

Introduction

The past years have witnessed exciting developments in the area of time-domain computations of Maxwell's equations. In particular, the nodal Discontinuous Galerkin Time-Domain (DGTD) Finite-Element approach [1] has emerged as serious rival for the well-tested Finite-Difference Time-Domain (FDTD) approach. DGTD approaches are applied to a large variety of electro-magnetic and optical problems including ordinary and ground penetrating radar, wireless communication, electro-physiology, plasma physics, and nano-photonics.

In particular, the DGTD method inherits the adaptive spatial resolution via unstructured grids and high-order spatial discretization of ordinary Finite Element techniques and combines them with explicit and high-order time-stepping schemes. As a result, DGTD allows one to effectively deal with some of the fundamental challenges associated with many nano-photonic problems: Complex geometries and multiple time and length scales [2].

Discussion

For instance, the essentially exact numerics provided by the DGTD approach may be utilized for assessing approximate coupled mode schemes for complex geometries [3]. Further, DGTD facilitates the modeling of advanced spectroscopic settings such as electron energy loss spectroscopy [4] and this significantly contributes in the interpretation of experimental data [5].

These encouraging results suggest to extent further DGTD's range of applicability through the development of advanced material models that can be efficiently integrated into a DGTD frame-work. This includes certain plasmonic systems where magneto-optical effects provide effective means of tuning their optical response [6]. By the same token, certain plasmonic systems exhibit (potentially) strong nonlocal and/or nonlinear optical properties where the standard description of metals as isotropic dispersive linear materials fails.

References

[1] J. Hesthaven and T. Warburton, J. Comput. Phys. **181**, 186 (2002)

[2] K. Busch, M. König, and J. Niegemann, Laser Photonics Rev. **5**, 773 (2011)

[3] K.R. Hiremath, J. Niegemann, and K. Busch, Opt. Express **19**, 8641 (2011)

[4] C. Matyssek, J. Niegemann, W. Hergert, and K. Busch, Photon. Nanostruct. **9**, 367 (2011)

[5] F. von Cube et al., Opt. Mater. Express **1**, 1009 (2011); F. von Cube et al., Nano Lett., in press (2013)

[6] C. Wolff, R. Rodriguez-Oliveros, and K. Busch, submitted (2013)

Generalized Source Method in Curvilinear Coordinates

A.A. Shcherbakov [1], A.V. Tishchenko [2]

[1] *Laboratory NFE, Moscow Institute of Physics and Technology, Dolgoprudny, Russia*
[2] *Laboratory Hubert Curien, University of Lyon, Saint-Etienne, France*
alex.shcherbakov@phystech.edu

This paper presents an extension of the generalized source method to curvilinear coordinates for modeling grating diffraction on 1D gratings. The method demonstrates linear time and memory complexity relative to the mesh node number.

The generalized source method (GSM) was recently developed for the light diffraction calculation on 2D periodic arbitrary shaped dielectric structures [1]. The method demonstrated $O(N \log N)$ of both time and memory consumption overwhelming widely used modal methods that have $O(N^3)$ complexity (N is a mesh node number). It is well-known that the Maxwell's equations can be written in the affine-invariant form when all the metric information is hidden in the constitutive relations. This fact was extensively used in computational electrodynamics for describing perfectly matched layers [2], and for introduction of adaptive spatial resolution in the Fourier Modal Method (FMM) [3]. In the last case curvilinear coordinates allowed for better adaptation to spatial field distributions and consequent reliable modeling of metallic gratings. Aiming at adapting the GSM to metallic gratings simulation we reformulate the method in a curvilinear coordinate system which contains a coordinate surface either coinciding with the corrugation profile if the latter is smooth or close to the profile if it contains sharp edges. The figure demonstrates an example of curvilinear coordinates introduced in a bounded region containing the grating.

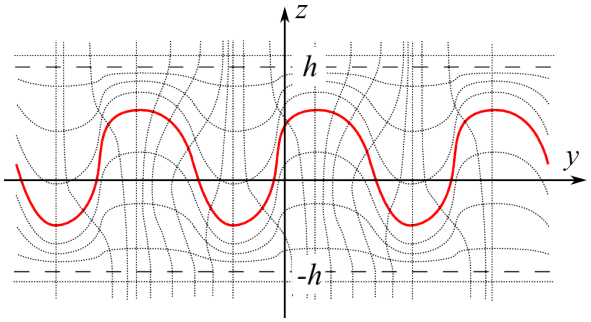

Illustrative example of curvilinear coordinates introduced inside a plane layer containing a 1D diffraction grating. One of coordinate surfaces coincides with the grating corrugation profile.

Acknowledgements

This work was supported in part by the Russian Ministry of Education and Science (agreement No. 14.A18.21.1946).

References

[1] A.A. Shcherbakov, A.V. Tishchenko, *New fast and memory-sparing method for rigorous electromagnetic analysis of 2D periodic dielectric structures,* JQSRT, 113, 158, 2012.
[2] W.C. Chew, W.H. Weedon, *A 3D perfectly matched medium from modified Maxwells equations with stretched coordinates,* Microwave Opt. Technol. Lett. 7, 599, 1994.
[3] G. Granet, *Reformulation of the lamellar grating problem through the concept of adaptive spatial resolution,* J. Opt. Soc. Am. A, 16, 2510, 1998.

Modified Optimal Variational Method to Study Modal Characteristics of Si Photonic Wire Waveguides

Kanchan Gehlot, Anurag Sharma

Department of Physics, Indian Institute of Technology Delhi, New Delhi 110 016, India
gehlot.kanchan@gmail.com, asharma@physics.iitd.ac.in

Earlier developed scalar VOPT method [1] is modified and a semi-vector approach is developed to study vector modes of high index contrast Si photonic wire waveguides. This iterative method is simple, fast and gives very accurate results.

Summary

In development of Si nanophotonics, Si photonic wire waveguide has emerged as a building block of various optical devices and interconnects for optoelectronic integrated circuits. High-index contrast and structural asymmetry of Si photonic wire waveguides give rise to large modal birefringence and it becomes essential to carry out vector mode analysis for the waveguide. Modified VOPT method is presented to provide an accurate semi-vector analysis of vector modes. This method uses a procedure similar to scalar VOPT to arrive at an iterative scheme for semi-vector wave equation. Accuracy of this method is tested by comparing present analysis with FEM results [2]. The waveguide considered in this paper consists of rectangular Si core surrounded by air cladding. At the operating wavelength of 1.55 μm, Si refractive index is taken as 3.50. For core height of 260 nm, fundamental E^x and E^y modes are calculated for wide range of waveguide width. In Fig. 1, variation of effective mode index, $n_{eff} = \beta/k$ for E^x_{11}, E^y_{11} mode and modal birefringence with waveguide width are plotted. Modal birefringence is defined as difference in n_{eff} of E^x_{11} and E^y_{11} mode. The comparison with FEM results shows that present method gives accurate results even for modes close to cut-off.

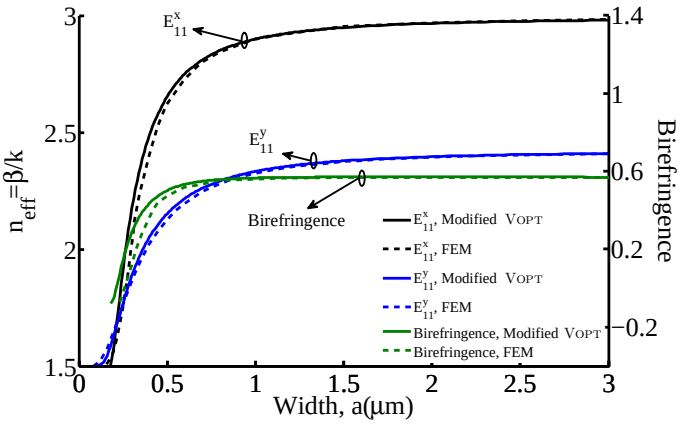

Fig. 1. Variation of n_{eff} for E^x_{11} and E^y_{11} modes (left scale) and modal birefringence (right scale) with width of waveguide core, a

This work was supported by grant from Council of Scientific and Industrial Research (CSIR), Govt. of India.

References

[1] A. Sharma, *Opt. Quant. Electron* **21**, 517–520 (1989)
[2] D. M. H. Leung et al. *Opt. Exp.*, **18**, 8528–8539 (2010)

Back-reflector optimization in thin-film silicon solar cells by rigorous FEM light propagation modeling

M. Blome [1], K. McPeak [2], S. Burger [1], F. Schmidt [1]

[1] *Computational Nano-Optics, Zuse Institute Berlin, Germany*
[2] *Optical Materials Engineering Laboratory, ETH Zürich, Switzerland*
blome@zib.de

We numerically optimize the light trapping efficiency of a periodic, pyramid structured back metal contact in thin-film amorphous silicon solar cells by rigorously solving Maxwell's equations. Identified optimal back contact geometries display a significant increase in short circuit current density over flat solar cells.

Introduction

Thin-film amorphous silicon based solar cells are an attractive design for providing cost-effective and efficient solar energy. Amorphous hydrogenated silicon (a-Si:H) can be deposited in thin layers on cheap substrate materials such as glass or plastic offering low fabrication costs suitable for mass production. Considering the large absorption length of amorphous silicon near its bandgap, the low absorber layer thicknesses typically employed necessitate light-trapping concepts for realizing efficient thin-film silicon solar cells.

Methodologies

Within this work we optimize geometry parameters of a periodic, pyramid structured back metal contact in a model (p-i-n type) thin-film solar cell. Our goal is to find optimal model parameters that considerably increase the solar cells light trapping efficiency compared to flat designs. We model the light propagation inside the investigated solar cell model using a frequency domain finite element Maxwell solver employing high order edge elements and adaptive perfectly matched layers for realizing transparent boundary conditions. To judge the efficiency of different solar cell models we compare computed short circuit current densities and reflection spectra.

For accurately predicting the material layer interfaces within the investigated solar cell model we employ a topology simulation method. The method simulates the chemical vapor deposition process that is typically used to fabricate thin-film solar cells by combining a ballistic transport and reaction model with a level-set method in an iterative approach.

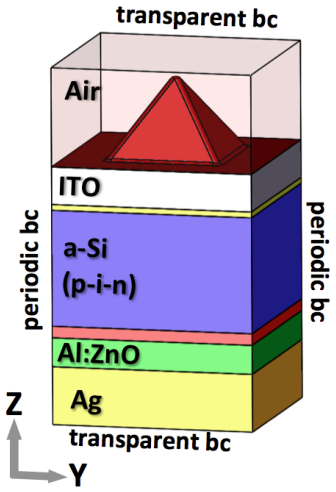

Sample CAD representation of the model (p-i-n type) solar cell considered.

Conclusions

In using our optimization approach we have identified nanostructured back reflector geometries that display a significant increase in short circuit current density over flat back reflectors. The employed topology simulation approach yield solar cell models that represent a far more realistic approximation to a real solar cell stack compared to solar cell models created by the frequently used conformal material layer growth assumption.

Tailoring meta-atoms for specific metamaterial applications

F. Lederer, S. Mühlig, C. Rockstuhl, R. Alaee, and C. Menzel
Institute of Condensed Matter Theory and Solid State Optics, Abbe Center of Photonics, Friedrich-Schiller-Universität Jena, Germany
falk.lederer@uni-jena.de

A strategic aim in contemporary optics is the desired control of light. Potentially this goal can be met by using metamaterials. We show how meta-atoms can be tailored to achieve various optical functionalities by a suitable multipole analysis of the scattered field.

Metamaterials are made of periodically or randomly arranged meta-atoms. Their optical properties are determined both by the arrangement and the shape of the respective meta-atoms. Sometimes a single meta-atom or an ensemble of a few of them provides also exciting functionalities, as e.g. optical nanoantennas. Thus there is an urgent requirement to develop tools that permit the control of the light field by tailoring the meta-atoms.
We describe here how to analyze the scattering response of individual meta-atoms in terms of multipole contributions. As a consequence the meta-atom can be modified such that particular multipole contributions are present or disappear depending on the envisaged functionality.
The scattered field of a selected meta-atom, calculated by rigorous means as FDTD, FEM, or FMM, is expanded into multipole contributions in spherical coordinates. These multipole moments are then transformed into their Cartesian counterparts. Thus the scattered field can be ultimately decomposed into contributions from arbitrary electric and magnetic multipole moments [1,2].

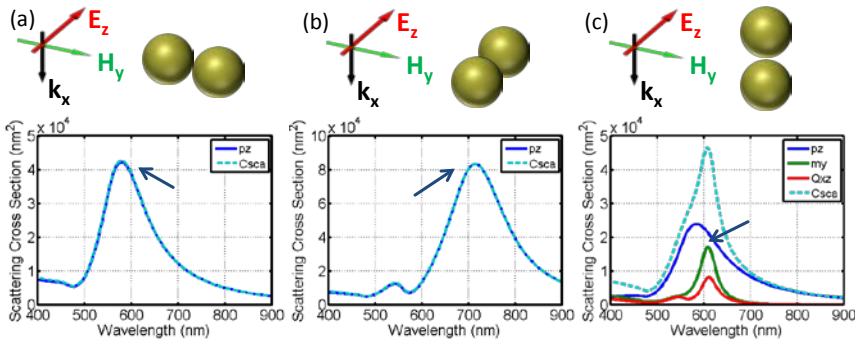

Contributing multipole moments to the scattered field of a gold dimer structure (radius = 40 nm, center-to-center distance = 83 nm) embedded into a dielectric host material (ε = 2.25) for three distinct illumination scenarios with a plane wave (a)-(c).

We use this powerful and versatile technique to design isotropic metamaterials consisting of both periodically (top down) and randomly (bottom up) arranged metaatoms. We show further that these metamaterials may be characterized by assigning genuine material parameters (permittivity and permeability) which do not depend on the wave vector of the exciting field (spatial dispersion) as it is usually the case. This can be achieved by tailoring the meta-atoms such that they exhibit only electric and magnetic dipole moments. A deep-subwavelength periodic or a random arrangement is further required to suppress spatial dispersion. It is also shown how nanoantennas can be designed the near-field of which contains a dominant quadrupole contribution thus fostering the excitation of dipole forbidden transitions in atomic systems.

References

[1] S. Mühlig, C. Menzel, C. Rockstuhl, and F. Lederer, *Multipole Analysis of Meta-Atoms*, Metamaterials 5, 64 (2011).
[2] C. Rockstuhl et al., *Scattering Properties of Meta-Atoms*, Phys. Rev. B83, 245119 (2011).

Lens equation for flat lenses made with hyperbolic metamaterials

J. Benedicto [1,2], E. Centeno [1,2], A. Moreau [1,2],

[1] *Université Blaise Pascal, Institut Pascal, BP 10448, F-63000 Clermont-Ferrand, France*
[2] *CNRS UMR 6602, F-63171 Aubière, France*
jessica.benedicto1@univ-bpclermont.fr

We give a general theory that enables the design of flat lenses based on hyperbolic metamaterials. The focal length can be finely controlled, and the losses are minimized by reducing drastically the amount of metal used. Super-resolution is obtained with a transmittance around 20 %.

Metamaterials are artificial medium with electric and magnetic effectif response that can be finely tuned. Pendry 's pioneer work, showing that a slab of such a material could be considered a perfect flat lens [1], is the best example of what can be achieved using such materials. Some metamaterials actually present a hyperbolic dispersion relation that allows for a self-collimation effect studied by P. Belov [2]. Near-field subwavelength images can be formed using hyperbolic metamaterials, which can be achieved by stacking dielectric and metallic layers. However, the flat lenses studied so far present a zero focal distance: the object and the image are formed at the very edge of the flat lens. Another way to stack the layers is to organize them in concentric circles. This forms an hyperlens, able to provide far-field images with subwavelength resolution [3].

In this study, a Fourier optics model is developed, providing a lens equation for flat lenses made of hyperbolic metamaterials. We demonstrate that, using a source on the edge of the lens, the focus can be arbitrarily chosen in a range extending from the very edge of the lens to one wavelength [4]. The numerical results show that the subwavelength resolution is preserved for a focal length below $\frac{\lambda}{2}$. Our approach even leads to an overall improvement of the transmission efficiency (the transmittance can be as high as 20%) of such lenses despite the optical losses induced by the metallic layers.

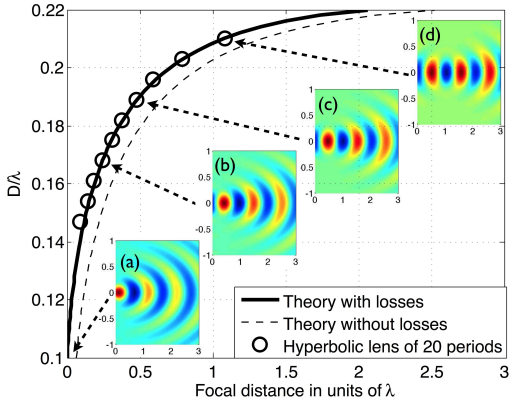

Variation of the focal distance as a function of the reduced frequency for a hyperbolic lens (20 periods). Theoretical calculations (solid line and circles) and full numerical simulations. (a-d) Field plot of the magnetic field. The focus is at a distance of 0, $\frac{\lambda}{4}$, $\frac{\lambda}{2}$ and λ of the edge.

References

[1] J.B. Pendry, *Negative Refraction Makes a Perfect Lens,* Physical Review Letters **85**, (18), 3966,2000.
[2] P.A. Belov, Y. Hao, *Subwavelength imaging at optical frequencies using a transmission device formed by periodic layered metal-dielectric structure operating in the canalization regime,* Physical Review B **73**, 113110,2006.
[3] Z. Liu, H.Lee, Y. Xiong, C. Sun, X. Zhang, *Far-field optical hyperlens magnifying sub-diffraction limited objects,* Science **315**, (5819), 1686, 2007.
[4] J. Benedicto, E. Centeno and A. Moreau, *Lens equation for flat lenses made with hyperbolic metametrials,* Optics Letters **37**, (22), 2012.

Tailoring the quadratic response of nanoantennas: use of a waveguide model

Shakeeb Bin Hasan*, Christoph Etrich, Robert Filter, Carsten Rockstuhl, and Falk Lederer
Institute of Condensed Matter Theory and Solid State Optics, Abbe Center of Photonics, Max-Wien-Platz 1, 07745 Jena, Germany. Tel. +49 3641 947179, Fax. +49 3641 947177
* shakeeb-bin.hasan@uni-jena.de

We employ a phenomenological model based on guided modes to access the localized resonances of plasmonic nanoantennas. It provides a systematic means to tune the resonance frequencies of antennas. In terms of quadratic nonlinearity, it is successfully exploited to achieve double resonant nanoantennas at both the fundamental and the second harmonic frequency to significantly boost the nonlinear interaction.

Unlike Kerr optical effect, which involves single frequencies, the majority of nonlinear processes involve multi-frequency interaction. These processes are significantly enhanced in plasmonic antennas, promoted by a subwavelength field confinement when the system sustains a resonance at one of the frequencies involved. The overall efficiency, however, could be further enhanced by achieving resonance at all involved frequencies. To this end, we consider the degenerate second harmonic generation in the presence of a dielectric medium exhibiting a strong $\chi^{(2)}$ nonlinearity ($LiNbO_3$). Without any loss of generality, we choose cylindrical metal wires as the geometry for the nanoantenna due to its amenability to both analytical and experimental studies. While more complicated antenna designs have been recently suggested for multiple resonances, we exploit the additional degree of freedom provided in terms of antenna termination for this purpose [Fig. 1(a)].

We view the localized resonances as standing-waves generated by the oscillations of guided modes supported by the cylindrical metal wire. Therefore, computing the modal dispersion and reflection coefficient of the guided mode provides us with all the data to locate the resonances supported by the structure. Allowing for resonances of different orders at fundamental harmonic (FH) and second harmonic (SH), we are able to identify frequency bands where these resonances appear at the FH and its corresponding SH. Figures 1(b-c) present one example in which double resonance is achieved for both FH (1st order) and SH (3rd order) to the betterment of the nonlinear interaction.

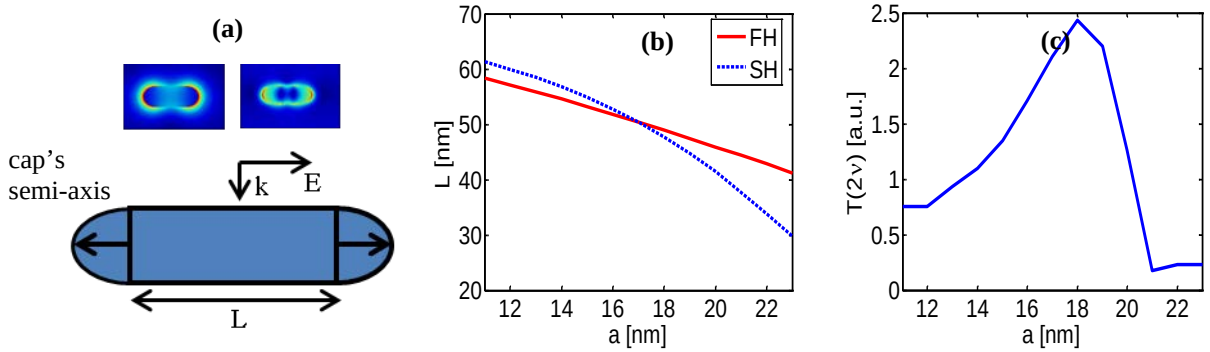

Figure 1: (a) Antenna geometry highlighting relevant geometrical features. Also shown is the amplitude distribution of the first and third order Fabry-Perot resonances FH and SH. (b) Antenna length and cap radius at which FH has 1st order (red) and SH has 3rd order (blue) resonances for the incident frequency ν_{FH} = 276THz. (c) SH transmission computed with the nonlinear FDTD at ν_{FH} = 276THz. FH is always kept resonant according to (b) but SH is resonant only when a = 17nm.

References:

[1] M. Ren, E. Plum, J. Xu, N. I. Zheludev, Nature Communications **3**, 833 (2012).
[2] M. Hentschel, T. Utikal, H. Giessen, M. Lippitz, Nano Lett. **12**, 3778 (2012).

Transmission of optical excitations through a linear chain of metal nanoparticles in the presence of a reflector

P.J. Compaijen, V.A. Malyshev, J. Knoester.

Zernike Institute for Advanced Materials, University of Groningen, Groningen, The Netherlands
p.j.compaijen@rug.nl

We study the transmission efficiency of optical signals in a linear chain of silver nanospheres in close proximity to a silver substrate and show that the coupling between surface plasmon polariton modes in the chain and on the interface enhances this efficiency. Studying the influence of the chain-interface spacing and polarization of the excitation, reveals a complicated interplay between several transmission channels.

Linear chains of Metal NanoParticles (MNPs) have been suggested for applications in nano-circuitry and nano-antennas (see, e.g., Ref. [1]). It has been shown that for such systems, the collective modes are Surface Plasmon Polaritons (SPPs) [2, 3]. The presence of a reflecting object in the proximity of the array may have a large influence on the collective modes of the chain and, therefore, on its ability to transmit optical signals. To explore this effect, we performed calculations of the dispersion relations and the Transmission Efficiency (TE), i.e. the ratio of the modulus squared of dipole moments of the last to the first MNP, assuming CW excitation of only the first particle.

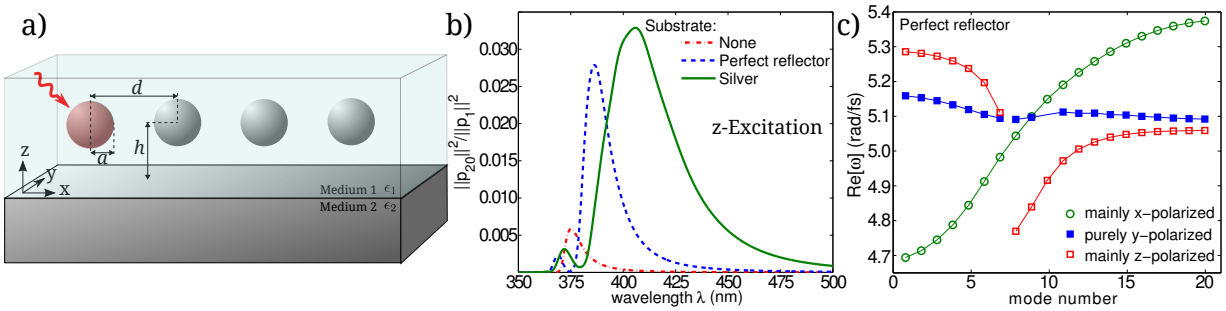

Fig. 1. a) Schematics of the system under consideration. b) TE for a chain of 20 MNPs with $a = 25$ nm, $d = 75$ nm and $h = 50$ nm for a chain over no substrate, a perfect reflector and a silver substrate. c) Dispersion relations for this chain over a perfect reflector.

Figure 1 shows that the presence of a reflector gives rise to an enhancement and an extra peak in the TE spectrum and that the main peak is red-shifted with respect to that of the isolated chain. The maximum transmission will occur for the mode with the highest group velocity (i.e. steepness of the dispersion curve) and the longest lifetime (not shown). This makes the calculation of dispersion relations a valuable tool for optimizing and understanding the TE. Interestingly, the silver substrate appears to give a stronger enhancement than a perfectly reflecting substrate, due to the possibility to decay into SPP modes of the silver substrate, which is manifested in both a broadening and an increase of the maximum transmission. Understanding the coupling between the SPP modes of the chain and the substrate, will allow to carefully manipulate the guiding properties of the MNPs.

References

[1] L. Novotny, B. Hecht, *Principles of Nano-Optics,* Cambridge University Press (2006).
[2] W.H. Weber, G.W. Ford, Physical Review B, **70**, 125429 (2004).
[3] A.F. Koenderink, A. Polman, Physical Review B, **74**, 033402 (2006).

Integrated Quantum Photonics

K. Aungskunsiri, D. Bonneau, J. Carolan, D. Fry, J. Hadden, S. Ho, J. Kennard, S. Knauer, E. Martin-Lopez, J. Meinecke, G. Mendoza, J. Munns, M. Piekarek, K. Poulios, X. Qiang, N. Russell, R. Santagati, A. Santamato, P. Shadbolt, P. Sibson, J. Silverstone, O. Snowdon, N. Tyler, J. Wang, C. Wilkes, S.R. Whittaker, J. Barreto, D. Beggs, X. Cai, P. Jiang, A. Laing, J.C.F. Matthews, G.D. Marshall, A. Peruzzo, X.-Q. Zhou, J.G. Rarity, M.G. Thompson, J.L. O'Brien and collaborators

Centre for Quantum Photonics, H.H. Wills Physics Laboratory
& Department of Electrical and Electronic Engineering, University of Bristol
www.phy.bris.ac.uk/groups/cqp

Quantum information science aims to harness uniquely quantum mechanical properties to enhance measurement, information and communication technologies, as well as to explore fundamental aspects of quantum physics. Of the various approaches to quantum computing [1], photons are particularly appealing for their low-noise properties and ease of manipulation at the single qubit level [2]. Encoding quantum information in photons is also an appealing approach to other quantum technologies [3], including quantum communication, metrology [4] and measurement [5]. We have developed an integrated waveguide approach to photonic quantum circuits for high performance, miniaturization and scalability [6–10]. We have begun to address the challenges of scaling up quantum circuits using new insights into how controlled operations can be efficiently realised [11], and demonstrated Shor's algorithm with consecutive CNOT gates [12] and the iterative phase estimation algorithm [13]. We have shown how quantum circuits can be reconfigured, using thermo-optic phase shifters to realise a highly reconfigurable quantum circuit able to perform almost any function on two photonic qubits [14], and electro-optic phase shifters in lithium niobate to rapidly manipulate the path and polarisation of telecomm wavelength single photons [15]. We have addressed miniaturisation using multimode interference coupler architectures to directly implement NxN Hadamard operations and the 'Boson sampling problem' [16], and by using high refractive index contrast materials such as SiO_x N_y , in which we have implemented quantum walks of correlated photons [17], and Si [18], in which we have demonstrated generation of orbital angular momentum states of light [19]. We have incorporated microfluidic channels for the delivery of samples to measure the concentration of a blood protein with entangled states of light [20]. We have begun to address the integration of superconducting single photon detectors [21] and diamond [22,23] and non-linear [24–6] single photon sources. Finally, we give an overview of recent work on fundamental aspects of quantum measurement, including a quantum version of Wheeler's delayed choice experiment [27].

References

[1] T. D. Ladd, F. Jelezko, R. Laflamme, Y. Nakamura, C. Monroe, and J. L. OBrien, ***Nature* 464**, 45 (2010).
[2] J. L. O'Brien, ***Science* 318**, 1567 (2007).
[3] J. L. O'Brien, A. Furusawa, and J.Vuckovic, ***Nature Photon.* 3**, 687 (2009).
[4] T. Nagata, R. Okamoto, J. L. O'Brien, K. Sasaki, and S. Takeuchi, ***Science* 316**, 726 (2007).
[5] R. Okamoto, J. L. O'Brien, H. F. Hofmann, T. Nagata, K. Sasaki, S. Takeuchi, ***Science* 323**, 483 (2009).
[6] A. Politi, M. J. Cryan, J. G. Rarity, S. Yu, and J. L. O'Brien, ***Science* 320**, 646 (2008).
[7] A Laing, A Peruzzo, A Politi, MR Verde, M Halder, TC Ralph, MG Thompson, JL O'Brien, ***Appl. Phys. Lett.* 97**, 211109 (2010)
[8] J. C. F. Matthews, A. Politi, A. Stefanov, and J. L. O'Brien, ***Nature Photon.* 3**, 346 (2009).
[9] A. Politi, J. C. F. Matthews, and J. L. O'Brien, ***Science* 325**, 1221 (2009).
[10] J. C. F. Matthews, A. Peruzzo, D. Bonneau, and J. L. O'Brien, ***Phys. Rev. Lett.* 107**, 163602 (2011)

[11] X-Q Zhou, TC Ralph, P Kalasuwan, M Zhang, A Peruzzo, BP Lanyon, and JL O'Brien, ***Nature Comm.*** **2** 413 2011

[12] E Martín-López, A Laing, T Lawson, R Alvarez, X-Q Zhou, JL O'Brien ***Nature Photon.*** doi:10.1038/nphoton.2012.259

[13] X.-Q. Zhou, P. Kalasuwan, T. C. Ralph, J. L. O'Brien, ***Nature Photon.*** in press; arXiv:1110.4276

[14] PJ Shadbolt, MR Verde, A Peruzzo, A Politi, A Laing, M Lobino, JCF Matthews, MG Thompson, JL O'Brien, ***Nature Photon.*** **6**, 45 (2012).

[15] D. Bonneau, *et al.* ***Phys. Rev. Lett.***, 108, 053601 (2012)

[16] A. Peruzzo, A. Laing, A. Politi, T. Rudolph, and J. L. O'Brien, ***Nature Comm.*** **2,** 224 (2011)

[17] A. Peruzzo, M. Lobino, J. C. F. Matthews, N. Matsuda, A. Politi, K. Poulios, X.-Q. Zhou, Y. Lahini, N. Ismail, K. Worhoff, Y. Bromberg, Y. Silberberg, M. G. Thompson, and J. L. O'Brien, ***Science*** **329**, 1500 (2010)

[18] D Bonneau, E Engin, K Ohira, N Suzuki, H Yoshida, N Iizuka, M Ezaki, CM Natarajan, MG Tanner, RH Hadfield, SN Dorenbos, V Zwiller, JL O'Brien, MG Thompson, ***New J. Phys.*** **14** 045003 (2012)

[19] X Cai, J Wang, MJ Strain, B Johnson-Morris, J Zhu, M Sorel, JL O'Brien, MG Thompson, S Yu ***Science*** **338**, 363 (2012)

[20] A. Crespi, M. Lobino, J. C. F. Matthews, A. Politi, C. R. Neal, R. Ramponi, R. Osellame, J. L. O'Brien, ***Appl. Phys. Lett.*** **100**, 233704 (2012).

[21] C. M. Natarajan, A. Peruzzo, S. Miki, M. Sasaki, Z. Wang, B. Baek, S. Nam, R. H. Hadfield, and J. L. O'Brien, ***Appl. Phys. Lett.*** **96**, 211101 (2010).

[22] J. P. Hadden, J. P. Harrison, A. C. Stanley-Clarke, L. Marseglia, Y.-L. D. Ho, B. R. Patton, J. L. OBrien, and J. G. Rarity, ***Appl. Phys. Lett.*** **97**, 241901 (2010)

[23] L. Marseglia, J. P. Hadden, A. C. Stanley-Clarke, J. P. Harrison, B. Patton, Y.-L. D. Ho, B. Naydenov, F. Jelezko, J. Meijer, P. R. Dolan, J. M. Smith, J. G. Rarity, J. L. O'Brien, ***Appl. Phys. Lett.*** **98**, 133107 (2011)

[24] C. Xiong, *et al.* ***Appl. Phys. Lett.*** **98**, 051101 (2011)

[25] M. Lobino, *et al*, ***Appl. Phys. Lett.*** **99**, 081110 (2011)

[26] E. Engin, *et al.* arXiv:1204.4922

[27] A. Peruzzo, P. Shadbolt, N. Brunner, S. Popescu J. L. O'Brien ***Science*** **338**, 634 (2012)

Looking in and through opaque material

Willem L. Vos

Complex Photonic Systems (COPS), MESA+ Institute for Nanotechnology, University of Twente, P.O. Box 217, 7500 AE Enschede, The Netherlands

Random multiple scattering of light is of fundamental physical interest and of great relevance for applications, as is apparent from the fact that it is readily observed in paper, paint, and biological tissue. From a theoretical perspective [1], light scattering allows the study of interference effects such as Anderson localization [2], the study of open transport channels in opaque media [3], and study of speckle correlations [4]. The importance of scattering to applications is obvious as scattering forms an obstacle to conventional high-resolution imaging and focusing.

Recently, the realization has arisen in Twente that the propagation of laser light in opaque scattering media can be controlled by shaping the incident wave front [5]. Such control is based on the realization that scattering by stationary media corresponds to a random linear transformation of incident light modes. Wave front shaping effectively inverts this transform. These advances have given rise to a surge of fundamental studies of light propagation and new modalities of imaging and focusing through and inside random photonic media [6-9]. These methods usually require some kind of calibration, such as the measurement of a transmission matrix [10], to characterize the scattering medium before imaging is possible [11].

We have demonstrated the use of speckle correlations to image objects through strongly scattering opaque layers without any invasive calibration [12]. This is the first ever high-resolution imaging method that uses only scattered light. We scan the angle of incidence of the light on the scattering layer, and record the resulting diffuse fluorescence from the object. Due to fluctuations in the overlap between the scattered speckle and the object the fluorescent signal fluctuates. These fluctuations contain sufficient information to allow us to obtain a high-resolution image of a small object with a typical size comparable to a cell. We will discuss the rapid progress in the development of imaging methods.

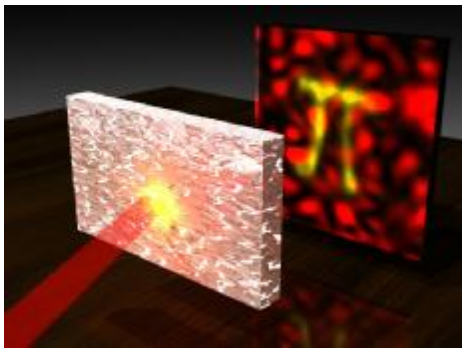

Figure 1*. Laser light that is incident on a strongly scattering screen is transmitted as a random speckle pattern. Speckle correlations can be used to focus light and retrieve image information, see Reference 12.*

References

[1] C. W. J. Beenakker, "*Random-matrix theory of quantum transport*," Rev. Mod. Phys. **69,** 731-808 (1997)
[2] A. Lagendijk, B. van Tiggelen, and D. S. Wiersma, "*Fifty years of Anderson localization*," Phys. Today **62**, 24 (2009).
[3] I. M. Vellekoop and A. P. Mosk, "*Universal Optimal Transmission of Light Through Disordered Materials*," Phys. Rev. Lett. **101,** 120601 (2008).
[4] E. Akkermans and G. Montambaux, "*Mesoscopic Physics of Electrons and Photons*," Cambridge University Press, 2007.
[5] I. M. Vellekoop and A.P. Mosk, "*Focusing coherent light through opaque strongly scattering media*," Opt. Lett. **32** 2309-2311 (2007).
[6] A. P. Mosk, A. Lagendijk, G. Lerosey, and M. Fink, "*Controlling waves in space and time for imaging and focusing in complex media*," Nature Photon. **6,** 283-292 (2012).
[7] O. Katz, E. Small and Y. Silberberg, "*Looking around corners and through thin turbid layers in real time with scattered incoherent light*," Nature Photonics **6**, 549-553 (2012).
[8] C. Hsieh, Y. Pu, R. Grange, G. Laporte, and D. Psaltis, "*Imaging through turbid layers by scanning the phase conjugated second harmonic radiation from a nanoparticle*," Opt. Express **18**, 20723-20731 (2010).
[9] T. Cizmár, M. Mazilu, and K. Dholakia, "*In situ wavefront correction and its application to micromanipulation*," Nat. Photon. **4**, 388 (2010).
[10] S. M. Popoff, G. Lerosey, R. Carminati, M. Fink, A. C. Boccara, and S. Gigan, "*Measuring the Transmission Matrix in Optics: An Approach to the Study and Control of Light Propagation in Disordered Media*," Phys. Rev. Lett. **104,** 100601 (2010).
[11] I. Freund, "*Looking through walls and around corners*," Physica A **168**, 49 (1990).
[12] J. Bertolotti, E. G. van Putten, C. Blum, A. Lagendijk, W. L. Vos, and A. P. Mosk, "*Non-invasive imaging through opaque scattering layers*," Nature **491**, 232–234 (2012).

Intriguing relations between "pseudo-Brewster incidence" and the plasmon mode at a metal surface.

A.V. Tishchenko, O. Parriaux
Laboratoire Hubert Curien UMR CNRS 5516, Université de Lyon à St-Etienne, F-42000 Saint-Etienne
* parriaux@univ-st-etienne.fr

There is nothing common between the "pseudo-Brewster condition" and the plasmon at a metal surface. Yet two puzzling features suggest that there is. What does it mean ?

Nothing common…

The so-called "pseudo-Brewster" incidence condition shows as a reflection minimum of a TM plane wave from a metal surface at a definite incidence angle θ_M [1]. The plasmon mode is a slow wave guided at the metal surface with a field which is purely evanescent in both adjacent media. One wave is above the light line, the other one below.

… yet two intriguing features

The ***first intriguing feature*** (Fig. 1) is the fact that the product of the effective index n_e of the plasmon mode by the horizontal projection of the incident wave k/k_0-vector $sin\theta$ in air is always very close to *1* at $\theta=\theta_M$ whatever the metal. By using the expression of the plasmon effective index n_e and finding out the incidence angle of minimum Fresnel reflection θ_M , this product is given by the following expression which is close to 1 for most metals since $\mathrm{Re}(\varepsilon_m)$ is negative:

$$n_e^2 \sin^2\theta_M = 1 - (\mathrm{Re}(\varepsilon_m) + |\varepsilon_m| + 4)/|\varepsilon_m|^2 \qquad (1)$$

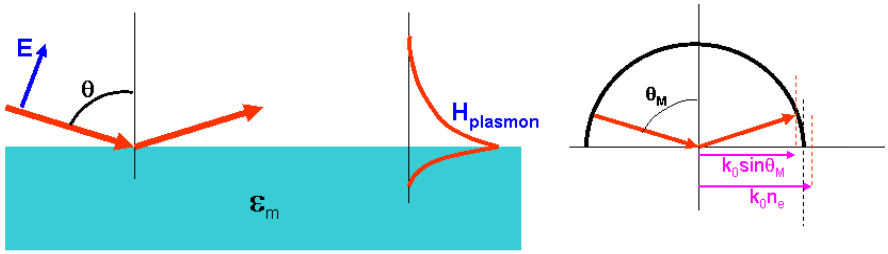

Fig. 1 Incident plane wave and plasmon fields. Right: the spatial frequencies whose product is k_0.

A ***second intriguing feature*** is that at the condition of minimum reflection, $\theta=\theta_M$, the reflection coefficient is purely imaginary, i.e., there is perfect matching between the line characteristic impedance (incident wave) and the load impedance. Pushing further and expressing the impedances as the normal components of the k-vector of the plane wave $k_0 cos\theta$ and of that, imaginary, of the plasmon, $k_0(1- n_e^2)^{1/2}$, and equating their modulus, leads to the simple analytical expression for θ_M:

$$\cos\theta_M = 1/(|1 + \varepsilon_m|)^{1/2} \qquad (2)$$

This expression fits with the numerical reflection minimum within much better than 1 degree with gold, silver, aluminium, nickel and even chromium in the visible and also with copper at 10.6 μm. Why two phase-mismatched waves of different nature show somehow related characteristics is still an interrogation for the authors who wish to submit the case to the attendance.

References

[1] A. Alsamman and R. M. A. Azzam, J. Opt. Soc. Am. A, Vol. 27, p. 1156 (2010)

Modelling of plasmonic waveguides

Z. Han and S. I. Bozhevolnyi*

Department of Technology and Innovation, University of Southern Denmark, Odense, Denmark

** seib@iti.sdu.dk*

Modelling of plasmonic waveguides is overviewed, considering different approaches for the description of strongly confined surface plasmon-polariton modes in various guiding configurations and paying special attention to accurate calculation of bending loss and optimization of the bending radius.

Recent years have seen an explosion of research into plasmonics instigated by a great promise of enabling energy-effective and highly-integrated optical interconnects that would exploit a special type of electromagnetic waves called surface plasmon-polaritons (SPP) propagating along and being controlled by metal circuitry, while also being strongly confined (beyond the diffraction limit) in the lateral cross section [1,2]. Modelling of SPP waveguides is an essential part of the development of SPP-based circuitry that allows one to properly choose the waveguide parameters in order to minimize the footprints of plasmonic components while keeping inevitable insertion losses associated with the radiation absorption by metals at an acceptable level. In this talk we overview different approaches to modelling of SPP waveguides paying special attention to the issue of bending loss. The latter determines not only the footprint but also the properties (e.g. quality factor is a ring resonator) of optical devices. For plasmonic waveguides, the bending loss comes from both propagation loss and radiation loss, which result in general an optimal bending radius in terms of transmission through the bends. The numerical calculation of bending loss can be achieved using the traditional method of conformal mapping of the refractive index in the bending area or using numerical simulations in the cylindrical coordinates. Here, we present the numerical results on the bending loss of some representative plasmonic waveguides [3] using the recently proposed transformation optics method [4]. A 90-degree bend of plasmonic waveguides in one Cartesian coordinates is conformably transformed to a straight waveguide in another Cartesian coordinates. The transmission through the 90-degree bends in different plasmonic waveguides can be calculated in the second coordinates, allowing us to determine the optimal bending radius.

References

[1] D. K. Gramotnev and S. I. Bozhevolnyi, *Plasmonics beyond the diffraction limit*, Nature Photonics **4**, 83 (2010).

[2] *Plasmonic Nanoguides and Circuits*, S. I. Bozhevolnyi, ed. (Pan Stanford, 2009).

[3] Z. Han and Sergey I. Bozhevolnyi, *Radiation guiding with surface plasmon polaritons*, Reports on Progress in Physics **76**, 016402 (2013).

[4] J. B. Pendry, D. Schurig, and D. R. Smith, *Controlling Electromagnetic Fields*, Science **312**, 1780 (2006).

Plasmon–soliton waves: towards realistic modelling

W. Walasik [1,2], Y. Kartashov [2], G. Renversez [1],

[1] *Institut Fresnel, CNRS, Université d'Aix-Marseille, Campus de St. Jérôme, 13013 Marseille, France*
[2] *ICFO, Universitat Politècnica de Catalunya, 08860 Castelldefels (Barcelona), Spain*
gilles.renversez@fresnel.fr

We study plasmon–soliton waves in multilayer nonlinear dielectric-metal planar structures using several improved vector models. We present, for the first time, low power plasmon–solitons in structures compatible with fabrication technology of chalcogenide waveguides.

Motivation

Nonlinear plasmon–soliton waves were predicted theoretically more than thirty years ago [1] and still attract a lot of attention [2]. Nevertheless, no experimental demonstration has been published so far due to the non-physically high power required. Our study is aimed to bring better understanding of the nature of plasmon–solitons and therefore facilitate the experimental observation of plasmon–solitons in realistic structures made of Kerr nonlinear dielectric, linear dielectric and metal.

Modelling plasmon–solitons

We use two complementary vector models based on Maxwell's equations to compute the nonlinear dispersion relation, the field profiles in structures shown below. The first one is a generalization of the model of Ref. [1] to 4-layers, and with an improved nonlinearity treatment. The nonlinearity is still treated in an approximate way, but it allows us to obtain the analytical formulas for the field shapes. The second model is an extension to 4 layers of a more recent model developed by Yin [3]. This model gives the dispersion relations with an exact nonlinearity treatment but the field shapes must be computed numerically. Moreover, we use a home made finite-element method adapted for Kerr nonlinear waveguides to verify our semi-analytical results. Thanks to these models we determined the types and the number of nonlinear solutions as a function of the structure parameters. We use the 1D nonlinear solution of the 4-layer structure to obtain a crude approximation of the 2D solutions.

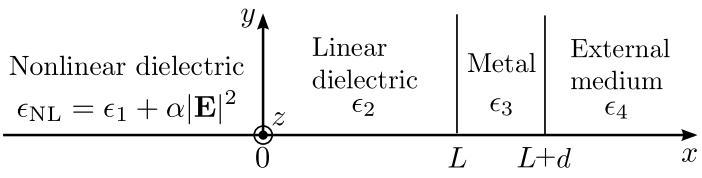

Geometry of the 4-layer configuration.

Using realistic material parameters, we were also able to design structures supporting plasmon–soliton coupling at significantly decreased light intensity ($\approx$1 GW/cm^2 that is 2 orders of magnitude less than in previous works) [4].

References

[1] V. M. Agranovich, V. S. Babichenko, and V. Y. Chernyak, *Nonlinear surface polaritons*, JETP. Lett. **32**, 512–515, 1980. J. Ariyasu, C. T. Seaton, G. I. Stegeman, A. A. Maradudin, and R. F. Wallis, *Nonlinear surface polaritons guided by metal films*, J. Appl. Phys. **58**, 2460–2466, 1985.

[2] E. Feigenbaum and M. Orenstein, *Plasmon–soliton*, Opt. Lett. **32**, 674–676, 2007. C. Miliàn, D. E. Ceballos-Herrera, D. V. Skryabin, and A. Ferrando, *Soliton-plasmon resonances as Maxwell nonlinear bound states*, Opt. Lett. **37**, 4221–4223, 2012.

[3] H. Yin, C. Xu, and P. M. Hui, *Exact surface plasmon dispersion relations in linear-metal-nonlinear dielectric structure of arbitrary nonlinearity*, Appl. Phys. Lett. **94**, 221102, 2009.

[4] W. Walasik, V. Nazabal, M. Chauvet, Y. Kartashov, and G. Renversez, *Low-power plasmon–soliton in realistic nonlinear planar structures*, Opt. Lett. **38**, 4579–4581, 2012.

Hybrid dielectric plasmonic slot guiding nanostructures – analysis with Fourier modal methods

P. Kwiecien[1], J. Čtyroký[2], I. Richter[1*]

[1] *Czech Technical University in Prague, Faculty of Nuclear Sciences and Physical Engineering, Department of Physical Electronics, Břehová 7, 11519 Prague 1, Czech Republic*

[2] *Institute of Photonics and Electronics AS CR, v.v.i., Chaberská 57, 182 51 Praha 8, Czech Republic*

* ivan.richter@fjfi.cvut.cz

Several different types of plasmonic guiding nanostructures, based on the hybrid plasmonic slot waveguide concept, has been recently proposed, simulated, and theoretically analyzed, based on our in-house 3D frequency-domain Fourier modal methods (BEX3, aRCWA).

Introduction

Plasmonic waveguides are finding their important place among other subwavelength-structured photonic and/or plasmonic nanostructures, especially as promising and versatile basic building blocks for the construction of extremely compact devices, targeted at various applications, i.e. for devices such as filters, switches, modulators, sensors, or lasers, in both passive and active regimes. Clearly, in parallel to experimental activities, there is also need for new theoretical exploitations of numerical methods and modeling activities in connection towards their direct application to realistic 3D geometries and problems within these plasmonic waveguides. A number of different types of plasmonic waveguide structures have been recently proposed, theoretically analyzed, and their properties experimentally verified [1]. Among them, one specific type, the hybrid dielectric-loaded plasmonic waveguide [2,3], have found particular interest. Our subtle modification, the hybrid dielectric-plasmonic slot waveguide (HDPSW) [4,5], exhibits very strong field confinement combined with tolerable losses which allows many applications in some integrated plasmonic devices.

Results

Recently, we have developed two independent 3D Fourier modal methods (aperiodic rigorous coupled wave analysis – aRCWA, bi-directional mode expansion propagation method – BX3) [6], based on the 2D approach developed earlier. We have applied our in-house methods to a number of challenging simulation problems, connected with HDPSW. Based on the optimization in terms of the mode effective area [4], and figures of merit [7], we have analyzed and discussed both simple HDPSW as well as more advanced devices such as directional couplers or multimode interference couplers.

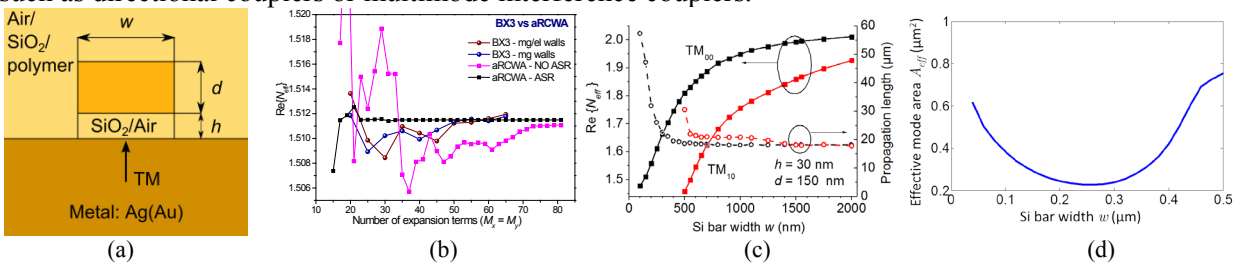

(a) (b) (c) (d)

Fig. 1: (a) Schematic cross-sectional view of HDPSW, (b) convergence of the real part of effective refractive indices - BEX3 × aRCWA, (c) the dependence of the effective refractive indices (solid) and the propagation length (dashed) of the HDPSW modes on the guide width w, (d) effective mode area of the HDPSW with respect to w of the high-index bar (d = 120 nm, gap size h = 30 nm, λ = 1500 nm).

Acknowledgements: This work was financially supported by the Czech Science Foundation (projects P205/10/0046 and P205/12/G118).

References

[1] P. Berini, I. De Leon, Nature Photonics **6**, 16 (2011).
[2] R. F. Oulton, et al., Nature Photonics **2**, 496 (2008).
[3] H.-S. Chu, Y. A. Akimov, P. Bai, E.-P. Li, JOSA B **28**, 2895 (2011).
[4] J. Čtyroký, P. Kwiecien, I. Richter, *submitted to* JEOS:RP (2013).
[5] P. Kwiecien, I. Richter, J. Čtyroký, Proceedings SPIE **8697**, 86971Y (2012).
[6] J. Čtyroký, J. Lightwave Technol. **30**, 3699 (2012).
[7] P. Berini, Optics Express **14**, 13030 (2006).

Analysis of layered media plasmonic waveguides by Multiple Multipole Program

A. Alparslan Ch. Hafner

Laboratory for Electromagnetic Fields and Microwave Electronics, ETH Zurich, 8092, Zurich, Switzerland
aytaca@ifh.ee.ethz.ch

The eigenvalue analysis of plasmonic waveguides is performed by Multiple Multipole Program (MMP) combined with modified layered media Green's functions (LMGF). By this new approach, the exact locations of the physical eigenvalues are determined, which is a troublesome task for all of the well known numerical methods.

Layered media are one of the mostly used building blocks of electromagnetical systems. In microwave regime, devices including microstrip antennas, transmission lines and waveguides were built by using the salient features of layered media for decades. Recent improvements in the fabrication process of materials made it possible to build structures with dimensions comparable with the wavelength range of the visible spectrum. Following these improvements, numerous nano-structures built in a general layered geometry, such as optical antennas and waveguides became popular research subjects in the electromagnetics society [1]. As a result of this interest, numerical tools that can perform the efficient and robust numerical analysis of nano-structures in layered geometries became very important. A candidate for such a tool is introduced by combining MMP [2], an efficient boundary discretization method for the solution of Maxwell's equations in general geometries, with LMGF [3], which are the fields generated by a point source in a layered geometry. The new tool can efficiently compute the scattering and the eigenvalue problems of nanostructures and it is implemented in the opensource environment OpenMAX [4]. In this talk, the eigenvalue analysis of plasmonic waveguides by the new tool is introduced. Since no truncation is needed for the layered geometries, problems originating from artificial truncation boundaries (such as absorbing boundary conditions and perfectly matched layers as in FDTD and FEM) are not present.

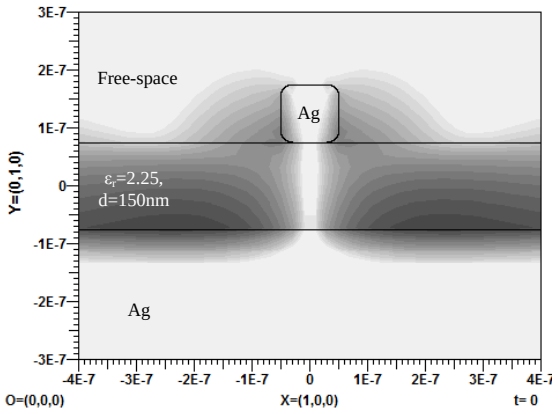

The eigenfield (magnitude of H field, z component in logarithmic scale) at $\lambda_0 = 600nm$ with the eigenvalue (out-of-paper wavenumber) $k_\gamma = (1.24+0.01i)k_0$. The waveguide is a rectangular single wire placed in a three layered geometry with the given material properties. The length of one of the sides of the wire is $100nm$ and the corners are rounded with $r = 20nm$.

References

[1] L. Novotny, *Effective wavelength scaling for optical antennas,* Phys. Rev. Lett. 98, 266802, 2007.
[2] Ch. Hafner, Generalized multipole technique for computational electromagnetics, Artech House Antenna library, Artech House, Boston, MA, 1990.
[3] A. Alparslan, M. I. Aksun, K. A. Michalski, *Closed-form greens functions in planar layered media for all ranges and materials,* IEEE Transactions on Microwave Theory and Techniques, 58, 2010.
[4] Ch. Hafner, A. Alparslan, *OpenMaX: OpenSource Maxwell solver package,* http://openmax.ethz.ch.


PhoeniX Software
Solutions for Micro and Nano Technologies


MESA+
INSTITUTE FOR NANOTECHNOLOGY


JCMwave


Optiwave


IEEE
photonics
SOCIETY


lumerical
illuminating the way


focal
vision & optics


LIONIX